

University of Central Florida

**STARS**

---

Electronic Theses and Dissertations

---

2006

## Design Optimization Of Solid Rocket Motor Grains For Internal Ballistic Performance

Roger Hainline

*University of Central Florida*



Part of the [Mechanical Engineering Commons](#)

Find similar works at: <https://stars.library.ucf.edu/etd>

University of Central Florida Libraries <http://library.ucf.edu>

This Masters Thesis (Open Access) is brought to you for free and open access by STARS. It has been accepted for inclusion in Electronic Theses and Dissertations by an authorized administrator of STARS. For more information, please contact [STARS@ucf.edu](mailto:STARS@ucf.edu).

---

### STARS Citation

Hainline, Roger, "Design Optimization Of Solid Rocket Motor Grains For Internal Ballistic Performance" (2006). *Electronic Theses and Dissertations*. 934.

<https://stars.library.ucf.edu/etd/934>

DESIGN OPTIMIZATION OF SOLID ROCKET MOTOR GRAINS  
FOR INTERNAL BALLISTIC PERFORMANCE

by

R. CLAY HAINLINE  
B.S. Southwest Missouri State University, 1998

A thesis submitted in partial fulfillment of the requirements  
for the degree of Master of Science  
in the Department of Mechanical, Materials, and Aerospace Engineering  
in the College of Engineering and Computer Science  
at the University of Central Florida  
Orlando, Florida

Summer Term  
2006

© 2006 R. Clay Hainline

## ABSTRACT

The work presented in this thesis deals with the application of optimization tools to the design of solid rocket motor grains per internal ballistic requirements. Research concentrated on the development of an optimization strategy capable of efficiently and consistently optimizing virtually an unlimited range of radial burning solid rocket motor grain geometries.

Optimization tools were applied to the design process of solid rocket motor grains through an optimization framework developed to interface optimization tools with the solid rocket motor design system. This was done within a programming architecture common to the grain design system, AML. This commonality in conjunction with the object-oriented dependency-tracking features of this programming architecture were used to reduce the computational time of the design optimization process.

The optimization strategy developed for optimizing solid rocket motor grain geometries was called the *internal ballistic optimization strategy*. This strategy consists of a three stage optimization process; approximation, global optimization, and high-fidelity optimization, and optimization methodologies employed include DOE, genetic algorithms, and the BFGS first-order gradient-based algorithm. This strategy was successfully applied to the design of three solid rocket motor grains of varying complexity.

The contributions of this work are the application of an optimization strategy to the design process of solid rocket motor grains per internal ballistic requirements.

This work is dedicated to my wife, Sachie, my parents, Roger and Nancy, and parents-in-law, Katsuhide and Chieno. Thank you for your support during the time it took to complete this thesis.

## ACKNOWLEDGMENTS

I would like to express sincere appreciation to my advisors, Jamal F. Nayfeh, Ph.D.; Alain Kassab, Ph.D.; and P. Richard Zarda, Ph.D. for their support and advise during my time as a graduate student. Special thanks are extended to Carlos G. Ruiz and Dean T. Kowal for technical advise and support shared while working on this research.

Gratitude is extended to Lockheed Martin, Missiles and Fire Control; Vanderplaats Research and Development Inc.; and TechnoSoft Inc. for supplying me the necessary software and licensing to successfully complete this research. The support received by the staff of the aforementioned companies was greatly appreciated.

## TABLE OF CONTENTS

LIST OF FIGURES .....	IX
LIST OF TABLES.....	XI
LIST OF TABLES.....	XI
CHAPTER 1: INTRODUCTION.....	1
1-1 Introduction .....	1
1-2 Scope of Work .....	3
1-3 Software Application and Integration.....	4
1-4 Research Contributions.....	6
CHAPTER 2: TECHNICAL SUMMARY.....	8
2-1 Principles of Optimization.....	8
2-1-1 Objective Function .....	9
2-1-2 Design Variables .....	10
2-1-3 Constraints.....	11
2-2 Objective Function: Damped Least Squared Method.....	12
2-3 Solid Rocket Motor Grains.....	13
2-3-1 Principle Components of a Solid Rocket Motor Grain .....	14
2-3-2 Solid Propellant Grain Geometry .....	16
2-3-3 Burn Process of a Solid Rocket Motor Grains .....	17
2-3-4 Nozzle Geometry.....	19
2-3-5 Thrust Calculations.....	20
2-4 Approximation Techniques .....	22
2-4-1 Design of Experiments (DOE) .....	22
2-4-2 Response Surface Methodology .....	24
2-5 Optimization Algorithms .....	25
2-5-1 First-order Gradient Based Methods .....	25
2-5-2 Second-order Gradient Based Methods.....	26
2-5-3 Genetic Optimization Methods .....	28
CHAPTER 3: THRUST OPTIMIZATION FRAMEWORK AND IMD ..	31
3-1 Adaptive Modeling Language .....	31
3-1-1 Object-Oriented Programming Language .....	32
3-1-2 Demand-Driven Dependency Tracking Language.....	34

3-1-3 Solid Rocket Motor Design Module .....	36
3-2 Optimization Interface .....	37
<b>CHAPTER 4: OPTIMIZATION PROBLEM STATEMENT .....</b>	<b>41</b>
4-1 Optimization Problem Statement.....	41
4-2 Design Variables.....	43
4-3 Design Constraints.....	44
4-4 Design Objective .....	45
<b>CHAPTER 5: OPTIMIZATION FORMULATION AND STRATEGY ..</b>	<b>46</b>
5-1 The Internal Ballistic Optimization Strategy .....	46
5-1-1 Internal Ballistic Optimization Strategy Overview .....	46
5-1-2 Internal Ballistic Optimization Strategy Stage 1: Design Approximation .....	48
5-1-3 Internal Ballistic Optimization Strategy Stage 2: Design Optimization .....	49
5-1-4 Internal Ballistic Optimization Strategy Stage 3: High-Fidelity Optimization ...	52
5-2 Optimization Formulation .....	54
5-2-1 Thrust Optimization Formulation.....	55
5-2-2 Burn-Area Optimization.....	56
5-3 Resolved Issues with the Optimization Strategy .....	57
5-3-1 Issue 1: Error in Surface Recession Model .....	57
5-3-2 Issue 2: Unexpected Halting of High Fidelity Optimization.....	58
<b>CHAPTER 6: OPTIMIZATION ANALYSIS .....</b>	<b>59</b>
6-1 Internal Ballistic Optimization Strategy Trial #1 .....	59
6-1-1 Optimization Model Definition .....	61
6-1-2 Internal Ballistic Optimization Strategy Stage 1: Design Approximation .....	65
6-1-3 Internal Ballistic Optimization Strategy Stage 2: Design Optimization .....	67
6-1-4 Internal Ballistic Optimization Strategy Stage 3: High-Fidelity Optimization ...	70
6-2 Internal Ballistic Optimization Strategy Trial #2 .....	74
6-2-1 Optimization Model Definition .....	75
6-2-2 Internal Ballistic Optimization Strategy Stage 1: Design Approximation .....	79
6-2-3 Internal Ballistic Optimization Strategy Stage 2: Design Optimization .....	81
6-2-4 Internal Ballistic Optimization Strategy Stage 3: High-Fidelity Optimization ...	85
6-3 Internal Ballistic Optimization Strategy Trial #3 .....	89
6-3-1 Optimization Model Definition .....	90
6-3-2 Internal Ballistic Optimization Strategy Stage 1: Design Approximation .....	94
6-3-3 Internal Ballistic Optimization Strategy Stage 2: Design Optimization .....	96
6-3-4 Internal Ballistic Optimization Strategy Stage 3: High-Fidelity Optimization ...	99

6-4 Investigated Optimization Strategies .....	104
6-4-1 Full-Factorial Design of Experiments Level of Analysis.....	104
6-4-2 High Fidelity Optimization starting at DOE Optimum .....	105
<b>CHAPTER 7: RESULTS AND DISCUSSION .....</b>	<b>107</b>
7-1 Ballistic Optimization Strategy Results.....	107
7-1-1 Internal Ballistic Optimization Strategy Stage 1 Results .....	107
7-1-2 Internal Ballistic Optimization Strategy Stage 2 Results .....	108
7-1-3 Internal Ballistic Optimization Strategy Stage 3 Results .....	109
7-1-4 Summary Results of Internal Ballistic Optimization Strategy .....	111
7-2 Conclusion of Work.....	112
7-3 Recommendations .....	113
<b>APPENDIX A: STAGE #1 – DESIGN APPROXIMATION .....</b>	<b>115</b>
A-1 Appendix Overview .....	116
A-2 Approximation Response Plots: Trials 1, 2, and 3 .....	117
A-3 Approximation Responses: Optimization Trial 1 .....	121
A-4 Approximation Responses: Optimization Trial 2 .....	127
A-5 Approximation Responses: Optimization Trial 3 .....	129
<b>APPENDIX B: STAGE #2 – DESIGN OPTIMIZATION.....</b>	<b>132</b>
B-1 Appendix Overview .....	133
B-2 Optimization Response Plots: Trials 1, 2, and 3 .....	134
B-3 Optimization Responses: Optimization Trial 1.....	138
B-4 Optimization Responses: Optimization Trial 2.....	142
B-5 Optimization Responses: Optimization Trial 3.....	146
<b>APPENDIX C: STAGE #3 – HIGH-FIDELITY OPTIMIZATION .....</b>	<b>149</b>
C-1 Appendix Overview .....	150
C-2 High-Fidelity Optimization Response Plots: Trials 1, 2, and 3 .....	151
C-3 High-Fidelity Opt. Responses: Optimization Trial 1 .....	155
C-4 High-Fidelity Opt. Responses: Optimization Trial 2 .....	158
C-5 High-Fidelity Opt. Responses: Optimization Trial 3 .....	159
<b>APPENDIX D: XM33E5 CASTOR SOLID FUELED ROCKET .....</b>	<b>162</b>
D-1 XM33E5 Castor Solid Fueled Rocket Datasheet.....	163
<b>REFERENCES</b>	<b>171</b>

## LIST OF FIGURES

Figure 1-1 – Three Solid Propellant Grains (a-c) that were optimized.....	2
Figure 1-2 – Software Integration Flowchart.....	4
Figure 2-1 – Sectional view of a solid propellant rocket booster. ....	14
Figure 2-2 – Two different Solid Rocket Motor Grains. ....	16
Figure 2-3 – Steps A--D depicting the surface recession of a solid propellant .....	18
Figure 2-4 – Pressure forces acting on rocket chamber/nozzle walls. ....	21
Figure 2-5 – The process of encoding a design set used in Genetic Algorithms.....	29
Figure 2-6 – Genetic Algorithm Flow Diagram using the Population Based Search. ....	30
Figure 3-1 – Graphical representation of a Table-object. ....	33
Figure 3-2 – Class hierarchy of object-oriented programming language. ....	33
Figure 3-3 – Grain Optimization Demand-Driven Dependency-Tracking Iteration. ....	36
Figure 3-4 – AMOPT Tabbed User-Interface Windows .....	40
Figure 4-1 – Three solid propellant grains shown in isometric and front view diagrams. (a-b) Multi-Cylinder Grain, (c-d) Star Grain, (e-f) Complex Grain. ....	42
Figure 4-2 – Geometric dimensions of complex-grain. ....	43
Figure 5-1 – Flow Diagram of the Internal Ballistic Optimization Strategy. ....	48
Figure 6-1 – (a) Multi-Cylinder Grain Design Solution and (b) Thrust-Time Requirement generated by this grain design.....	60
Figure 6-2 – (a) Initial Multi-Cylinder Grain Design and (b) corresponding Thrust-Time Product. ....	60
Figure 6-3 – Dimensioned cross-section of the multi-cylinder grain. ....	62
Figure 6-4 – (a) Approximated Multi-Cylinder grain model and (b) Thrust-Time Product. .....	67
Figure 6-5 – (a) Optimized Multi-Cylinder Grain Model and (b) Thrust-Time Product..	69
Figure 6-6 – (a) Optimized Multi-Cylinder Grain Model and (b) Thrust-Time Product..	72
Figure 6-7 – The (a) initial grain design; (b) the initial grain design with Castor’s case dimensions; (c) the thrust time requirement of the XM33E5 Castor solid fueled rocket; .....	75
Figure 6-8 – Cross Section of Solid Rocket Motor Grain in Star Configuration. ....	76
Figure 6-9 – (a) Approximated 4 Fin Star Grain Model and (b) Thrust-Time Product....	81
Figure 6-10 – (a) Approximated 5-Fin Star Grain Model and (b) Thrust-Time Product.	81
Figure 6-11 – (a) Optimized 4-slotted Star Grain Model and (b) Thrust-Time Product. .	84
Figure 6-12 – (a) Optimized 5-slotted Star Grain Model and (b) Thrust-Time Product. .	84

Figure 6-13 – (a) High-Fidelity Optimized 5-slotted Star Grain Model and (b) Thrust-Time Product.....	88
Figure 6-14 – Complex Grain and Burn-Area versus Web-Distance Requirement. ....	90
Figure 6-15 – Complex grain with annotated dimensions.....	91
Figure 6-16 – (a) Approximated Complex grain and (b) corresponding burn-area-versus-distance product plotted against the requirement.....	96
Figure 6-17 – Optimized Complex Grain and corresponding Burn Area versus Distance plotted versus the Requirement.....	99
Figure 6-18 – High-Fidelity Optimized Complex Grain and corresponding Burn Area versus Distance plotted versus the Requirement. ....	102
Figure A-1 – DOE approximation responses from the Multi-cylinder grain design. ....	118
Figure A-2 – DOE approximation responses from the Star grain design. ....	119
Figure A-3 – DOE approximation responses from the Complex grain design.....	120
Figure B-1 – Optimization responses from the Multi-Cylinder grain design.....	135
Figure B-2 – Optimization responses from (a) the Star grain design with 5-slots and (b) the Star grain design with 4-slots.....	136
Figure B-3 – Optimization responses from the Complex grain design. ....	137
Figure C-1 – Optimization Response Plot of the Multi-Cylinder Grain Design. ....	152
Figure C-2 – Optimization Response Plot of the Star Grain Design. ....	153
Figure C-3 – Optimization Response Plot of the Complex Grain Design.....	154

## LIST OF TABLES

Table 2-1 – Data Set for 3 Design Variables in a Level 3 Full Factorial DOE. ....	23
Table 5-1 – Parameter Settings for Genetic Algorithm. ....	50
Table 5-2 – Parameter Settings for BFGS Algorithm.....	53
Table 6-1 – Initial design variable configuration for multi-cylinder grain. ....	63
Table 6-2 -- Constraint values of initial design configuration.....	64
Table 6-3 – Design variable values for approximated Multi-Cylinder grain design. ....	66
Table 6-4 – Parameter Setting Definitions for the Genetic Algorithm used in Trial #1...	68
Table 6-5 – Parameter Setting Definitions for the BFGS Algorithm used in Trial #1. ....	71
Table 6-6 – Multi-cylinder grain design variable values for optimum versus solution....	73
Table 6-7 – Initial design variable configuration for star grain. ....	77
Table 6-8 – Constraint values of initial design configuration.....	78
Table 6-9 –Design Variable configurations for Star grain design approximations. ....	80
Table 6-10 – Parameter Setting Definitions for the Genetic Algorithm used in Trial #2.	82
Table 6-11 – Parameter Setting Definitions for the BFGS Algorithm used in Trial #1. ...	86
Table 6-12 – Star grain design variable values for optimum versus Castor grain design.	88
Table 6-13 – Initial design variable configuration for cylinder grain.....	92
Table 6-14 – Design variable values for best approximated Complex grain design. ....	95
Table 6-15 – Parameter Setting Definitions for the Genetic Algorithm used in Trial #3.	97
Table 6-16 – Parameter Setting Definitions for the BFGS Algorithm used in Trial #1.	101
Table 6-17 – Initial design variable configuration for cylinder grain.....	103
Table 7-1 – Summary of approximation results from three optimization trials. ....	108
Table 7-2 – Summary of optimization results from three optimization trials.....	109
Table 7-3 – Summary of high-fidelity optimization results from three optimization trials. .....	110
Table 7-4 – Summary of results from the internal ballistic optimization strategy. ....	111
Table A-1 – Multi-cylinder grain full-factorial 3-level DOE approximation responses.	121
Table A-2 – Star grain full-factorial 3-level DOE approximation responses. ....	127
Table A-3 – Complex grain full-factorial 3-level DOE approximation responses. ....	129
Table B-1 – Multi-cylinder grain abridged genetic optimization response. ....	138
Table B-2 – Every tenth optimization response for the Star grain design with 4-slots. .	142
Table B-3 – Every tenth optimization response for the Star grain design with 5-slots. .	144
Table B-4 – Complex grain abridged genetic optimization response.....	146

Table C-1 – Multi-cylinder grain high-fidelity optimization response.....	155
Table C-2 – Star grain high-fidelity optimization response.....	158
Table C-3 – Complex grain high-fidelity optimization response. ....	159

## CHAPTER 1: INTRODUCTION

This chapter serves as an introduction to the work completed. Descriptions of the optimization problem, applications of this work, and specific research contributions are contained in follow sections.

### 1-1 Introduction

This paper presents the application of optimization tools and techniques to the computer-aided design of solid rocket motor grains. Optimization techniques were applied to the design of solid rocket motor grains within a system level missile design and analysis software titled, *Interactive Missile Design* (IMD) developed by Lockheed Martin, Missiles and Fire Control in Orlando, Florida. Historically, techniques for designing grain geometries in IMD involved a series of methodical inefficient time consuming steps. Through the use of design optimization tools, techniques and strategy were invented to circumvent these historical techniques and provide a more effective method to efficiently and consistently design solid rocket motor grains for internal ballistic requirements.

Sophisticated methods were employed to model solid rocket motor grain geometries. To model grain geometries, IMD used a set of geometric primitives (blocks, cylinders, cones, extrusions, etc.) to construct complicated grain geometries, and through Boolean operations these primitive geometries were joined together in order to realize the burn surface area of the grain. However, while IMD has the methods to model solid

rocket motor grains, simulate surface recession, and perform ballistic analyses, it lacks optimization tools capable of optimizing grain geometries for internal ballistic requirements. The research presented in this paper discusses optimization strategies and tools developed for optimizing solid rocket motor grains for internal ballistics.

Once the *internal ballistic optimization strategy* was developed, three solid rocket motor grains of varying complexities were optimized to prove the strategy. Figure 1-1 illustrates these three center perforated radial burning grain geometries where (a) represents a multi-cylinder grain, (b) represents a slotted grain, and (c) represents a complex grain. More details on each of these three grains will be presented throughout this paper.

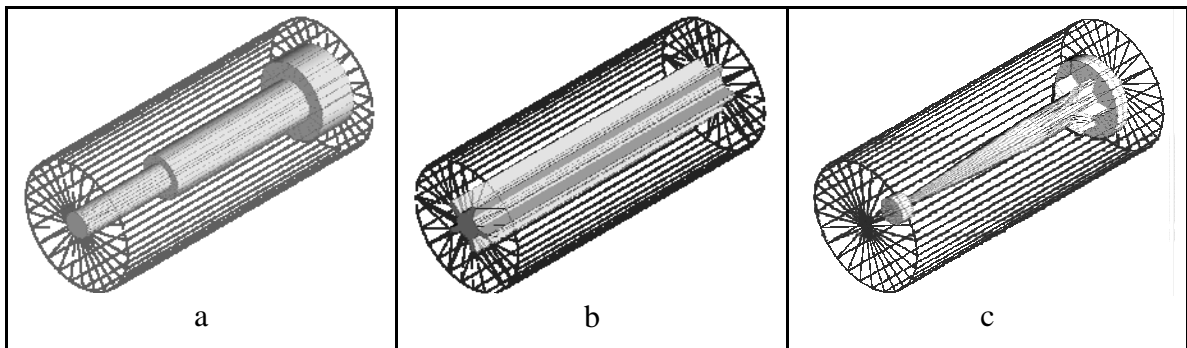


Figure 1-1 – Three Solid Propellant Grains (a-c) that were optimized.

Finally, the *internal ballistic optimization strategy* demonstrated the ability to improve solid rocket motor grains geometry with respect to internal ballistic performance requirements. Optimization techniques applied within the optimization strategy included design of experiments, genetic algorithms, and gradient-based algorithms. Some solid

rocket motor characteristics considered to rate the merit of respective designs include thrust versus time, burn area versus distance, total impulse, and propellant weight.

## 1-2 Scope of Work

The tools of optimization are currently being accelerated faster than ever into industry. Work presented in this thesis demonstrates how optimization functionality can be applied to the design process of solid rocket motor grains. Advantages of optimization strategies in the solid rocket motor design process include a reduction in the design time, and the ability to efficiently and consistently realize design behavior. The scope of work is summarized in the following bullets:

1. Develop an optimization strategy capable of optimizing a solid rocket motor grain geometry for a ballistic requirement of thrust.
2. Investigate methods of approximation that will reduce the computational time required to converge to optimum solid rocket motor grain designs.
3. Integrate the solid rocket motor design interface and the optimization interface using AML, a demand driven, dependency tracking programming language.
4. Optimize three solid propellant grains of varying complexity within a demand driven, dependency tracking interface.
5. Identify optimization algorithm(s) with the most efficient and most consistent rates of convergence.
6. Recommendation future investigations in this arena.

### 1-3 Software Application and Integration

Software required for this research included software for modeling solid rocket motor grains, an optimization algorithm software suite, and a software interface between the grain modeling software and the optimization algorithm suite. The flow of software integration is shown in Figure 1-2.

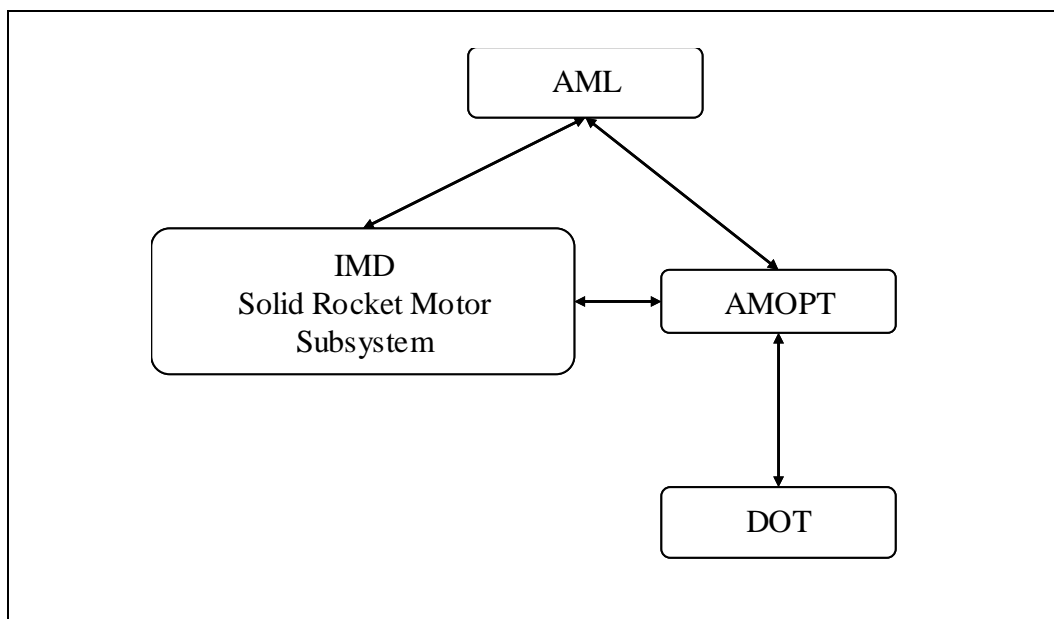


Figure 1-2 – Software Integration Flowchart.

First, software was required to model solid rocket motor grain geometries and inspect internal ballistic properties. This was accomplished by composing a system similar to the solid rocket motor subsystem of Interactive Missile Design (IMD). This system was used to model solid rocket motor grain geometries, simulate surface

recessions, and perform internal ballistic analyses of solid rocket motor grains. This system was coded using Adaptive Modeling Language (AML), a demand-driven dependency-tracking programming language developed and supported by TechnoSoft Inc. Furthermore, AML is the underlying programming language of IMD. IMD was developed by Lockheed Martin, Missiles and Fire Control and was designed as a system level missile design and analysis tool that streamlined the conceptual and preliminary missile design and development process.

Next, a suite of optimization algorithms was required to optimize solid rocket motor grain geometries. Two optimization algorithm suites were used. First, Design Optimization Tools (DOT) developed by Vanderplaats Research and Development was used as it contained first and second order gradient-based algorithms. Next, algorithms integrated into the optimization interface AMOPT, developed by TechnoSoft Inc., were also used. AMOPT is discussed in the next paragraph.

Finally, an interface was required to tie the solid rocket motor modeling system to the third-party optimization algorithm suite. AMOPT provided this interface. AMOPT was developed to link the optimization algorithms in DOT and manage optimization models. From this interface, the optimization process in its entirety was executed, and with its AML architecture it could take advantage of all the demand-driven dependency-tracking features of the programming language.

## 1-4 Research Contributions

The research contributions of this work are summarized in the list below and discussed throughout this thesis.

1. The *Internal Ballistic Optimization Strategy* was developed as a strategy for optimizing solid rotor motor grain designs per internal ballistic requirements.
2. The *Internal Ballistic Optimization Strategy* was applied to the design of solid rocket motor grains in three optimization trials involving three different solid rocket motor grain designs.
3. The *Internal Ballistic Optimization Strategy* is capable of optimizing solid rocket motor grains per one of two internal ballistic properties: thrust-time and burn-area versus distance.
4. Optimization methodologies used in the optimization strategy were studied and chosen based on the different optimization techniques employed by these methodologies; these different optimization techniques compliment each other in converging to optima.

This research concentrated on the application of optimization to the design of solid rocket motor grains. Solid rocket motor grains were optimized on merits comprised of internal ballistic properties. Emphasis was placed on the development of a strategy that would efficiently and consistently optimize any center perforated radial-burning solid rocket motor grain design. This strategy is referenced throughout this paper as the *internal ballistic optimization strategy*.

The *internal ballistic optimization strategy* was developed using AML, an object-oriented dependency-tracking programming language. Also, because AML was the underlying programming language of the solid rocket motor grain modeling system within IMD, full advantage was taken of the object-oriented dependency-tracking behavior of AML.

During the three trials of the *internal ballistic optimization strategy*, optimal results were recorded with the use of non-gradient based optimization methodologies at the start of the optimization process. This was caused by the formulation of the optimization models. However, as the optimization converged and there was less variation in the optimum response, and gradient based optimization methodologies proved to be an effective component to the *internal ballistic optimization strategy*.

## CHAPTER 2: TECHNICAL SUMMARY

This chapter serves to introduce the technical topics of this thesis. Technical topics presented fit two major categories: optimization and solid rocket motor grains. Principles of optimization are presented first, followed by an introduction to solid rocket motor grains. Finally, a detailed discuss of optimization techniques (including optimization algorithms) are presented. Optimization algorithms discussed include gradient based, non-gradient based, and genetic algorithms.

### 2-1 Principles of Optimization

Present day software design tools require the use of sophisticated optimization tools to efficiently solve design problems. Examples of some engineering software that currently supply optimization design tools include PRO-E by Product Development Company, I-DEAS by Structural Dynamics Research Corporation and CODE V by Optical Research Associates. In order for these optimization tools to be implemented efficiently, the formulation of the optimization design problem must adhere to the formulation criterion shown in Equation 2-1. [1] This basic formulation consists of three principle components listed on the next page and discussed in subsections that follow. Note the nomenclature below will be used throughout this paper.

1. *Objective/Merit function* represented by  $F(\bar{X})$ ,
2. *Design variables* represented by the vector  $\bar{X}$ ,
3. *Constraints* represented by  $g_i(\bar{X})$ ,  $h_j(\bar{X})$ , or  $\bar{X}$  with upper and lower bounds.

$$\begin{array}{llll}
 \text{Minimize :} & F(\bar{X}) & & \\
 \text{Such that :} & g_i(\bar{X}) \leq 0 & i = 1, \dots, n_g & \\
 & h_j(\bar{X}) = 0 & j = 1, \dots, n_h & \\
 & X_k^{lower} \leq X_k \leq X_k^{upper} & k = 1, \dots, n_m & 
 \end{array} \quad \text{Equation 2-1}$$

### 2-1-1 Objective Function

The objective function,  $F(\bar{X})$ , provides the criterion for rating design improvement during the optimization process. This function is a function of the design variables chosen to describe a particular system. Without this dependence, the design variables would be unable to influence the design.

Optimization problems are typically tasked with finding the minimum condition for a system. Problems seeking a maximum condition can be converted into minimization problems by minimizing the negative of the objective function,  $-F(\bar{X})$ .

[1]

Optimization algorithms operate by sampling the objective function iteratively at different perturbations of the design variables until the objective function converges to a solution, within an acceptable tolerance. Therefore, the formulation of objective function is a key determinant to the convergence rate of the optimization process, and the

objective function must be formulated in terms of its sensitivity to small perturbations of the design variables throughout the entire design space. Objective functions that are insensitive to changes in the design variables can suffer from early optimization process termination. Likewise, hyper-sensitive formulations run the risk of becoming unbound which also can result in early termination. [2]

### 2-1-2 Design Variables

Design variables are parameters chosen to describe a design, and are denoted by the vector  $\bar{X}$ . In the case of a box design, the design variables would be the height, width and depth of the box. Design variables are manipulated by a search direction or search strategy to drive the objective function to a minimum. An example of an optimization problem involving a box is the problem of maximizing a volume while minimizing surface area.

Design variables can take one of two forms: continuous and discrete. [1] Continuous design variables can be assigned any real numerical value within a specified range. Discrete design variables can be assigned only discrete values that exist within a data set or range. One design variable used in this thesis was discrete and the rest were continuous.

Selecting design variables to represent a system is the first step of the optimization process. These variables must be chosen carefully in order to effectively describe the design. Another consideration for choosing design variables is quantity of design variables selected. The quantity of design variables chosen to represent a system directly relates to the complexity of the optimization problem, and the more complex the

optimization problem, the more it costs to solve. [1] Therefore, the less design variables the better.

One way to reduce the number of design variables is through variable decomposition. [1] This method eliminates variables from an optimization problem by formulating one or more variables in terms of another. For example, if a box is to be optimized for maximum volume and that box must be twice as tall as it is wide, the design variable for box *height* can be replaced with  $2 \cdot (\text{box width})$  every time it appears in the problem. This reduces the number of design variables by one and makes the optimization problem that much easier to solve.

Finally, it is good practice to eliminate large variations in the magnitudes of design variables and constraints through normalization. [1] Design variables may be normalized to unity by scaling, and often unity represents the largest value the design variables will ever see. Normalization is important as many optimization software packages are not numerically robust enough to handle this condition.

### 2-1-3 Constraints

Constraints are used to bound on the solution space of optimization problems to a *feasible region*. There are three types of constraints used in optimization; inequality, equality, and side constraints. Referencing Equation 2-1,  $g_i(\bar{X})$  represents inequality constraints,  $h_j(\bar{X})$  represents equality constraints, and  $X_k$  represents side constraints. To have influence on the optimal design, constraints must be influenced by at least one design variable. [3]

The choice of constraint depends on the problem. Inequality are used more often than equality constraints as they are less restrictive of the design. [3] More feasible solutions exist between a range of values than at a specific value as deemed necessary by equality constraints. On the other hand, they can be used to reduce the number of design variables. [1]

For an optimization problem to produce a feasible solution, all constraints must be satisfied. [1] This means that even though a set of design variables may evaluate to an optimum, if even one constraint is violated the solution is considered infeasible.

## 2-2 Objective Function: Damped Least Squared Method

Since 1960, the damped least-squares method (DLSM) has been implemented in objective functions for many optimizers. [4] This method fits the genre of what are known as *downhill optimizers* where in a system with multiple minima, it is supposed to find the nearest local minimum. [5] It is possible that the local minimum could correlate with the global minimum; however, this is unlikely and it is often advised to start the optimization process multiple times each time using a different initial starting position. One downside of using the DLSM is that this function suffers from stagnation, yielding slow convergence to local minima. To rectify this, however, designers over the years have found ways to overcome this deficiency by learning to manipulate the damping factors. [5]

The damped least-squares function is a continuation of the least-squares method (LSM) formulated by summing the squares of operands,  $f_i$  multiplied by weighting

factors,  $w_i$ . These operands must be a functions of the design variables,  $\bar{X}$ , in order for the formulation to be properly influenced and thus be an objective function. This formulation is shown in Equation 2-2 below where  $y_i$  represents a reference point from which a difference is calculated. [4]

$$DLS = \sum_{i=1}^n w_i f_i(\bar{X}) = \sum_{i=1}^n w_i f_i(\bar{X}) - y_i \quad \text{Equation 2-2}$$

### 2-3 Solid Rocket Motor Grains

A solid rocket motor grain is the physical mass of propellant used in solid rocket motors. Solid rocket motor grains are burned to convert energy stored in the propellant into kinetic energy, *thrust*. A typical scenario for a solid rocket motor grain is produce large amounts thrust at the instant of motor ignition and then reduce the amount of thrust to an acceptable point after lift-off to prevent overstressing of the rocket during maximum dynamic pressure. [6] The burn characteristic of a solid rocket motor grain is greatly influenced by the shape, size, and geometry of that grain.

This section presents the subject of solid rocket motor grains. Technical information includes a component overview of solid rocket motor grains, a description of solid rocket motor grain geometry and its relationship to thrust, a description of how the burn of a solid rocket motor grain is modeled, and finally, a description of how a solid rocket motor produces thrust.

### 2-3-1 Principle Components of a Solid Rocket Motor Grain

Solid rocket motor grains have five principle components: propellant, combustion chamber, nozzle, and igniter. [7] These components and relevant subcomponents are diagramed in Figure 2-1 and described in the order in which they appear in the figure.

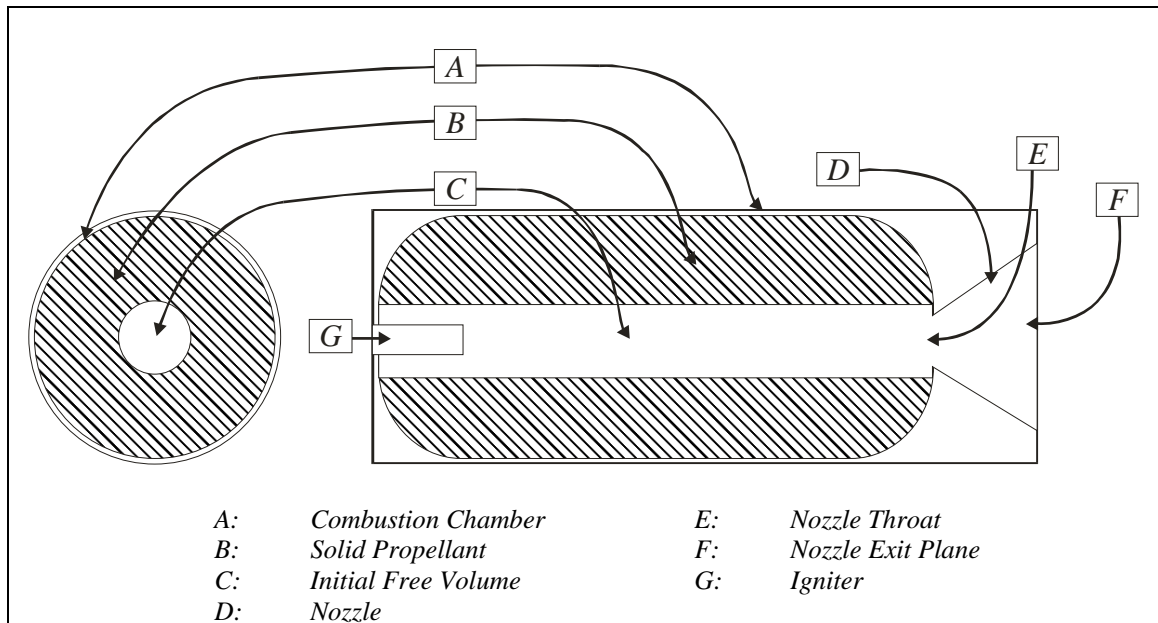


Figure 2-1 – Sectional view of a solid propellant rocket booster.

First, referring to Figure 2-1, the *combustion chamber*, A, represents the housing for the *solid propellant grain* shown as the hatched area labeled B. The combustion chamber is also the mechanism that limits the maximum volume of solid propellant in the grain. Therefore, a variation in thrust for any specific propellant is highly a function of the propellant grains geometry rather than the volume of actual propellant. [7] Solid propellant grain geometry will be discussed in the next section.

The *initial free volume*,  $B$ , of a solid propellant grain is a hollow geometrical perforation in the propellant ported to the rocket nozzle. This is where the propellant reacts to produce hot high pressure gases that are expelled through the nozzle to provide thrust. [5] The propellant in reference figure is in the shape of a cylinder, and the initial free volume is shown as a cylindrical perforation inside the propellant. The surface area of the initial free volume is the exposed area of the grain known as the *burn surface area*. A grain's initial free volume can take on a variety of shapes, from the simplest cylinder to something orders of magnitude more complex. Throughout this paper, the shape of the initial free volume is also referred to as *grain geometry*.

The *nozzle* and components thereof, ( $D, E$ , and  $F$ ) in Figure 2-1, represent the mechanism for regulating pressure inside the combustion chamber, and ultimately the exhaust velocity, and thrust. Component adjustments that effect the exhaust velocity include the area ratio of the nozzle throat  $E$  to the nozzle exit plane  $F$ , and the pitch angle of the nozzle. [7]

Lastly, the *igniter* ( $G$ ) serves to ignite the propellant. It is assumed in this paper that this device ignites the entire burn surface area instantaneously.

Components that highly contribute to the thrust of a solid propellant grain are the geometry of the grain's initial free volume, the entrance and exit areas of the nozzle, and the burn rate of the propellant. [8] The next section describes the grain geometry, the shape of the initial free volume.

### 2-3-2 Solid Propellant Grain Geometry

The initial free volume geometry (grain geometry) of a solid rocket motor grain is the principle component that influences solid rocket motor internal ballistics. [7] This geometry ultimately defines the *burn surface area*. The *burn surface area* is the surface area of a grain's initial free volume, and the area of the propellant exposed to the environment through the nozzle. Figure 2-2 shows two solid rocket motor grain models. These models represent two solid rocket motor grains through the parametric shape of their respective initial free volumes. In these figures, the solid objects inside the wire-frame volumes are the initial free volumes of the grains, and the wire-frame volumes surrounding the free volumes represent the propellant.

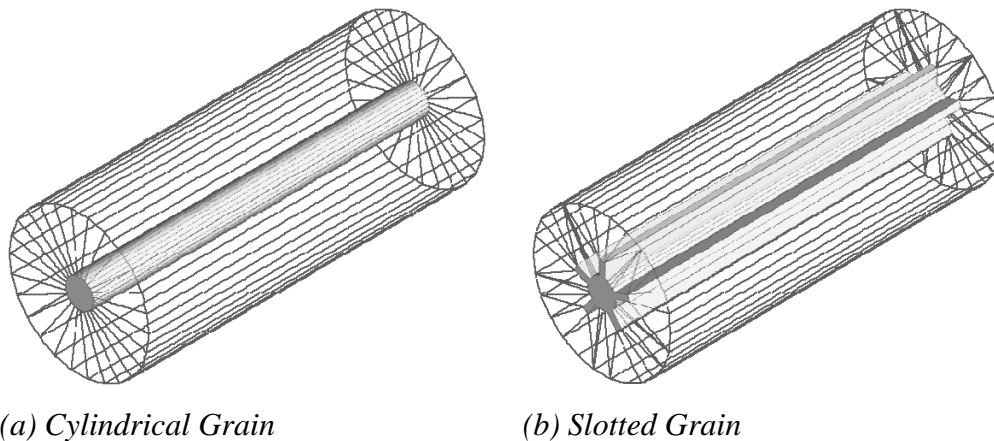


Figure 2-2 – Two different Solid Rocket Motor Grains.

Solid rocket motor grain geometries are commonly modeled using geometric primitives. These primitives include geometric shapes (blocks, cylinders, cones, spheres, etc). Also, through the use of Boolean operands (union, and intersection), primitive

geometric shapes are collected into a single geometric entity that can be grown in a direction normal to its burn surface area. [8]

A feature of solid rocket motor grains is they lend themselves to mechanically constrained design volumes. According to George P. Sutton, “Since a given combustion chamber will be able to hold only a limited amount of propellant, the variation of thrust for any specific propellant has to be obtained by varying the geometric form and therefore the exposed burning surface of the propellant charge.” This quote states that solid propellant grains are versatile in the mission characteristic they satisfy. Just by changing the grain geometry, not the physical envelop allocated to the grain, the thrust-time curve for a grain can be altered to satisfy the requirements of different missions.

### 2-3-3 Burn Process of a Solid Rocket Motor Grains

In the burn process of solid rocket motor grains, propellant recedes in a direction normal to the burn surface area of the grain. [7, 8] As propellant recedes, the burn surface area changes as a function of time, burn rate, and grain geometry. At the start of the burn process, there is a transient phase where the burn rate increases rapidly until it reaches a constant rate determined by the design pressure of the motor and burn rate of the propellant. However, for motors that are designed to reach a steady state design pressure, the transient phase only lasts a few milliseconds. The volume of propellant burned per second is called the *web*. [7] Additionally, the time a propellant grain burns is commonly expressed in a *web distance*, a linear distance of propellant, normal to the current burn surface, that would burn in a specified amount of time. Solid propellant

grain surface recession is commonly expressed in terms of burn area versus web distance, a dependent of thrust versus time.

To exemplify the burn process, consider the center perforated cylindrical grain in Figure 2-2a on page 16. When this grain burns the cylindrical perforation, the initial free volume of the grain, grows concentrically larger receding the propellant until all is consumed. For this simple grain geometry, the burn area versus web is easy to mathematically predict. However, for grains of more complex geometries, it becomes more difficult to efficiently make such mathematically predictions and computers are used to simulate the burn process of solid rocket motors.

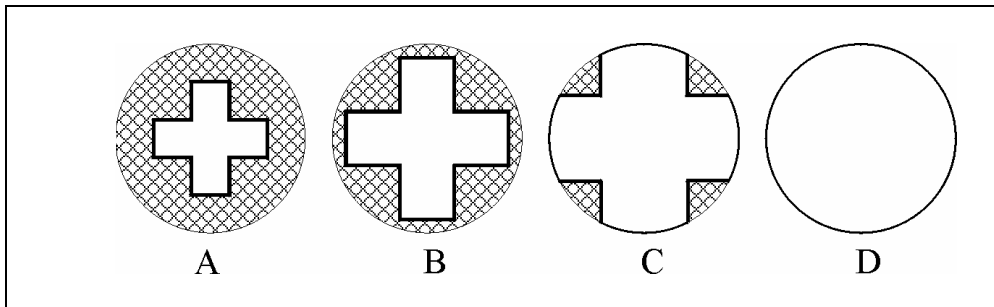


Figure 2-3 – Steps A--D depicting the surface recession of a solid propellant

Finally, for a more complicated grain example, Figure 2-3 represents two-dimensional cross-sections of a four-slotted star grain at four increments during the burn process. An isometric view of this grain appears similar to the five-slotted star grain shown in Figure 2-2b on page 16. The hatched area represents the remaining propellant, and the dark outline represents a cross section of the burn surface area. This figure depicts the propellant receding in a direction normal to the burn surface area. Where as mathematical representations of burn surface area versus web are not difficult for steps A

and B, once the propellant recession starts intersecting the case, predicting the burn surface area gets quite rigorous. Without iterating the mathematics used to calculate web versus distance for this grain, the mathematical difficulty is empirically expressed.

#### 2-3-4 Nozzle Geometry

The nozzle component of a solid propellant rocket is the exit port to the combustion chamber. The shape of the nozzle is used to convert the chemical energy released in combustion into kinetic energy. [7] Nozzles have several key parameters shown in Figure 2-1 on page 14 including the *nozzle throat* and the *nozzle exit plane*. The nozzle throat is the point in the nozzle with the smallest cross-sectional area, and the nozzle exit plane is rear exit area of the nozzle. Also important but not labeled in the figure are the *convergent* and *divergent* cones of the nozzle.

To aid in the flow of exhaust gases out of the combustion chamber the nozzle has a convergent cone and a divergent cone. The convergent cone is designed to funnel exhaust gases from the combustion chamber into the nozzle throat, and the divergent cone is designed to control pressures and exhaust velocities. The convergent section of the nozzle is in a space of the grain where the kinetic energy is relatively small, “and virtually any symmetrical and well-rounded convergent shape has very low losses”. [7] Conversely, the shape of the divergent section of the nozzle is more critical. The nozzle throat represents the plane in the nozzle with the smallest cross-sectional area. There is a relationship between the nozzle throat area and the nozzle exit plane called the *area ratio* which is the ratio between these two areas. This number in conjunction with the

divergent angle of the cone represents the two performance driving characteristics of a solid rocket nozzle.

### 2-3-5 Thrust Calculations

Thrust is an internal ballistic property of solid rocket motors. Internal ballistics deal with solid rocket motor properties such as thrust, pressure exponent, burn rate, etc. resulting from burning a solid propellant in a rocket motor or gas generator. External ballistics, in contrast, deal with the trajectory aspects of rockets.

Solid propellant rocket engines are reaction engines that produce thrust based on the Newtonian principle that “to every action there is an equal and opposite reaction.” Thrust is the reaction force on the rocket structure caused by the action of the pressure of the combustion gases against the combustion chamber and nozzle surfaces. [7] When solid propellant is ignited, propellant evaporates into hot high pressure gases that exhaust through the rockets nozzle at high velocities.

Axial thrust is determined through the integration of the pressure in the combustion chamber and nozzle over all the respective area elements. This is described mathematically in Equation 2-3 and visually in Figure 2-4.

$$Thrust = \int P dA$$

Equation 2-3

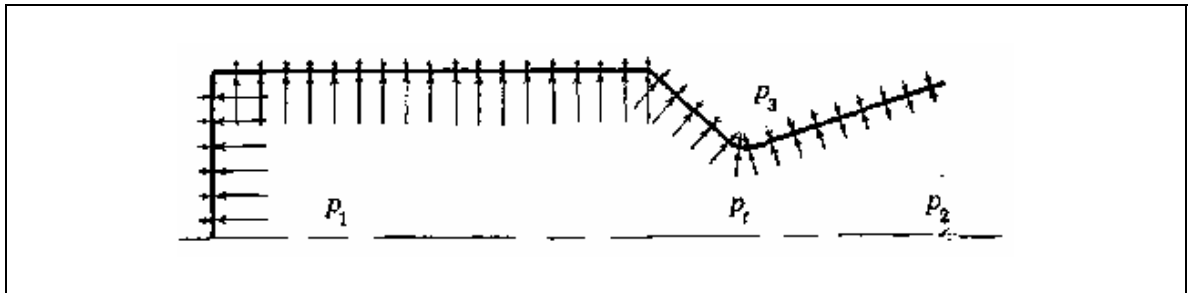


Figure 2-4 – Pressure forces acting on rocket chamber/nozzle walls.

In this research, rocket thrust was calculated using algorithms supplied by Lockheed Martin, Missiles and Fire Control. These algorithms use a highly simplified combustion model known as St. Robert's Law. This model assumes the normal burning rate of the propellant is a function of the chamber pressure. The combination of this normal burning rate and burn surface area of the grain is used to determine the volume of propellant burned in the chamber at any given time step. This is then used to determine the chamber pressure, and ultimately thrust. The general form of the normal burning rate law is expressed in Equation 2-4.

$$r = a \left( \frac{P}{P_{ref}} \right)^n \quad \text{Equation 2-4}$$

where:

$r$  = normal burning rate in inches/second.

$a$  = reference burning rate. (propellant characteristic)

$P$  = chamber pressure.

$P_{ref}$  = reference chamber pressure.

$n$  = burn rate exponent. (propellant characteristic)

## 2-4 Approximation Techniques

Design optimization strategies typically involve multiple steps of performing iterative optimization analyses. Often for a design problem to converge to a solution individual analyses must be repeated. Each analysis step has a cost associated with it, and as the number analyses increase, this cost can become significant to the point of being prohibitive. Approximation techniques can be use ahead of optimization to understand the design space of an abstract problem. Significant cost savings can be realized through the use of approximation techniques. This section discusses approximation techniques including DOE and regressions.

### 2-4-1 Design of Experiments (DOE)

Design of Experiments (DOE) represents a group of methodologies used to quantitatively sample the design space of a system with relatively few design points. In this project and others, DOEs are routinely employed as a precursor to the optimization process.

There are two major advantages to running DOEs. First, by sampling the objective response over the design space, system behavior is ascertained over the design space and design points with the highest merit can be used as starting points for optimization processes. Second, performing regression analysis on DOE output relating the variance of the objective response to the design variables reveals design variable sensitivities, and with this information, the vector of design variables can be altered and/or revised as appropriate. Accuracy of these mathematical models depend upon of

the system response behavior and the DOE methodology used to collect the system response.

One of the most common DOE methodologies is the full-factorial DOE. The full-factorial DOE samples the effects of all design variables and their interactions. This methodology is run as a level-two or level-three experiment. For level-two DOEs, design variables are sampled at the upper and lower bound of their defined domains, where as for level-three DOEs, design variables are sampled at the upper, lower, and midpoint of each variables domain. For example, Table 2-1 lists all experiments for level-three full factorial DOE with variables *DV1*, *DV2*, and *DV3* defined in the domain from -1 to 1. The number of iterations required to sample the design space in a three level DOE is the 3 raised to a power equal to the number of design variables; e.g.  $3^3 = 27$  iterations. A two-level DOE with the variables listed in the table below would have  $2^3 = 8$  iterations.

Table 2-1 – Data Set for 3 Design Variables in a Level 3 Full Factorial DOE.

<i>Iteration</i>	<i>DV1</i>	<i>DV2</i>	<i>DV3</i>
1	-1	-1	-1
2	-1	-1	0
3	-1	-1	1
4	-1	0	-1
5	-1	0	0
6	-1	0	1
7	-1	1	-1
8	-1	1	0
9	-1	1	1
10	0	-1	-1
11	0	-1	0
12	0	-1	1
13	0	0	-1
14	0	0	0
15	0	0	1
16	0	1	-1
17	0	1	0
18	0	1	1
19	1	-1	-1
20	1	-1	0
21	1	-1	1
22	1	0	-1
23	1	0	0
24	1	0	1
25	1	1	-1
26	1	1	0
27	1	1	1

Different requirements mandate the need for running a level-two or level-three full factorial DOE. Level-two DOEs are used on systems when a linear response is expected and information on all design variables and their interactions are desired. Level-three experiments are used when a non-linear response is expected. A disadvantages of full factorial DOEs is a large number of experiments are required for designs with a large number of design variables. [9]

In summary, DOEs sample the solution space of a design with a limited number of design points. Designs are sampled without the need for derivative or gradient calculation used by many optimization algorithms, and furthermore, results of DOE methodologies significantly minimize time, and thus, cost of a design. [10]

#### 2-4-2 Response Surface Methodology

One of the most common methods of “global approximation” is the response surface methodology. [1] The first step to create a response surface approximation is to sample the objective function at multiple experimental design points. Often DOE techniques are used to generate a sum of experiments to be run. Next, an analytical expression is fit to the data. This expression, typically a polynomial, is used to predict system performance at multiple design points.

Fidelity of response surface approximations are highly subject to the number of experiments sampled and size of the design space. It is standard to run at least three sets of experiments. [10] Also, the order of the polynomial fit is an important contributor to approximation accuracy; e.g. if a system has a cubic response, a linear response surface would not likely produce an accurate fit. [1]

## 2-5 Optimization Algorithms

The probability of finding an optimum solution is highly related to the optimization formulation and what optimization algorithm is used as the optimizer. Records of optimization techniques being used in structural design date back to the eighteenth century, and when the aerospace industry recognized the importance of minimum weight in aircraft marks another milestone in the development of optimization techniques. [1] This section focuses on optimization algorithms grouped under the following categories: first and second order gradient based algorithms, and genetic algorithms.

### 2-5-1 First-order Gradient Based Methods

First-order gradient based optimization methods utilize the gradient of the objective function to increase the convergence rate to optima. These methods apply to unconstrained optimization problems, and are usually more efficient than zero-order (non-gradient) based methods given certain conditions are valid. [11] First-order gradient based methods inherently have a higher cost to operate driven by gradient information that must be supplied analytically or by finite differencing calculations. However, even though the cost per iteration may be higher for these methods than for zero-order methods, the trade is a lesser number of iterations required to achieve an optimum solution.

$$\bar{S} = -\nabla F(\bar{X})$$

Equation 2-5

The simplest first order gradient based algorithm is known as the method of *steepest descent*. [11, 12]. The search direction of this algorithm moves with the negative gradient of the objective function, see Equation 2-5. Note, if the search direction moved with the positive gradient, this algorithm would be named the method of steepest *ascent*. [3] This is but one example of first-order gradient based algorithms. Other algorithms have adapted this principle to produce algorithms with much more efficient performance.

Next, second-order gradient based methods will be discussed.

### 2-5-2 Second-order Gradient Based Methods

Second-order gradient based optimization methods provide a more accurate representation of the objective function than first-order methods, and with the inclusion of second order information the convergence rate becomes more efficient. [3]

Second-order gradient based methods utilize function values, gradient of the objective function, and the Hessian matrix,  $H$ , in the optimization process. [3, 11] The Hessian matrix, shown in Equation 2-6, is a matrix of second derivatives of the objective function with respect to the design variables. By using the Hessian matrix in the formulation of the search direction  $\vec{S}$ , see Equation 2-7, functions that are truly quadratic in the design variables can be optimized in only one iteration. [3, 11]

$$\mathbf{H} = \begin{bmatrix} \frac{\partial^2 F(\bar{X})}{\partial X_1^2} & \frac{\partial^2 F(\bar{X})}{\partial X_1 \partial X_2} & \dots & \frac{\partial^2 F(\bar{X})}{\partial X_1 \partial X_n} \\ \frac{\partial^2 F(\bar{X})}{\partial X_2 \partial X_1} & \frac{\partial^2 F(\bar{X})}{\partial X_2^2} & \dots & \frac{\partial^2 F(\bar{X})}{\partial X_2 \partial X_n} \\ \vdots & \vdots & \ddots & \vdots \\ \frac{\partial^2 F(\bar{X})}{\partial X_n \partial X_1} & \frac{\partial^2 F(\bar{X})}{\partial X_n \partial X_2} & \dots & \frac{\partial^2 F(\bar{X})}{\partial X_n^2} \end{bmatrix} \quad \text{Equation 2-6}$$

$$\bar{\mathbf{S}} = -[\mathbf{H}(\bar{X}^q)]^{-1} \nabla F(\bar{X}^q) \quad \text{Equation 2-7}$$

Differing from the first-order gradient base methods examined in previous sections, these methods are applied to constrained optimization problems. Though second-order methods approach the use of constraints differently, a common approach alters the search direction to “push away” from the constraint boundary before it is violated. [11]

Common to second-order gradient based algorithms is the use of the Kuhn-Tucker conditions. These conditions, shown in Equation 2-8 to Equation 2-10 are used in the determination of global optimality. Equation 2-8 requires the values of all design variables exist within a feasible domain. Equation 2-9 requires for all inequality constraint(s),  $g_j(\bar{X})$ , that are not exactly satisfied (e.g. not critical), the corresponding Lagrange multiplier,  $\lambda_j$ , must equal zero. Finally, the third Kuhn-Tucker condition, Equation 2-10, requires search directions satisfying both usability and feasibility requirements will be precisely tangent to the constraint boundary and the line in which the objection function is constant. [1] “A feasible direction is one in which all constraints

are satisfied, and a usable direction is one in which the objective function is improved.”

[10]

$$\bar{X}^* \text{ is feasible} \quad \text{Equation 2-8}$$

$$\lambda_j g_j(\bar{X}^*) = 0 \quad \text{Equation 2-9}$$

$$\nabla F(\bar{X}^*) + \sum_{j=1}^m \lambda_j g_j(\bar{X}^*) + \sum_{k=1}^l \lambda_{m+k} \nabla h_k(\bar{X}^*) = 0 \quad \text{Equation 2-10}$$

$$\lambda_j \geq 0$$

$$\lambda_{m+k} \text{ unrestricted in sign}$$

### 2-5-3 Genetic Optimization Methods

Genetic optimization methods originated in genetics, biology, and computer science. Genetic optimization methods operate differently than conventional optimization methods by relying on a *survival of the fittest* type approach in the hunt for optima. Just as biological creatures evolve by passing on useful characteristics and discarding not so useful ones, genetic optimization processes work by retaining design sets that give the best figure of merit while the design sets that do not have such good merit ratings are discarded. [7]

Genetic methods have many renditions. For reference purposes, a popular method, titled population-based search, is now presented. A flow diagram depicting the encoding process is shown in Figure 2-5. This process is started with the selection of several design sets within a feasible design space. The first iteration design sets are

called *parent values*. Next, each design set is encoded into a binary chain of ones and zeros. These chains of numbers are called chromosomes. [7]

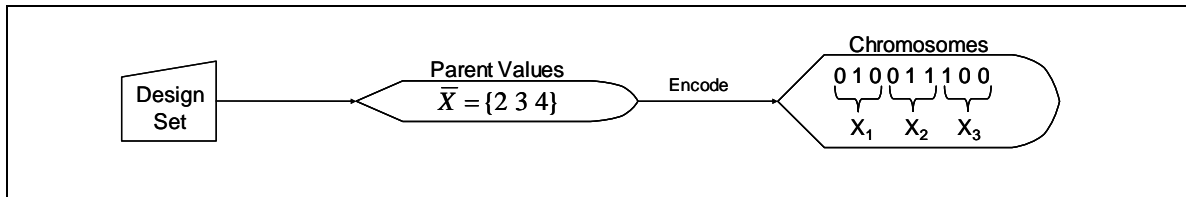


Figure 2-5 – The process of encoding a design set used in Genetic Algorithms.

Genetic algorithms are stochastic search techniques that guide a population of solutions using the principles of evolution and natural genetics. Once the design sets have been encoded into chromosomes, they are manipulated in one of two ways to form new design sets shown Figure 2-6. The *crossover* method swaps sections of chromosome to form new chromosomes, and the *mutation* method changes the values of one or more binary bits of the chromosomes to form new chromosomes. Finally, these new chromosomes are decoded back into the base of the parent values, e.g. binary to decimal, and the objective function is evaluated.

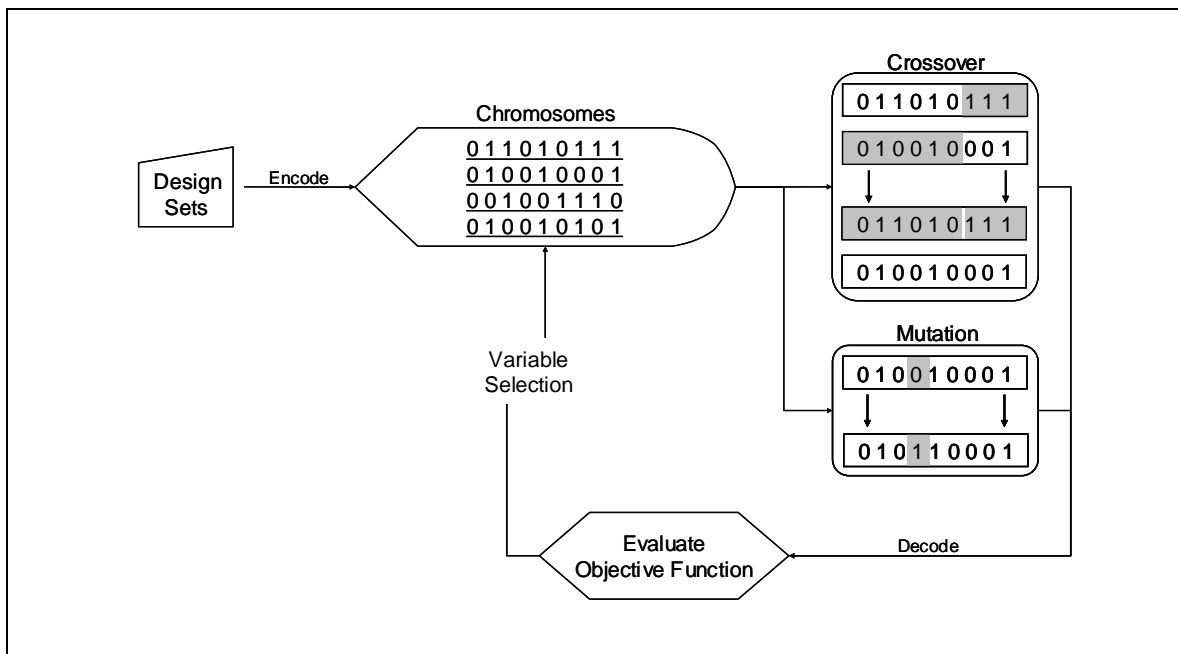


Figure 2-6 – Genetic Algorithm Flow Diagram using the Population Based Search.

The main disadvantage of genetic algorithms is they require numerous evaluations of the objective function (on the order of thousands) to find optima. This increases the cost of using the algorithms. Conversely, there are two main advantages. First, genetic algorithms have a higher potential than conventional algorithms of finding the global optima. By searching stochastically, genetic algorithms are less likely to get stuck in local minima. Second, genetic algorithms are easily coded, and because of that there are many free algorithms available.

## CHAPTER 3: THRUST OPTIMIZATION FRAMEWORK AND IMD

This chapter presents the optimization framework created to optimize solid rocket motor grains for a given thrust versus time profile. First, presented is the programming language used to build the interface between the solid rocket motor grain module and the optimization module. Next, the system used to model solid rocket motor grain geometries and surface recessions is presented. Note, this chapter only presents the program and what it does. Discussions of the workings of solid rocket motor grains and how they are modeled are presented Chapter 2. Finally, presented is the optimization interface system.

### 3-1 Adaptive Modeling Language

Adaptive Modeling Language (AML) developed by TechnoSoft Inc. was the programming language chosen to build the optimizer to grain model interface. Several specific features made this language conducive to this interface. These software features including a object-oriented environment, dependency-tracking demand-driven computations, and an ability to capture many applications into a unified model. Additionally, AML is already being used as the underlying architectural language for Interactive Missile Design (IMD) developed by Lockheed Martin, Missiles and Fire Control and TechnoSoft Inc.. IMD is a large scale industrial system that enables rapid design and analysis of conceptual and preliminary missile models.

This section describes the aforementioned features of AML and how they were used in the application of the research presented in this paper. Also, a brief introduction to IMD will be presented at the close of this section.

### 3-1-1 Object-Oriented Programming Language

Object-oriented programming languages (OOPL) offers a powerful model for designing complex computer software. In OOPLs, relations are established between classes and subclasses in a hierarchical order. Classes can be defined from existing classes or instantiated with independently defined properties. In the class hierarchy, classes can inherit properties from other classes or predefined objects in AML. An example showing the principles of OOPL is next.

For example, consider the class *table-class* created in AML. This class is graphically represented in Figure 3-1. Table-class has the fundamental properties of a table including a rectangular box surface with four cylindrical legs. These table components are generated through the use of five predefined subclasses; one box-object and four cylinder-objects. Figure 3-2 below represents the class hierarchy of table-class. Classes, subclasses, and property names are shown on the left, and values assigned to properties are shown on the right of the table. Parentheses indicate an object or property inheritance from the property or object labeled within the parentheses. Each subclass under table-class inherits from one of two predefined AML objects; box-object or cylinder-object.

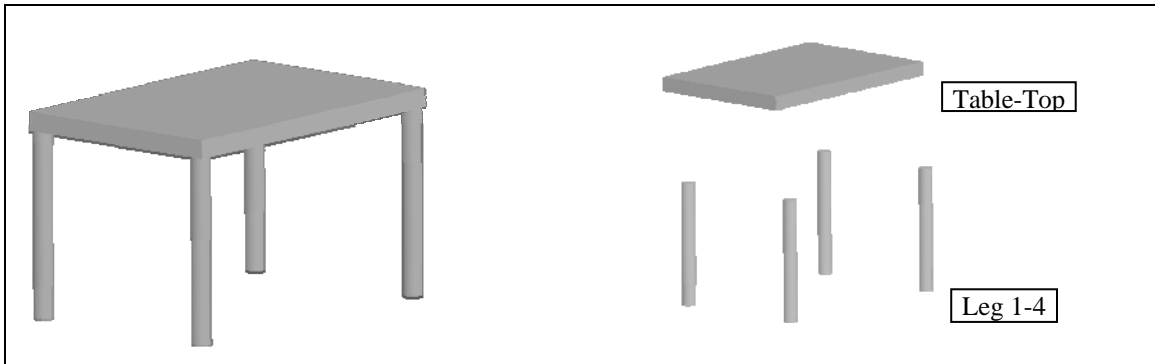


Figure 3-1 – Graphical representation of a Table-object.

Figure 3-2 – Class hierarchy of object-oriented programming language.

<b>Table-Class</b>		<b>Class</b>
<i>table-length</i>	9	Property
<i>table-width</i>	6	"
<i>table-depth</i>	0.5	"
<i>leg-height</i>	5	"
<i>leg-diameter</i>	0.5	"
<b>Table-Top</b>		<b>Subclass</b>
<i>Length</i>	<i>(table-length)</i>	Property
<i>Width</i>	<i>(table-width)</i>	"
<i>Depth</i>	<i>(table-depth)</i>	"
<i>Position</i>	<i>(0 0 0)</i>	"
<b>Leg-1</b>		<b>Subclass</b>
<i>Height</i>	<i>(leg-height)</i>	Property
<i>Diameter</i>	<i>(leg-diameter)</i>	"
<i>Position</i>	<i>F[(table-length, table-width, leg-diameter)]</i>	"
<b>Leg-2</b>		<b>Subclass</b>
<i>Height</i>	<i>(leg-height)</i>	Property
<i>Diameter</i>	<i>(leg-diameter)</i>	"
<i>Position</i>	<i>F[(table-length, table-width, leg-diameter)]</i>	"
<b>Leg-3</b>		<b>Subclass</b>
<i>Height</i>	<i>(leg-height)</i>	Property
<i>Diameter</i>	<i>(leg-diameter)</i>	"
<i>Position</i>	<i>F[(table-length, table-width, leg-diameter)]</i>	"
<b>Leg-4</b>		<b>Subclass</b>
<i>Height</i>	<i>(leg-height)</i>	Property
<i>Diameter</i>	<i>(leg-diameter)</i>	"
<i>Position</i>	<i>F[(table-length, table-width, leg-diameter)]</i>	"

When a class inherits from a predefined object, that class inherits the objects properties. Therefore, if a class inherits from box-object, that class will have properties that define the dimensions and position of a box.

This example demonstrated the advantages of inheritance. First, in regard to object inheritance, once an object or class is defined it does not have to be redefined. Notice a cylinder-object was used four times to create the table legs, but it only had to be created once. To carry this further, table-class could be inherited by another class to create a whole restaurant of tables. Second, in regard to property inheritance, property inheritance allows the dimensions of this table to be controlled by just five properties immediately under table-class. All the subclasses of table-class inherit from these properties to specify their dimensions and positions. By using property inheritance, the height of the table leg does not have to be specified four separate times and by doing so, the model becomes much more efficient. If this were an optimization example, property inheritance could be use to reduce the number of design variables and cause the optimization process to be more efficient.

### 3-1-2 Demand-Driven Dependency Tracking Language

Demand-driven dependency-tracking behavior, supported by AML, is an important feature for processing the complex internal ballistics and optimization algorithms presented in this paper. Demand-driven behavior refers to the fact that properties are only evaluated when the property value is demanded. This eliminates the need for unnecessary calculations and therefore, reduces the convergence time of optimization routines.

Dependency-tracking behavior keeps track of computational dependencies in order to increase computational speed. If a property was demanded and the model had changed such that the demanded property or dependencies of the demanded property had become invalid, those dependencies would be evaluated as necessary to insure the value of the demanded property is representative of the current model. For example, consider the thrust calculation of a solid rocket motor grain. Dependencies of the thrust calculation include the grains' geometry. If the grain geometry changes, the thrust property value automatically changes to *unbound* in AML signifying the model has changed in a way that invalidated the result of the thrust formula. When the value of that property is demanded, the surface recession of the solid propellant grain is simulated automatically as a dependency of the thrust calculation before the thrust property value is available.

Finally, Figure 3-3 presents a flow chart showing the demand-driven dependency track behavior of an optimization iteration performed on a solid propellant grain. First, the value of the objective function is demanded. Next, the dependencies of the objective function are demanded followed by their dependencies. Once all layers of dependencies have been evaluated the objective function is evaluated. In the figure below, arrows relay the chain of dependencies, and the data flow. The process is as follows.

First, the objective function is demanded and in turn, the objective function demands the values of its dependencies: Grain Thrust and Thrust Weighting Values. Grain Thrust has dependencies of its own and they are in turn demanded. Finally, data ripples back up the tree, the objective function is evaluated and returned to the demanding property. The point is, to evaluate the objective function only the objective

function had to be demanded. Beyond the objective function, AML evaluated the dependencies to ensure the value of the objective function is current. No special code had to be written to validate the dependencies of the objective function prior to its evaluation.

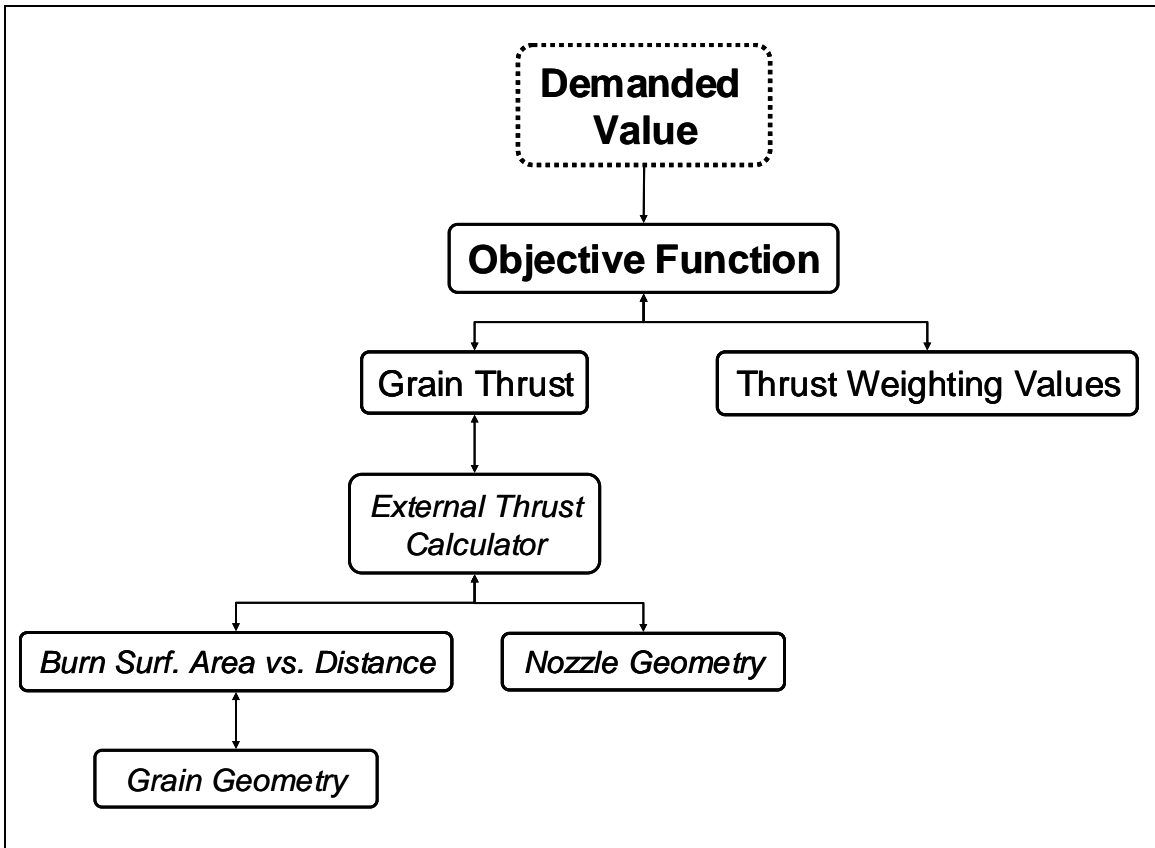


Figure 3-3 – Grain Optimization Demand-Driven Dependency-Tracking Iteration.

### 3-1-3 Solid Rocket Motor Design Module

The Solid Rocket Motor Design Module is an interactive solid rocket motor design tool that runs in an AML environment. Like most solid rocket motor modelers,

this module utilizes geometric primitives (blocks, cylinders, cones, spheres, etc.) to construct solid propellant grains. Through Boolean (union, intersect, and cut) and non-Boolean operations geometric primitives are formed into more complex geometries, and constructions of geometric primitives are joined to form single geometric entities, solid propellant grains.

Each geometric primitive used in grain construction has its own set of parametric controls, and through these controls the grain is made to grow normal to itself. The surface recession of the solid rocket motor grain is modeled graphically during evaluation, and is a dependency of the thrust calculation. Internal ballistic calculations on the grain produce *burn area versus distance* and *thrust versus time* results.

To aid the design of solid rocket motor grains, the Solid Rocket Motor Design Module has the ability to use optimization techniques to target the merit of *thrust versus time* or *burn-area versus distance*. Given a base design, once the user enters a *thrust versus time* or *web versus distance* requirement the design merit is evaluated against that requirement using a built-in merit function. It is also possible to weight a portion of the requirement profile in the merit function.

Next, the optimization interface that brings the power of optimization to the design of solid rocket motor grains is described.

### 3-2 Optimization Interface

The optimization algorithm to solid-propellant-grain-design tool interface was managed by a tool suite titled AMOPT developed by TechnoSoft Inc. Since this tool runs in an AML environment, it inherently takes advantage of the demand-driven

dependency-tracking environment discussed in section 3-1-2. This is an important feature for reducing computational time in optimization processes. AMOPT provided three important components of the thrust optimization framework; optimization algorithms, an interface to Design Optimization Tools (DOT) by Vanderplaats R&D, Inc., and a common user interface.

First, AMOPT contains a host of design optimization algorithms. These algorithms are based on several optimization methodologies including, design of experiments, and non-gradient based methods. The design of experiments method is an approximation method, and the rest are optimization methods. These methods do not require additional licensing, but for more complex problems and faster convergence rates, more complex algorithms are suggested.

Second, in addition to the included optimization algorithms AMOPT is able to link to the third-party Design Optimization Tools (DOT). DOT is a gradient-based numerical optimization package developed by Vanderplaats R&D, Inc. designed to solve a wide variety of non-linear optimization problems. Algorithms contained in DOT include first and second order gradient-based algorithms. These algorithms are designed to work on large scale problems with a large number of design variables. First and second order gradient-based optimization algorithms, by design, offer a faster rate of convergence than non-gradient based methods. [11]

Third, the user-interface through which optimization problems are defined plays an important role in the efficiency of the optimization process. If the process of setting up a problem consumes a significant amount of time or requires the user to know a cryptic syntax, it is unlikely the optimization capability would be used to its full potential.

AMOPT employs an efficient common user-interface that puts little burden on the user to define optimization problems. The interface is common between optimization algorithms. Therefore, the optimization model definition consisting of design variables, constraints, and objective function(s) only needs to be input once and any available optimization algorithms can be chosen to do the optimization.

Three tabs of the AMOPT user-interface are shown in Figure 3-4a-c below. The first tab (a) was used to define the optimization model. Exclusive sections are available for selecting AML properties to be used a design variables, constraints, and objective function(s). As stated in the previous paragraph, once these selections are made, they are fixed and can be used for several optimization algorithms. The next AMOPT tab (b) is used to select an optimization algorithm and specify control parameters specific to that algorithm; maximum number of iterations, derivative sensitivity, step size, etc. Finally, tab (c) is used to run the optimization process and view the optimization response. When the optimization process is run, design variable values are set and applied to the design. Next, the object function and constraint values (if specified) are demanded. Finally, these values are sent to the optimization algorithm, the current solution is compared to the exit criterion, and barring a criterion being satisfied, a new search direction is calculated and process starts again.

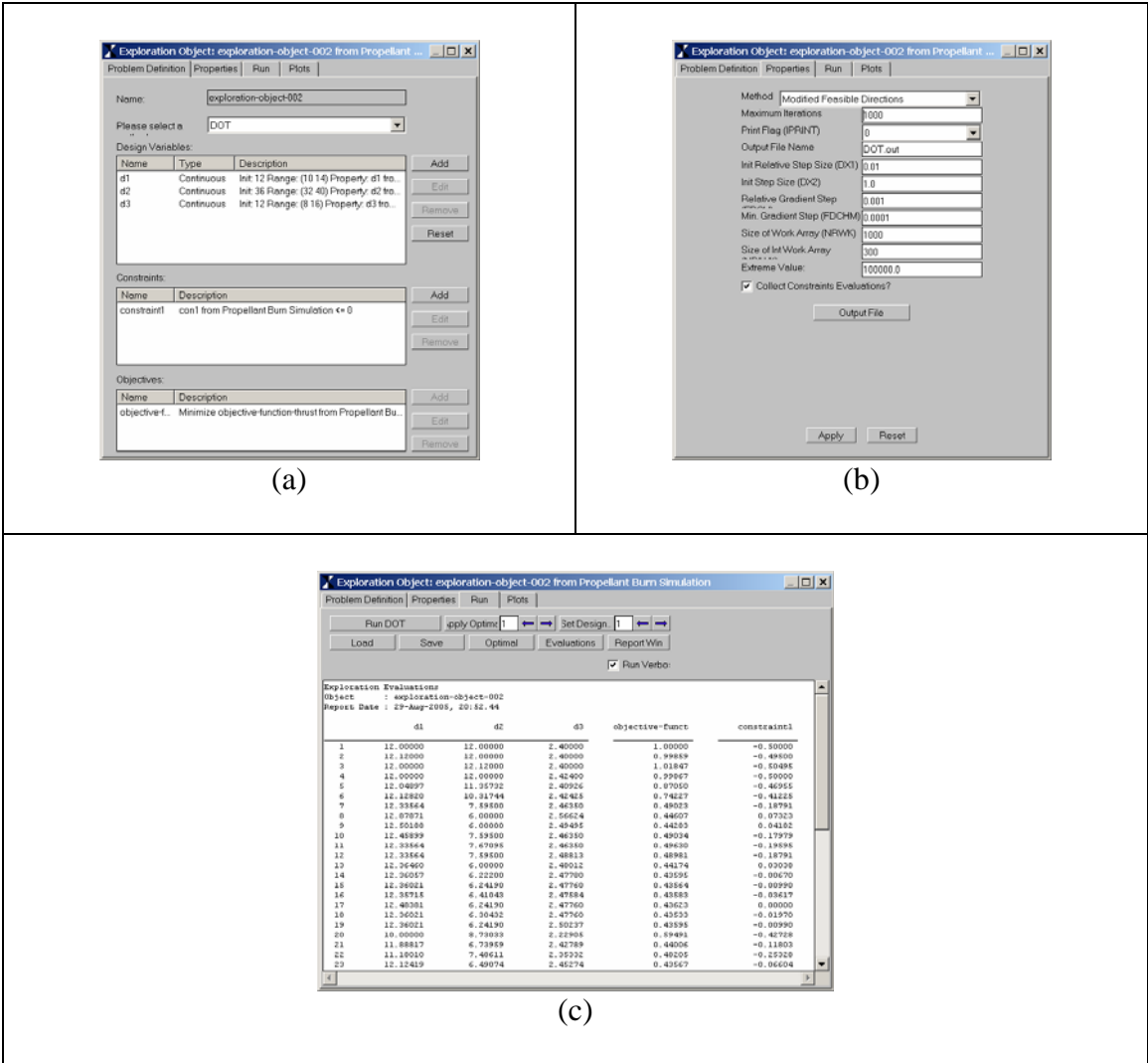


Figure 3-4 – AMOPT Tabbed User-Interface Windows

## CHAPTER 4: OPTIMIZATION PROBLEM STATEMENT

This section presents detailed discussion of the problem subject of this thesis. Also included in this section are subsections dedicated to the formulation of the problem. These subsections include topics of the objective function, design variables, and constraints.

### 4-1 Optimization Problem Statement

The problem posed by Lockheed Martin, Missiles and Fire Control was a constructive investigation into the application of optimization techniques to the design process of solid rocket motor grains within in IMD type environment. The large scale missile design software Interactive Missile Design (IMD) developed by Lockheed Martin is currently absent of any tools or methods designed to optimize solid rocket motor grains. To circumvent the quasi *hunt-and-peck* method utilized by propulsion engineers in solid rocket motor grain design, the objective of that proposed was to capture a process capable of optimizing the a solid rocket motor grain geometry for internal ballistic requirements (i.e. thrust versus time).

To test the optimization process developed, three different grains of varying complexity were used: a multi-cylinder-grain, a slotted-grain, and a complex-grain. These three grains are shown in Figure 4-1a-f. Each grain is shown in an isometric view and end view and are placed in order of increasing complexity. The wire-frame cylinder in these figures represents the volume of the combustion chamber, and the object

appearing solid in these figures represents the initial free volume and initial burn surface area.

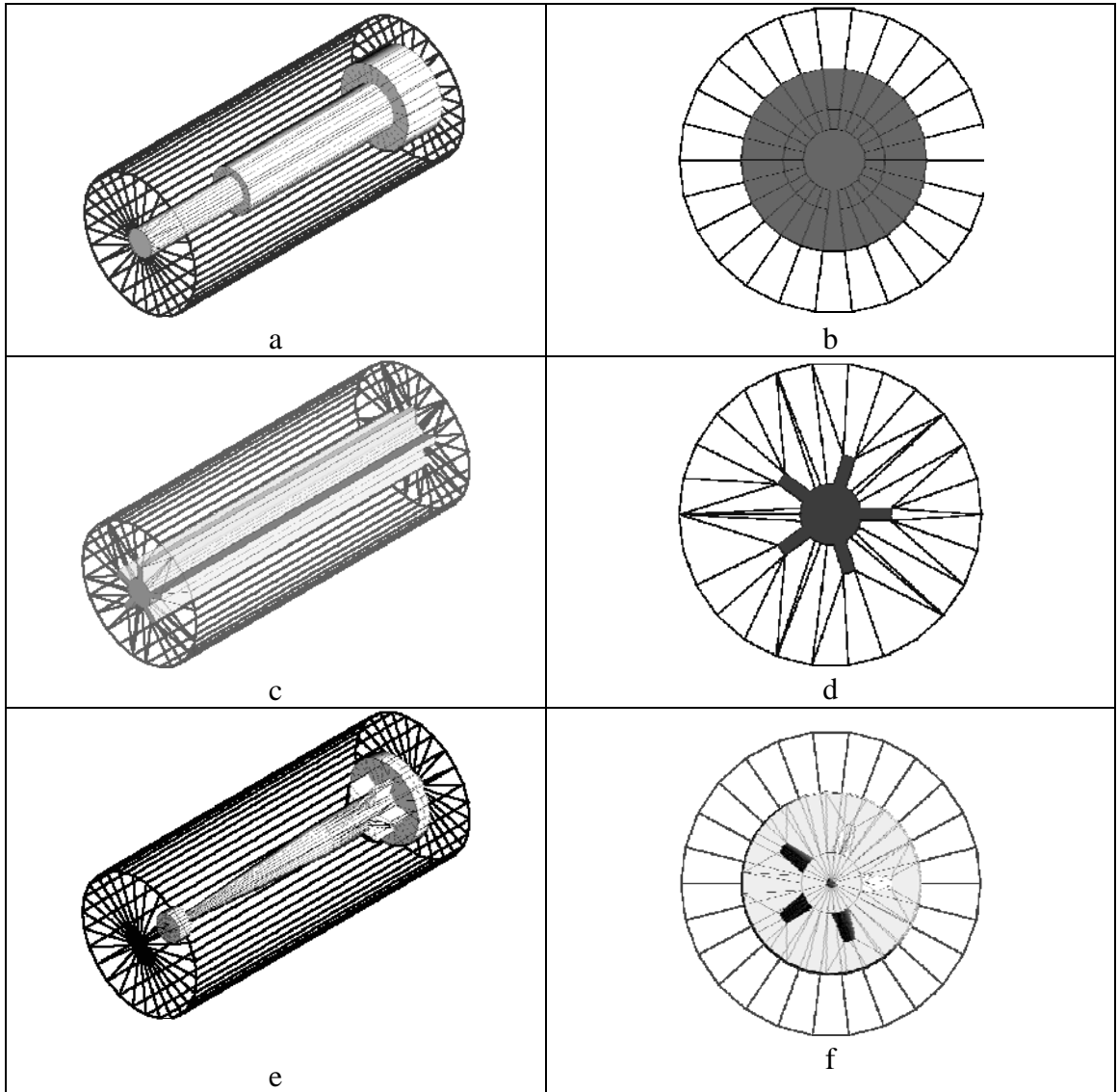


Figure 4-1 – Three solid propellant grains shown in isometric and front view diagrams. (a-b) Multi-Cylinder Grain, (c-d) Star Grain, (e-f) Complex Grain.

## 4-2 Design Variables

The objective of the optimization problem described in the previous section was to achieve a desired thrust product from a grain through the geometric manipulation of the grains geometry. Therefore, the design variables used in this problem were the geometric parameters that defined the respective grain geometries.

Different grains have a different number of design variables. Referencing Figure 4-1 on the previous page, the cylinder grain (a) has three defining geometric dimensions that are potential design variables. The star grain (b) has four additional potential design variables, and the complex grain (c) had more than eleven potential design variables. Figure 4-2 shows a dimensioned profile of the complex grain. However, not all dimensions that define a grains geometry have to be used as design variables.

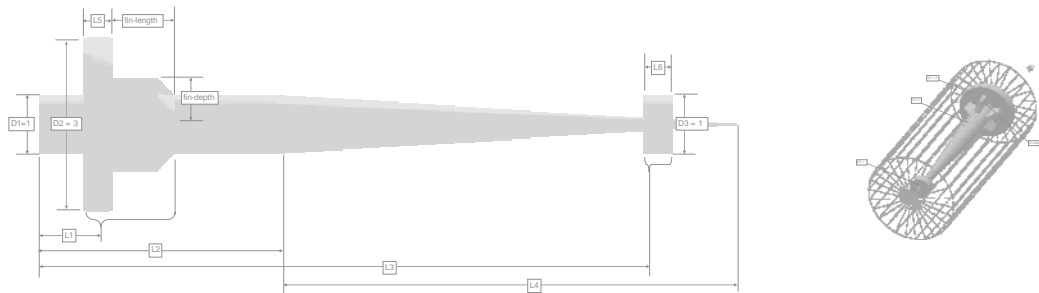


Figure 4-2 – Geometric dimensions of complex-grain.

Two types of design variables were utilized in this problem; continuous and discrete. All but one of the design variables were continuous. All of the continuous variables represented geometric dimensions. The single discrete design variables represented the quantity of slots/fins the slotted and complex grain.

### 4-3 Design Constraints

Two types of design constraints were used to bound the solid space of the thrust optimization problem. First, in every optimization run, side constraints played an important role in bounding the domain of the design variables. These side constraints helped to maintain a feasible grain design and reduced the amount of ill conditioning throughout the optimization process. For example, fins on the star and complex grains were prevented from becoming too thick or thin. Equation 4-1 formulates this example. In this example, the design variable  $X_i$  represents a the fin thickness of a grain and that thickness is only allowed to exist in a domain from 4 to 8 inches.

$$4'' \leq X_i \leq 8'' \qquad \text{Equation 4-1}$$

Second, inequality constraints,  $g_i(x)$ , were used to bound the values of grain properties. For example, a inequality constraint that could be used was the space factor constraint. The space factor constraint controlled the propellant volume to combustion chamber volume ratio formulated in Equation 4-2.

$$\frac{V_{Grain}(\bar{X})}{V_{Chamber}} - 1 \leq 0 \qquad \text{Equation 4-2}$$

0.6

Most of the time inequality/equality of constraints were not used, and once weighting of the objective function used instead. Ultimately, these constraints reduced the number of iterations required to find a feasible solution.

#### 4-4 Design Objective

The objective of this optimization research was to develop an optimization design tool and strategy for optimizing solid rocket motor grains for the internal ballistic of thrust. The development of this tool was structured such that it could optimize any geometrically parameterized grain regardless of configuration and complexity. Section 5-2-1 will provide detailed discussions on how the optimization problem was formulated to account for variations in grain configurations.

The optimization problem used by the optimization design tool was formulated as a minimization problem, and is summarized in Equation 4-3 below. This formulation minimizes the deviation between the thrust time curve of the grain being designed and the thrust-time requirement.

$$\begin{array}{ll} \text{Minimize} & F(\bar{X}) = DLS = \sum_{i=1}^n w_i (T^i(\bar{X}) - T_o^i)^2 \\ \text{w.r.t.} & X_i \quad i = 1 \dots n \\ \text{Such that :} & (\text{Lower Limit}) \leq \bar{X} \leq (\text{Upper Limit}) \\ & g_j(\bar{X}) \leq 0 \quad j = 1 \dots k \end{array} \quad \text{Equation 4-3}$$

The number of design variables, for solid propellant grains optimized in this paper, varied between three (for the slotted-grain) and eleven (for the complex-grain). More complex grains with more design variables could be optimized; however, more design variables causes the cost and time merits of the optimization process to increase. The objective function,  $F(\bar{X})$ , was based on the damped least squares method.

## CHAPTER 5: OPTIMIZATION FORMULATION AND STRATEGY

The process of applying design optimization to the design process of solid propellant grains involved the orchestration of several events. Beyond the construction of the initial solid propellant grain described in Chapter 2, the optimization strategy had to be planned and formulated. Presented in this chapter are the optimization strategy, formulation of the standard objective/merit function for grain optimization, and problems encountered during development of the optimization process.

### 5-1 The Internal Ballistic Optimization Strategy

This section discusses the *internal ballistic optimization strategy*, a strategy developed through research documented in this thesis to efficiently optimize solid rocket motor grain for internal ballistic requirements of thrust and burn-area versus web-distance. This optimization strategy was developed as a three stage process encompassing design approximation, global design optimization, and high-fidelity design optimization. This chapter presents, first, an overview of the ballistic optimization strategy followed by three sections containing detailed discussions on individual stages of the strategy.

#### 5-1-1 Internal Ballistic Optimization Strategy Overview

The *internal ballistic optimization strategy* was the label given to the optimization strategy for optimizing solid rocket motor grain designs for a given thrust-time or burn-

area-versus-distance requirement. This strategy involved a three stage process. Starting with a base grain geometry and a thrust-time requirement, the design was approximated. Next, using the optimum approximation from the first stage of the strategy, the design was optimized using a global design optimization technique. Finally, after the grain had converged to a quasi optimal design configuration, a high-fidelity optimization technique was employed to *fine tune* the design to meeting the requirement. A flow diagram in Figure 5-1 illustrates this optimization strategy, where each block in the diagram represents an important step in the optimization process, and arrows connecting the blocks indicate the grain design transitioning from one step to another.

Sections that follow discuss individual stages of the ballistic optimization strategy shown in blocks 3 – 5 in the figure below.

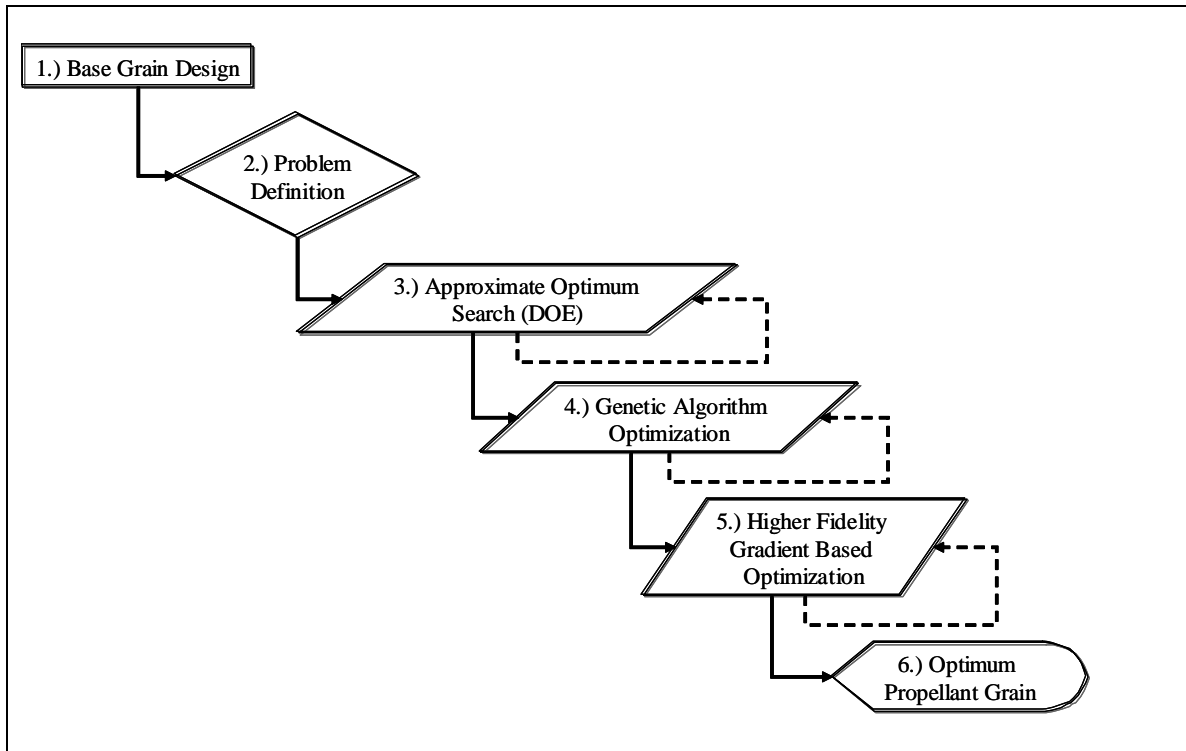


Figure 5-1 – Flow Diagram of the Internal Ballistic Optimization Strategy.

#### 5-1-2 Internal Ballistic Optimization Strategy Stage 1: Design Approximation

The first stage of the internal ballistic optimization strategy approximated the solid rocket motor grain design using a full-factorial design of experiments (DOE). DOE worked by sampling the objective function response (design merit) over the entire design space of a grain. The primary reason for choosing this experiment was the full factorial DOE samples the effect of design variables and interactions between all design variables.

Furthermore, the full factorial DOE was executed as a three-level design as the objective response was non-linear and ill-conditioned. A three-level full-factorial DOE experiment was choice as it produced the most comprehensive set of results. However,

for solid rocket motor grains with seven or more design variables, a three-level DOE produced a prohibitive number of experiments ( $> 2187$ ). To mitigate this problem, designs with large number of design variables were approximated using a subset of the most response sensitive variables, and then the full set of design variables were used in the following stages of the strategy. Further advantages of three-level DOEs are discussed in section 2-4-1 .

The AML optimization interface (AMOPT) used to execute DOEs and developed by TechnoSoft allowed the sequence of experiments in a full-factorial DOE to be altered and/or amended. This feature allowed DOEs to become especially powerful as several potential optima could be discovered at several values of discrete design variables.

Following DOE execution in the first stage of the internal ballistic optimization strategy, the best grain design approximation was selected and used as the base design for the second stage of the strategy, global design optimization.

### 5-1-3 Internal Ballistic Optimization Strategy Stage 2: Design Optimization

The second stage of the internal ballistic optimization strategy optimized the solid rocket motor grain design using a global optimization approach. Global optimization was applied through the use of a genetic algorithm. See section 0 for a discussion of genetic algorithms.

Genetic algorithms are effective at performing a global search. Other algorithms, such as hill-climbing algorithms, perform local searches using a “convergent stepwise procedure, which compares the values of nearby points and moves to the relative optimal points”. [13] This was an important feature due to the formulation of the ballistic

optimization problem. The damped least squares method utilized as the objective function and described in section 2-2, has a tendency to stagnate at local minima. Genetic algorithms successfully mitigate this situation through an evolutionary stochastic nature of searching for optima. Rather than climb into a pit, analogous to a local minimum, the evolutionary search method effectively utilizes the convexity of a problem to insure that any local optima is a global optima. [13] This was the primary reason for selecting this algorithm as the optimizer.

Table 5-1 – Parameter Settings for Genetic Algorithm.

<i>Population Size</i>
<i>Number of Generations</i>
<i>Noise Power</i>
<i>Extreme Value</i>

Before the optimization process could begin, however, four parameter settings of the genetic optimization algorithm were defined. These parameter settings are listed in Table 5-1 above and are discussed referencing genetic algorithms terminology outlined in section 2-5-3. First, the parameter labeled *Population Size* defined the numeric precision of the design variables by specifying the bit length of each chromosome. This value was calculated using Equation 5-1. Next, the parameter labeled *Number of Generations* represented the number of iterations though which each chromosome was allowed to mutate. [13] This value was chosen to be 50 percent of the *population size* insuring

enough iterations to utilize/vary all bits of the chromosomes. [13] Third, the parameter setting labeled *Noise Power* represented the design variable increment and was used to calculate the *Population Size* parameter. Lastly, the *Extreme Value* setting represented the largest expected objective function response value. If such response values increased beyond the *Extreme Value* setting, the optimization process would terminate.

$$2^{(Population\ Size)} \geq \sum_i \frac{X_i^U - X_i^L}{v_i^{incr}} + 1$$

Equation 5-1

where  $X_i^U \equiv$  The Upper Limit of Design Variable  $i$

$X_i^L \equiv$  The Lower Limit on Design Variable  $i$

$v_i^{incr} \equiv$  The *Noise Power*

The genetic algorithm was selected and executed through AMOPT. The genetic algorithm provided through AMOPT was developed by TechnoSoft Inc., also the developers of AML and AMOPT.

Following the global optimization execution, the solid rocket motor grain design should be fitness significantly improved from that of the approximated design (the base design of this stage of the optimization strategy). The thrust-time product of the grain should resemble the requirement; however, the thrust-time product may still depart from the requirement in several key areas at this point. Therefore, following the execution of the second stage of the ballistic optimization strategy, the optimum grain design was

selected and used as the base design to the third and final stage of the strategy, high-fidelity optimization.

#### 5-1-4 Internal Ballistic Optimization Strategy Stage 3: High-Fidelity Optimization

The third and final stage of the internal ballistic optimization strategy used high-fidelity optimization techniques to *fine tune* the solid rocket motor grain design to satisfy the thrust-time requirement. Experimental data indicated the thrust response of the optimized grain design from the previous stage would track with the requirement, however, the *total impulse* (area under the thrust-time curve) of the grain may still deviate from the requirement. Two reasons this deviation could still exist at this point were (1) the global optimization from the previous stage had converged to a local optimum (rather than the global optimum) or (2) the objective function had stagnated due to a decrease in response sensitivity to changes in the design variables.

High-fidelity optimization used the Broyden, Fletcher, Goldfarb, and Shanno (BFGS) first-order gradient based algorithm to optimize the solid rocket motor grain from the second stage of the internal ballistic optimization strategy. This algorithm discussed in section 2-5-1 used gradient information from the objective function at the current design point to calculate the optimum search direction. This was a *hill climbing* algorithm that operated unlike the genetic algorithm from the second stage; thus, it was expected to overcome weaknesses and stagnation points of the second stage of the optimization strategy. This was the primary reason for selecting it.

Table 5-2 – Parameter Settings for BFGS Algorithm.

<i>Initial Relative Step Size (DX1)</i>
<i>Initial Step Size (DX2)</i>
<i>Relative Gradient Step (FDCH)</i>
<i>Min. Gradient Step (FDCHM)</i>
<i>Extreme Value</i>

The BFGS algorithm was part of an optimization algorithm suite contained within Design Optimization Tools 5.0 (DOT) developed and supported by Vanderplaats Research and Development, Inc. This algorithm required the following five parameters settings shown in Table 5-2 to be defined. First, the parameter setting labeled *Initial Relative Step Size (DX1)* defined the maximum relative change in the design variable attempted on the first optimization iteration. Next, the parameter labeled *Initial Step Size (DX2)* represented the maximum absolute change in a design variable attempted on the first optimization iteration. These two parameters were used to estimate the initial move in a one-dimensional search and were updated as the optimization progressed. Third, the *Relative Gradient Step (FDCH)* parameter represented the relative finite difference step used when calculating gradients, and forth, the parameter labeled *Min. Gradient Step (FDCHM)* represented the minimum absolute value of the finite difference step when calculating gradients. This prevented the step size from becoming too small. Finally, the parameter labeled *Extreme Value* represented an upper limit value to the response value. [14] If response values occur higher than the specified parameter, the optimization process will terminate. These parameters were all set within AMOPT.

In addition to using a gradient based optimization algorithm in this stage, the weights were applied to the objective function to increase the response sensitivity. Up until this point, weights had not been applied to the objective function as doing so would have been premature. Now that the grain had been optimized in the second stage of the internal ballistic optimization strategy the thrust-time response should approach the thrust-time requirement at several data points, but at other points the thrust-time response may still deviate from the requirement. Whenever a thrust-time data point becomes satisfied its contribution to the objective function becomes zero, thus reducing the response sensitivity. Upon inspection of the thrust-time response in relation to the thrust-time requirement, the objective function should be weighted at points corresponding to a significant deviation from the requirement. This increased the response sensitivity at critical points, which decreased the chance of premature optimization process termination.

Finally, following completion of high-fidelity optimization the grain should satisfy the requirement. Advantages of this stage include a fast convergence rate to optima thanks to the high-fidelity gradient based algorithm, and a chance to weight the objective function. Disadvantages of this stage include a higher probability of premature termination of optimization using the BFGS algorithm.

## 5-2 Optimization Formulation

Two methodologies were used to formulate the solid rocket motor design optimization model. The first methodology based formulation on a reference thrust-time curve, and the second methodology based formulation on a reference burn-area versus

web-distance curve. The first methodology optimizes solid propellant grains for thrust versus time; where as, the second methodology optimizes solid propellant grains for burn-area versus web-distance. The next two subsections discuss formulation of the solid rocket motor optimization model for thrust and burn-area ballistics.

### 5-2-1 Thrust Optimization Formulation

The figure of merit for solid rocket motor grain optimization on the basis of thrust was measured by the deviation of a grains' thrust-time curve from the requirement, respectively. To efficiently compare the thrust time curve of a grain design with a reference curve, the damped least squares (DLS) method was employed. This method, summarized in Equation 5-2, was defined as a sum of differences between  $n$  selected points on the grains' thrust time curve  $T^i(\bar{X})$  and the given data points  $T_o^i$ . Finally, this difference was multiplied by a weighting factor  $w_i$ .

$$F(\bar{X}) = \sum_{i=1}^n w_i (T^i(\bar{X}) - T_o^i)^2 \quad \text{Equation 5-2}$$

Three major advantages of the DLS method prompted its use in the optimization formulation. First, this formulation was adaptable enough to accommodate variations in thrust optimization problem definitions. Optimization processes developed in this paper were independent of grain configuration. Furthermore, different grain configurations have different thrust time requirements, and thus, slightly different problem definitions. Second, thrust, for all practical purposes, is an implicit function of the design variables,

and the DLS method allows for expressing the merit of a solid rocket motor grain as a function of the design variables. Finally, the DLS method has been used in countless design optimization tools and has proven its functionality. [4]

### 5-2-2 Burn-Area Optimization

Optimization on the ballistic merit of burn-area versus web-distance was a simplification of optimization on the merit of thrust time. Burn-area was a dependent of thrust, and therefore, by optimizing directly on the merit of burn-area, the overhead associated with thrust calculations were eliminated. This methodology is used for preliminary and conceptual designs.

The figure of merit for burn-area optimization problems was measured by the deviation of a grains' burn-area versus web-distance curve from the required curve. This deviation was compared using the DLS method, the same way it was compared for thrust optimization. The formulation of burn-area optimization is summarized in Equation 5-3 using the DLS method where the grains' burn-area versus web-distance curve is represented by  $B^i(\bar{X})$  and the required data points,  $B_o^i$ . Finally, this difference was multiplied by a weighting factor  $w_i$ .

$$F(\bar{X}) = \sum_{i=1}^n w_i (B^i(\bar{X}) - B_o^i)^2 \quad \text{Equation 5-3}$$

### 5-3 Resolved Issues with the Optimization Strategy

During implementation of the optimization strategy described above several major issues were encountered that threatened the success of the optimization strategy. This section describes the major issues experienced along with their resolutions.

#### 5-3-1 Issue 1: Error in Surface Recession Model

During early optimization processes of the center perforated star and complex grains, shown first in Figure 1-1 on page 2, the objective versus iteration response indicated unusually high convergence rates to optima. Upon inspection of several optimum grain designs, it was discovered the corresponding surface recession models were terminating early thus resulting in shortened internal ballistic responses. The cause of the early termination was determined to be inherent to how the burn-surface-area of the grain was interpreted by AML when the corners of the grains' fins began intersecting themselves. However, just because the surface recession of the grain model terminated early was no reason for the objective function to evaluate to a minimum. In fact the opposite should have occurred.

The issue was resolved by reformulating the objective function to penalize itself if the grain surface recession terminates early or late with respect to the requirement. This was formulated as a progressive penalty such that the earlier (or later) grain surface recession terminates the more penalty is added to the objective function.

### 5-3-2 Issue 2: Unexpected Halting of High Fidelity Optimization

The second unexpected issue encountered in the optimization process of solid rocket motor grains was unexpected halting of the high-fidelity gradient-based optimization. This would occur when optimization was attempted in the third stage of the *internal ballistic optimization strategy*. The optimization process would be started but after two to four iterations, the process would terminate.

The cause of this early termination of the optimization process was determined to be a result of reduced sensitivity in the objective function. Following the completion of stage two of the internal ballistic optimization process (global optimization) many data-points along the thrust-time curve were satisfied or near satisfied. This made the contribution to the objective function for those respective data-points zero or near zero. To mitigate this reduction in objective function sensitivity, weights were applied to data-points which deviated by more than 10% from the requirement, respectively. Weights that were applied were on the order of 5 to 10X. Following the application of weights and renormalization of the objective function, the high-fidelity gradient-based optimization process would optimize the grain without early termination.

## CHAPTER 6: OPTIMIZATION ANALYSIS

A strategy labeled the *internal ballistic optimization strategy* was developed as a plan for designing solid rocket motor grains to satisfy ballistic requirements using optimization tools. This chapter describes the optimization methodologies, the optimization formulations, and the design results of this strategy as it was applied to the design of three different solid rocket motor grains; the multi-cylinder grain, the star grain, and the complex grain.

The strategy for optimizing each solid rocket motor grain is discussed in separate sections described as optimization trials #1 through #3. Within each trial an overview of each grain and design optimization goal is presented followed by discussion of the optimization model definitions, respectively. Next, the optimization methodologies and results are discussed in subsections dedicated to each stage of the optimization strategy as applied to each grain. This chapter ends with a discussion of other optimization strategies and formulations that were considered.

### 6-1 Internal Ballistic Optimization Strategy Trial #1

The first trial of the *internal ballistic optimization strategy* involved the optimization of a multi-cylinder solid rocket motor grain for a thrust-time internal ballistic requirement. The goal of this trial was to optimize a center perforated multi-cylinder-grain geometry per a thrust-time requirement generated by a multi-cylinder grain

of different geometric configuration. This created an optimization design experiment with a known solution.

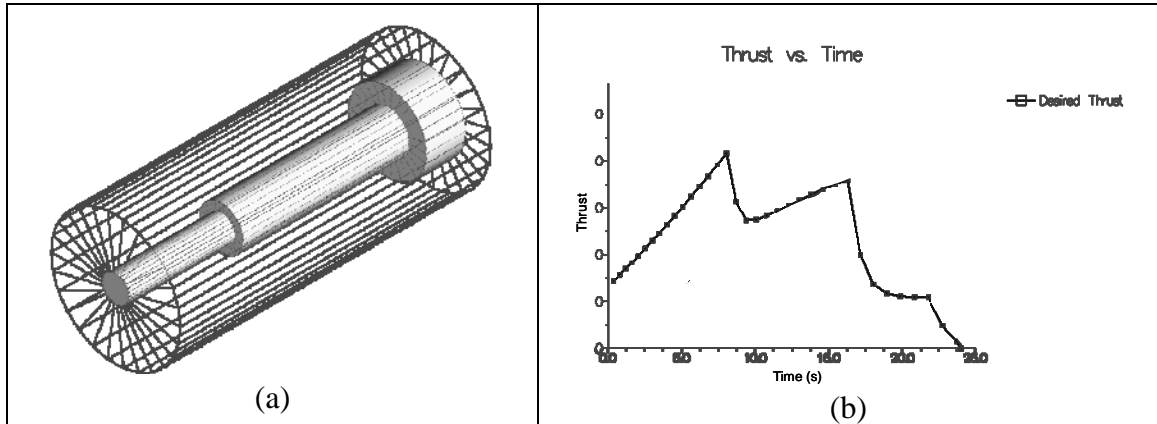


Figure 6-1 – (a) Multi-Cylinder Grain Design Solution and (b) Thrust-Time Requirement generated by this grain design.

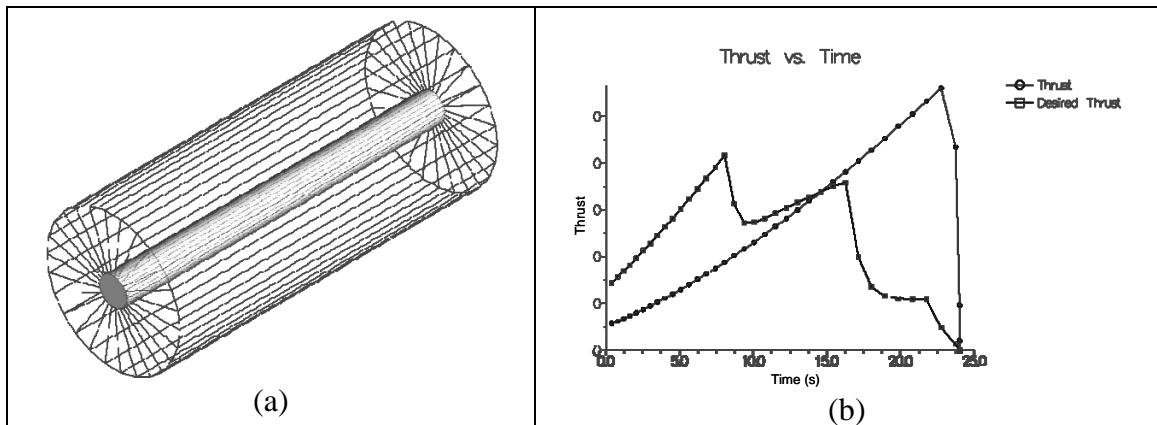


Figure 6-2 – (a) Initial Multi-Cylinder Grain Design and (b) corresponding Thrust-Time Product.

The thrust requirement for this optimization trial was generated from the multi-cylinder grain model shown in Figure 6-1a. Figure 6-1b shows a corresponding plot of this thrust-time requirement.

Next, five geometric parameters defining the grain geometry were changed resulting in the altered multi-cylinder grain geometry shown in Figure 6-2a. Each of the three cylinders composing this grain design had congruent diameters and lengths essentially transforming the grain into a simple center perforated grain. Furthermore, resulting from the change in grain geometry, the thrust-time product became significantly different when compared to the requirement, see Figure 6-2b.

With a different thrust-time product the design challenge had been created; optimize the multi-cylinder grain geometry shown in Figure 6-2a to produce a thrust-time product that satisfies the requirement. The next four subsections discuss the optimization problem definition, the optimization methodology and the design results at each of the three stages of the optimization process: approximation, optimization, and high-fidelity optimization.

#### 6-1-1 Optimization Model Definition

This section discusses the multi-cylinder solid rocket motor grain design optimization model definition for ballistic optimization strategy trial #1. The optimization problem definitions outlined in this and the next two trials were setup using the three step process described in section 2-1 titled Principles of Optimization.

First, design variables were selected to represent the center perforated multi-cylinder grain geometry. The real grain model in AML consisted of three AML cylinder objects, and the grain geometry was controlled by five dimensions. Figure 6-3 represents a cross-sectional view of the multi-cylinder grain with controlling dimensions labeled. Assuming all other controlling dimensions/orientations/positions were constant

(including the nozzle dimensions), these five dimensions were chosen as the continuous design variables.

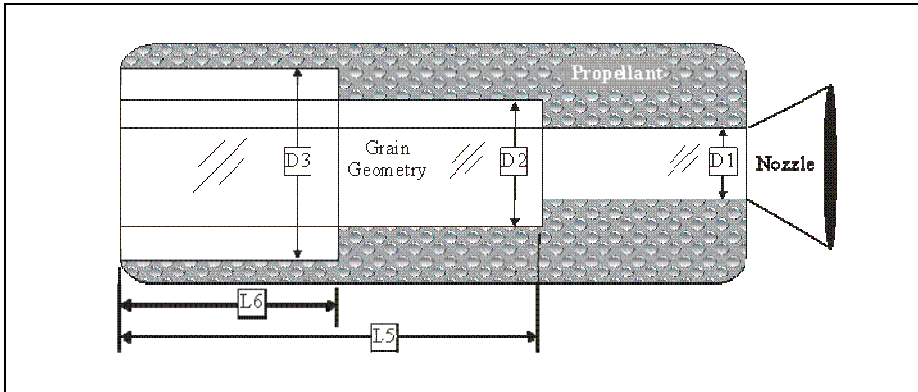


Figure 6-3 – Dimensioned cross-section of the multi-cylinder grain.

To eliminate wide variations in the magnitudes of the design variables each variable was normalized [1] with respect to the combustion chamber dimensions (the object containing the propellant in Figure 6-3). For example, if a design variable varied by diameter, it was normalized to the combustion chamber diameter, and likewise, if a design variable varied by length it was normalized to the combustion chamber length. This operation converted the design variables to ratios existing between zero and one. Table 6-1 lists these variables along with descriptive remarks, initial values, and upper and lower bounds (UB and LB).

Table 6-1 – Initial design variable configuration for multi-cylinder grain.

Variable Name	Variable Description	Initial Value	LB	UB
<i>DV-D1</i>	<i>Diameter of Cylinder 1</i>	0.20	0.15	0.90
<i>DV-D2</i>	<i>Diameter of Cylinder 2</i>	0.33	0.15	0.90
<i>DV-D3</i>	<i>Diameter of Cylinder 3</i>	0.60	0.15	0.90
<i>DV-L5</i>	<i>Length of Cylinder 2</i>	0.66	0.50	0.90
<i>DV-L6</i>	<i>Length of Cylinder 3</i>	0.33	0.1	0.45

Second, the design constraints were formulated. Initially, side constraints were imposed on all design variables to restrict the domain to which they existed, see the upper (UB) and lower (LB) bounds listed in Table 6-1. Next, two inequality constraints, see Equation 6-1 and Equation 6-2, were formulated to maintain the hierarchy of cylinder diameters in the grain (Prefixes of the design variable names (*DV-*) are omitted in these equations). Referencing the constraint descriptions in Table 6-2 on the next page, all of these constraints were satisfied and *active* in the initial design; an *active* constraint is one whose value resides on a constraint boundary.

$$\text{Constraint 1} \quad \frac{D1 - D2}{D1} \leq 0 \quad \text{Equation 6-1}$$

$$\text{Constraint 2} \quad \frac{D2 - D3}{D2} \leq 0 \quad \text{Equation 6-2}$$

Table 6-2 -- Constraint values of initial design configuration.

Constraint	Variable Description	Initial Value	Condition	
1	<i>Diameter of Cylinder 2</i>	0.00	$\leq$	0.00
2	<i>Diameter of Cylinder 3</i>	0.00	$\leq$	0.00

Third, the objective function was formulated. The objective function was formulated using the damped least squares formulation discussed in section 4-4. Dependencies of this formulation were the data-points from the thrust-time requirement and data-points from the thrust-time product of the grain design.

Additionally, the objective function was formulation was scripted in AML to take advantage of the languages demand-driven dependency-tracking features. Upon evaluating the objective function, the objective function would automatically fetch data-points from the thrust-time requirement and execute a surface recession simulation of the grain to generate the thrust-time product of the grain. This created a seamless operation conducive to an iterative optimization environment.

Lastly, the objective function was normalized to itself. This created an initial design merit value of 1.0 (one); designs with higher merit have values approaching zero. This operation was performed ahead of each stage of the optimization process.

This optimization model definition was used throughout the entire ballistic optimization strategy. The next three sub-sections describe the three stages of the

internal ballistic optimization process: design approximation, design optimization, and high-fidelity optimization.

#### 6-1-2 Internal Ballistic Optimization Strategy Stage 1: Design Approximation

The first stage of the internal ballistic optimization strategy, outlined in section 5-1-2, centered on approximating the multi-cylinder solid rocket motor grain design using design of experiments (DOE). This approximation technique provided an inexpensive vehicle for characterizing the design space of the grain. The goal of this stage was to approximate the grain design driven by a thrust-time requirement and identify a grain design approximation(s) that best satisfied that requirement with the intent of optimizing that design(s) in the second stage of the strategy.

The multi-cylinder grain design was approximated using full-factorial level-three DOE. This DOE was executed as a three-level design as the response was known to be nonlinear. Additionally, the thrust-time response between variations in the grain geometry proved to be highly ill-conditioned over anything but a finite change in grain geometry. Therefore, the comprehensive full-factorial DOE methodology was chosen as the most efficient approximation technique as it measures the response of every possible combination of design variables for the level of design chosen. With five design variables representing the grain geometry, the full-factorial three level DOE consisted of 243 experiments.

The multi-cylinder grain design approximation results are plotted in Figure A-1 under Appendix A-2 and listed in Table A-1 under Appendix A-3. The aforementioned plot represents the results in two series; The *Raw DOE Response* series

represented the responses from all 243 experiments, and the *Sorted Feasible DOE Response* series represented only the feasible responses (designs satisfying all constraints) sorted in order of increasing design merit. Only one third of all the responses satisfied all of the constraints. Results plotted in the former series indicated only one appreciable local minimum. This was confirmed by the results plotted in the later series as among the designs of highest merit (lowest objective function value), no significant differences were observed between the designs.

Table 6-3 – Design variable values for approximated Multi-Cylinder grain design.

Variable Name	Variable Description	Value
<i>DV-D1</i>	<i>Diameter of Cylinder 1</i>	0.15
<i>DV-D2</i>	<i>Diameter of Cylinder 2</i>	0.525
<i>DV-D3</i>	<i>Diameter of Cylinder 3</i>	0.9
<i>DV-L5</i>	<i>Length of Cylinder 2</i>	0.5
<i>DV-L6</i>	<i>Length of Cylinder 3</i>	0.1

Finally, the best approximated multi-cylinder grain design was loaded into AML and validated to be free of defect. The merit value of this design was 0.31 which marked a 69 percent design improvement relative to the base design. Table 6-3 lists the design variable values for the best approximated grain, and Figure 6-4 shows a model of the best approximated multi-cylinder solid rocket motor grain design and a plot of its thrust-time product plotted against the thrust-time requirement and the thrust-time product of the

base grain. This plot clearly shows a significant design improvement with respect to the requirement.

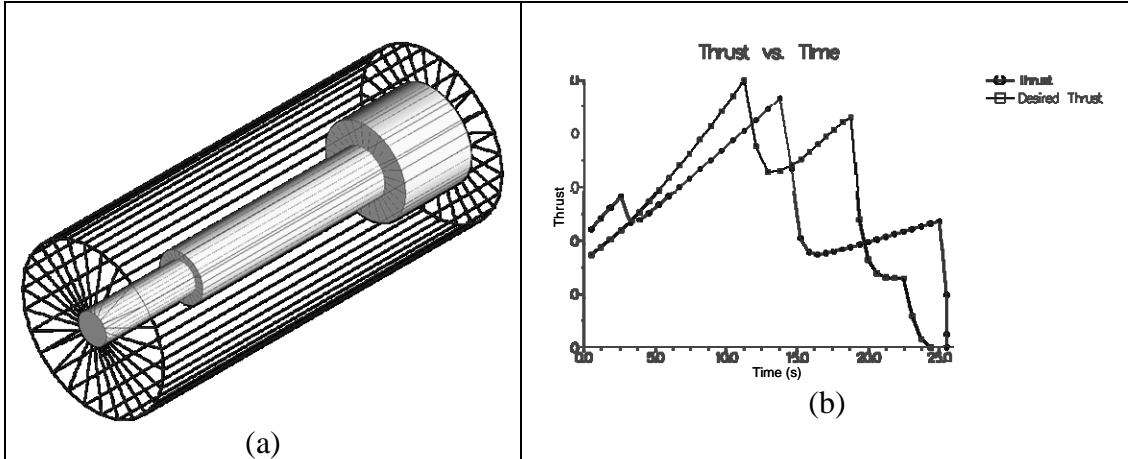


Figure 6-4 – (a) Approximated Multi-Cylinder grain model and (b) Thrust-Time Product.

### 6-1-3 Internal Ballistic Optimization Strategy Stage 2: Design Optimization

The second stage of the internal ballistic optimization strategy, discussed in section 5-1-3, centered on the optimization of the multi-cylinder solid rocket motor grain design. The goal of this stage was to optimize the best approximated multi-cylinder grain design (shown in Figure 6-4) per the stated thrust-time requirement. This strategy employed a global optimization routine using the genetic optimization algorithm from the AMOPT optimization interface developed by TechnoSoft; genetic algorithms are discussed in section 2-5-3.

First, the approximated multi-cylinder grain design (from the first stage of the strategy) was prepared for optimization. The AML optimization interface AMOPT provided an elegant widget for performing this operation. While still in the approximation mode of AMOPT, the DOE experiment producing the best feasible

response was selected and set as the concurrent working design. Next, the objective function was renormalized to a unit value of one. At this point, the grain model and optimization model definition was setup for optimization, however parameter settings of the optimization algorithm remained undefined.

Table 6-4 – Parameter Setting Definitions for the Genetic Algorithm used in Trial #1.

<i>Population Size</i>	50
<i>Number of Generations</i>	25
<i>Noise Power</i>	0.001
<i>Extreme Value</i>	4

Next, four parameter settings of the genetic algorithm were defined. These parameter settings are listed in Table 6-4 above and what these parameters represent are discussed in section 5-1-3. The first parameter, *Population Size*, was calculated using Equation 5-1 and the design variable information in Table 6-1. The next parameter, *Number of Generations*, was chosen to be 50 percent of the *population size*. [13] The product of these two parameters defined the maximum number of optimization iterations. The third setting, *Noise Power*, represented the design variable increment. Lastly, the *Extreme Value* setting represented the largest expected objective function response value. If such response values increased beyond the *Extreme Value* setting, the optimization process would terminate.

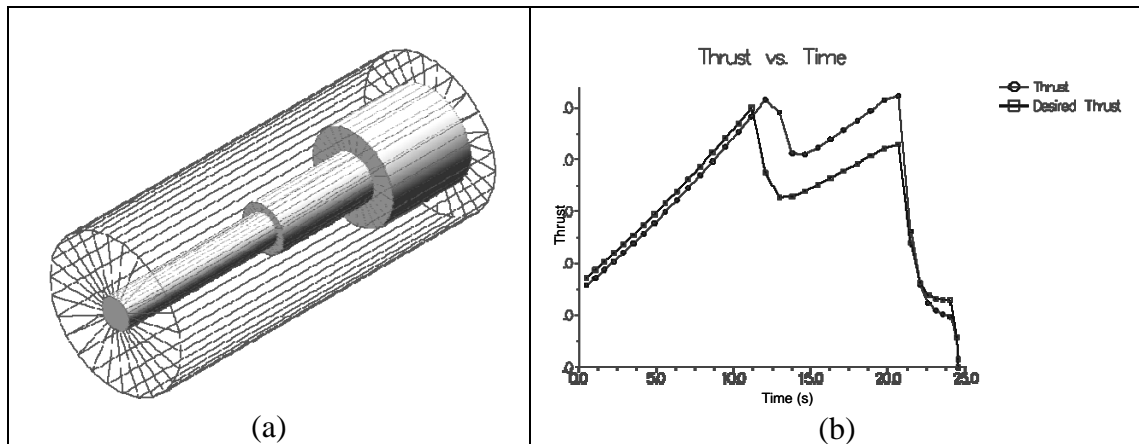


Figure 6-5 – (a) Optimized Multi-Cylinder Grain Model and (b) Thrust-Time Product.

Once the optimization model and optimization algorithm were setup, the optimization process was initiated. The optimization process ran successfully without premature termination. A plot of the multi-cylinder grain optimization response is shown in Figure B-1 under Appendix B-2 and Table B-1 under Appendix B-3 lists every tenth response of the total 1250 responses. Design improvement per iteration occurred rapidly in the beginning of the optimization process improving the design merit by approximately 90 percent.

The optimized multi-cylinder grain model and corresponding thrust-time product are shown above in Figure 6-5. This plot indicated the thrust-time product of the optimum grain design was in phase with the requirement and followed a similar trend; a significant improvement from the approximated grain design. However, the total impulse (area under the thrust-time curve) of the optimum grain still deviated from that of the requirement. This departure will be dealt with in the third stage of the internal ballistic optimization strategy.

Accomplishments from this stage of the internal ballistic optimization strategy included a multi-cylinder grain design with a design merit improvement of 99 percent, and combining this improvement with the improvement from stage one of the strategy yielded an design improvement of 98 percent.

#### 6-1-4 Internal Ballistic Optimization Strategy Stage 3: High-Fidelity Optimization

The third, and final stage of the internal ballistic optimization strategy, discussed in section 5-1-4, centered on high-fidelity optimization of the multi-cylinder grain design. At this point the previous two stages of the ballistic optimization strategy had approximated/optimized the multi-cylinder grain design to have a thrust-time product with a merit 98 percent higher than the base design; however, this thrust-time product still departed from the requirement in several critical areas. Therefore, the goal of this final stage of the ballistic optimization strategy was to optimize the multi-cylinder grain design per the stated thrust-time requirement to have an overall merit 90 percent better than the base grain using the high-fidelity BFGS gradient-based optimization algorithm. This algorithm is discussed in section 2-5-1.

The high-fidelity optimization process started with the optimized grain design produced from the second stage of the strategy described in the previous section; Figure 6-5 shows the grain model and thrust-time characteristic of the grain at this stage. Next, key features of the high-fidelity optimization process will be described.

First, the optimized multi-cylinder grain design (from the second stage of the internal ballistic optimization strategy) was prepared for high-fidelity optimization. Within the AML optimization interface AMOPT, the optimization iteration producing the

optimum design was selected and set as the concurrent design. Next, the objective function was renormalized to a unit value of one. At this point, the model and high-fidelity optimization problem definition was setup, however parameter settings of the optimization algorithm remained unset.

Table 6-5 – Parameter Setting Definitions for the BFGS Algorithm used in Trial #1.

<i>Initial Relative Step Size (DX1)</i>	0.01
<i>Initial Step Size (DX2)</i>	1
<i>Relative Gradient Step (FDCH)</i>	0.001
<i>Min. Gradient Step (FDCHM)</i>	0.0001
<i>Extreme Value</i>	50

Next, five DOT parameter settings were defined to control the BFGS algorithm. These parameter settings are listed in Table 6-5 and what these parameters represent are discussed in section 5-1-4. All of these parameter definitions were left at their default values except for the *Extreme Value* parameter. This parameter was increased to the value shown above to avoid premature termination of the optimization process when finite differences was used to recalculate the gradient of the objective function. When these occurred at several times during the optimization process the response was higher than normal.

After settings to the optimization algorithm were defined, the objective function was weighted in areas corresponding to the thrust response of the multi-cylinder grain having greater than ten percent departure from the requirement (see Figure 6-5b above).

This increased the response sensitivity in these areas. The objective function was weighed 5x on areas of the thrust-time curve that deviated from the requirement by more than ten percent. By using weights to increase the objective function sensitivity in areas of needed improvement the probability of premature termination of the optimization process was mitigated.

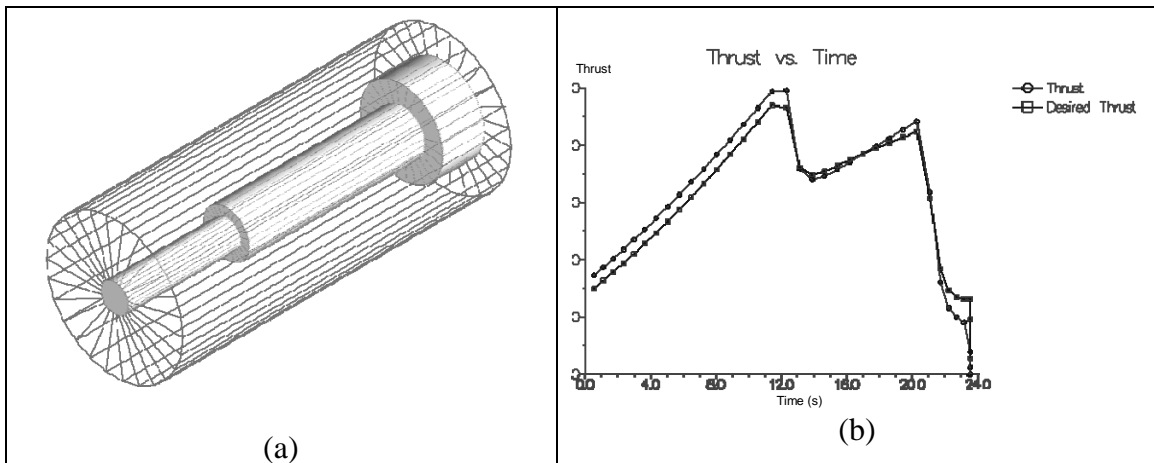


Figure 6-6 – (a) Optimized Multi-Cylinder Grain Model and (b) Thrust-Time Product.

The high-fidelity optimization was carried out in AML through the AMOPT interface using the BFGS algorithm. The high-fidelity optimization process converged to a solution quickly generating a multi-cylinder solid rocket grain design with a merit improvement of 92 percent over the grain design produced from the second stage of the ballistic optimization strategy. The optimized multi-cylinder grain model and a plot of the corresponding thrust-time product are shown in Figure 6-6. This plot indicates high correlation between the thrust-time product of the grain design and thrust-time requirement.

Table 6-6 – Multi-cylinder grain design variable values for optimum versus solution.

Variable Name	Variable Description	Optimum Design	Design Solution
<i>DV-D1</i>	<i>Diameter of Cylinder 1</i>	0.23	0.20
<i>DV-D2</i>	<i>Diameter of Cylinder 2</i>	0.31	0.33
<i>DV-D3</i>	<i>Diameter of Cylinder 3</i>	0.6	0.6
<i>DV-L5</i>	<i>Length of Cylinder 2</i>	0.53	0.66
<i>DV-L6</i>	<i>Length of Cylinder 3</i>	0.25	0.25

In summary, accomplishments from this stage of the optimization strategy include a multi-cylinder solid rocket motor grain design that satisfies the thrust-time requirement imposed on the grain. The high-fidelity optimization increased the design merit of the grain by 92%, and combining this improvement in design merit with that from previous two stages of the internal ballistic optimization process yielded a design merit improvement of 99.98%. Additionally, since there was a known solution to this design project, comparisons were made between the final optimum grain design and the grain design used to generate the thrust-time requirement. These comparisons are shown below in Table 6-6 where design variable values are listed for the optimum design and the design solution representative of the grain design that generated the requirement. Comparisons show the optimum grain design highly correlates with the design solution on all except one design variable: *DV-L5* (the length of the middle section of the multi-cylinder grain). Given the excellent agreement between the thrust-time products of the

two grains, it was assumed the design was insensitive to variations in this particular variable, and this is an alternate design solution.

## 6-2 Internal Ballistic Optimization Strategy Trial #2

The second trial of the internal ballistic optimization strategy involved the optimization of a star/slotted solid rocket motor grain per the thrust-time requirements of a real solid fueled rocket motor, the Thiokol XM33E5 Castor. This rocket motor has been used in the solid rocket boosters of the Delta D launch vehicle, and as the second stage of the NASA Scout launch vehicle.

The Thiokol XM33E5 Castor rocket motor requirements were obtained directly from the Chemical Propulsion Information Analysis Center (CPIA), however this information is also published by John Hopkins University in the CPIA/M1 Rocket Motor Manual. For reference, the portion of the CPIA/M1 Rocket Motor Manual used in the paper is posted in 0.

This optimization trial initiated with the star grain shown in Figure 6-7a as the base solid rocket motor grain model. This base model was acquired from a library of generic grains. Figure 6-7b shows the same grain model with combustion chamber dimensions per the Castor requirement. Figure 6-7b shows the thrust-time requirement of the Castor rocket motor plotted against the thrust product of the base model.

The next four subsections discuss the optimization model definition, the optimization methodology and the design results at each of the three stages of the optimization process: approximation, optimization, and high-fidelity optimization.

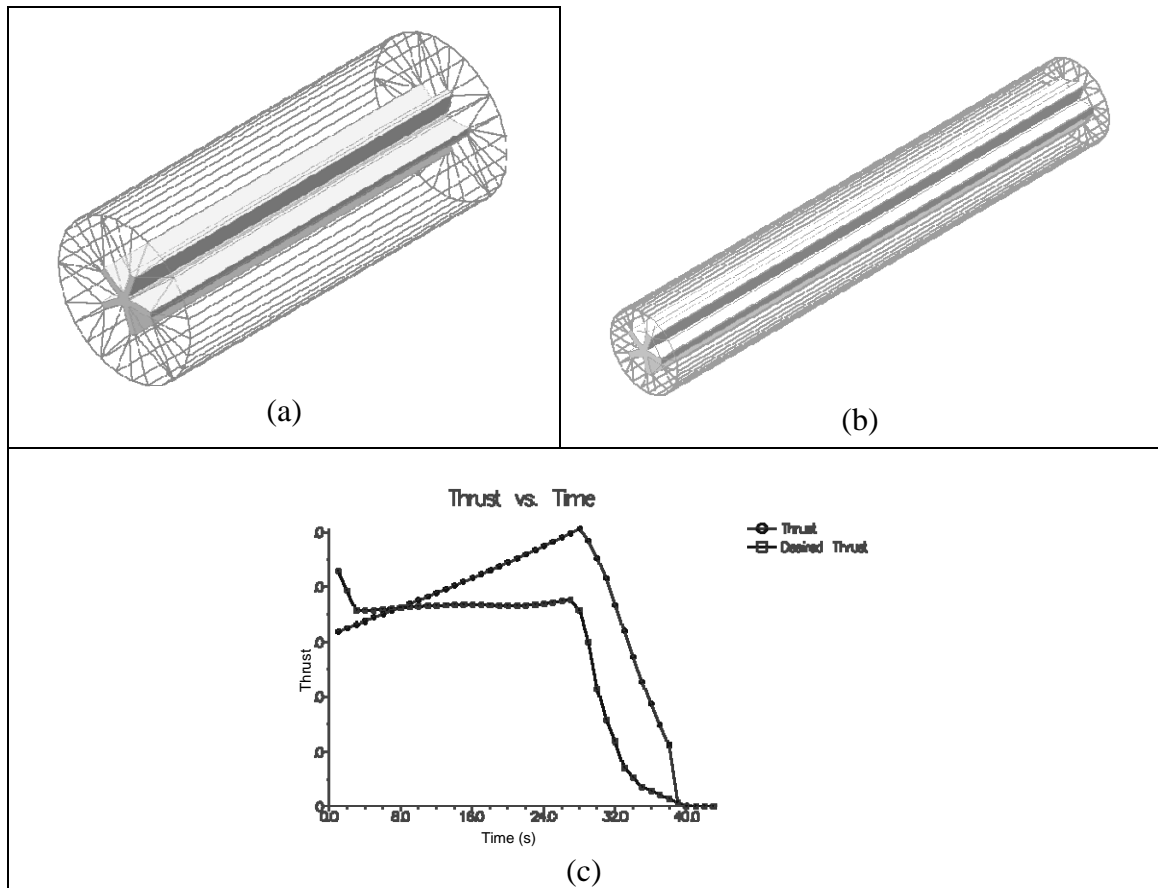


Figure 6-7 – The (a) initial grain design; (b) the initial grain design with Castor’s case dimensions; (c) the thrust time requirement of the XM33E5 Castor solid fueled rocket;

### 6-2-1 Optimization Model Definition

This section discusses the optimization model definition for the star solid rocket motor grain design. The optimization model definition outlined in this section follows a three step process discussed in section 2-1 .

First, design variables were selected to represent the parametric geometry of the star grain. The star grain was constructed in an AML and consisted of a fin-object and a cylinder object. These objects perforated the grain and were invariant along the grain's entire length. The fin-object *inherited* (terminology defined in section 3-1 ) from three separate objects that defined (1) the profile of a fin, (2) the extrusion of the fin profile, and (3) the pattern of fins. For a visual reference, a cross-section of the grain and an illustration of the objects involved in its construction are shown in Figure 6-8. This group of separate objects were joined (using a union object) to make one geometry, the center perforated star-grain.

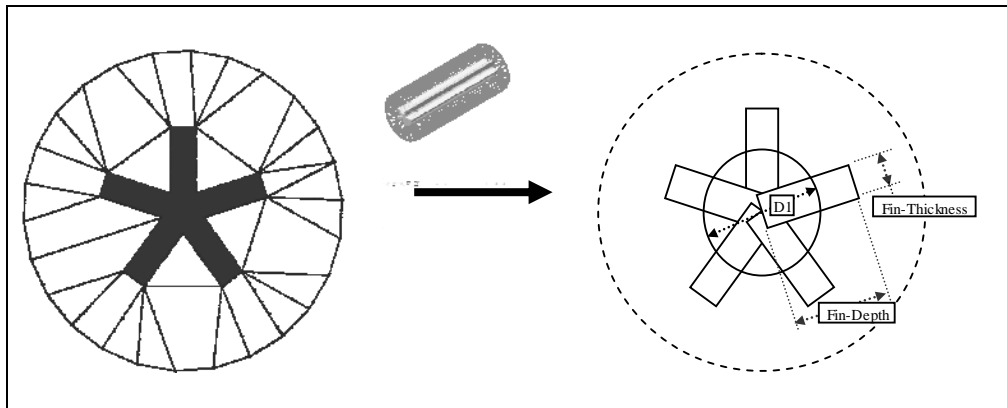


Figure 6-8 – Cross Section of Solid Rocket Motor Grain in Star Configuration.

With the grain construction geometry known, the choice of design variables was clear. Referencing Figure 6-8, Table 6-7 below lists the design variables along with their initial values, and upper (UB) and lower (LB) bounds. This geometry was represented by four design variables; two continuous variables and one discrete variable. The discrete variable represented the

number of fins in the grain and was labeled *No-of-Fins*. Finally, all variables were normalized with respect to the diameter of the combustion chamber; see discussion towards the end of section 6-1-1 regarding normalizing the design variables.

Table 6-7 – Initial design variable configuration for star grain.

Variable Name	Variable Description	Initial Value	UB	LB
<i>No-of-Fins</i>	<i>Quantity of Fins</i>	5	<i>Domain { 4 5 6 }</i>	
<i>DV-Fin-Depth</i>	<i>Depth of Fins</i>	0.260	0.08	0.40
<i>DV-Fin-Thickness</i>	<i>Thickness of Fins</i>	0.079	0.015	0.10

Second, design constraints were applied to the model. Side constraints were imposed on all design variables, see the upper (UB) and lower (LB) bounds listed in Table 6-7. In this problem, side constraints were used primarily to control (1) the fin thickness, and (2) the size of the grain geometry with respect to the combustion chamber. It was intended that these constraints posed minimum restriction on the allowable design space.

Next, two inequality constraints were formulated to control the weight of propellant per a derived requirement. These constraints are formulated in Equation 6-3 where  $W$  represents the weight of the grain model and  $W_{Target}$  represents the target weight. The initial constraint boundaries are listed in Table 6-8. Note, both constraints were formulated such that they were satisfied with negative values per the guidelines of optimization tool Design Optimization Tools (DOT).

$$\frac{W_{T\text{arget}} - 0.85 \cdot W}{W_{T\text{arget}}} < 0 \quad \text{Constraint 1}$$

Equation 6-3

$$\frac{1.15 \cdot W - W_{T\text{arget}}}{W_{T\text{arget}}} < 0 \quad \text{Constraint 2}$$

Table 6-8 – Constraint values of initial design configuration.

Constraint No./Name	Variable Description	Initial Value	LB	UB
1.) <i>Propellant-Weight</i>	<i>LB on Prop. Weight</i>	-0.14	-0.15	0
2.) <i>Propellant-Weight</i>	<i>UB on Prop. Weight</i>	-0.05	-0.15	0

Third, the objective function was formulated. This was done by, first, entering data points for the target thrust time. For this optimization trial the thrust-time requirement, discussed above on page 74, was the thrust requirement of the Thiokol XM33E5 Castor solid fueled rocket obtained from the CPIA/M1 Solid Rocket Motor Manual. The normalized target thrust time curve is shown above in Figure 6-7c. Next, the objective function was automatically formulated through the use of demand-driven dependency-tracking AML code. Before the optimization process began, the objective function was normalized to a value of one.

This optimization model definition was used throughout the entire ballistic optimization strategy. The next three sub-sections describe the three stages of the ballistic optimization process: design approximation, design optimization, and high-fidelity optimization.

## 6-2-2 Internal Ballistic Optimization Strategy Stage 1: Design Approximation

The first stage of the internal ballistic optimization strategy, outlined in section 5-1-2, center on approximating the star solid rocket motor design using DOE. This approximation technique provided an inexpensive vehicle for characterizing the design space of the grain. The goal of this stage was to approximate the grain design driven by a thrust-time requirement of the Thiokol XM33E5 Castor solid fueled rocket and identify grain design approximation(s) that best meet that requirement with the intent of optimizing that design(s) in the second stage of the strategy.

The star grain design was approximated using a full-factorial level-three DOE. In this case the cost (number of experiments) of running a full-factorial level-three DOE was insignificant as there was such a small number of design variables, and the same conditions existed in this trial as did in the previous trial (discussed in section 6-1-2) that justified this DOE methodology. With three design variables representing the star grain geometry, the full-factorial three level DOE consisted of 27 experiments.

The star grain design approximation results are plotted in Figure A-2 under Appendix A-2 and listed in Table A-2 under Appendix A-4. The aforementioned plot represents the results in two series; The *Raw DOE Response* series represented the responses from all 27 experiments, and the *Sorted Feasible DOE Response* series represented only the feasible responses (designs satisfying all constraints) sorted in order of increasing design merit. Only one third of all the responses satisfied all of the constraints. Plotted results correlated with source data indicated two local minima, one with a geometric grain configuration employing 4 fins and the other employing 5 fins.

Table 6-9 –Design Variable configurations for Star grain design approximations.

<i>Variable Name</i>	<i>Star Grain 1</i>	<i>Star Grain 2</i>
<i>No-of-Fins</i>	4	5
<i>DV-Fin-Depth</i>	0.4	0.4
<i>DV-Fin-Thickness</i>	0.0575	0.0575

Finally, since two local minima were discovered in the approximation process, two designs were saved to pass to the second stage of the optimization strategy. The best approximated star grain with 4 fins had a merit value 0.39, and the best approximated star grain with 5 fins had a merit value of 0.55. This marked design improvements of 61% and 45%, respectively. Table 6-9 lists the design variable values for the best approximated grains; *Grain1* in this table refers to the approximated grain with 4 fins and *Grain2* refers to the approximated star grain with 5 fins. Figure 6-9 and Figure 6-10 show model of the best approximated 4 fin and 5 fin solid rocket motor grain designs and plots of their thrust-time products plotted against the thrust-time requirement, respectively. These plots clearly show significant design improvements from the base star grain with respect to the requirement.

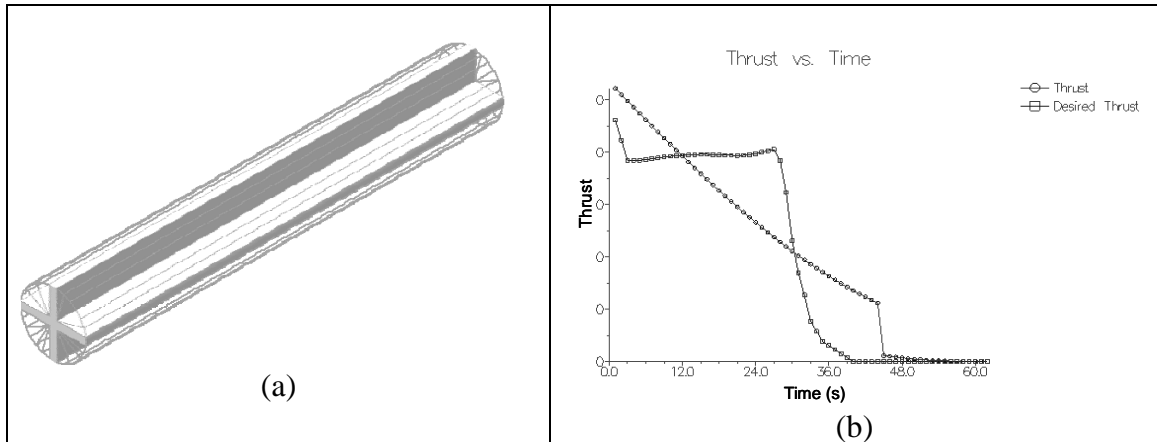


Figure 6-9 – (a) Approximated 4 Fin Star Grain Model and (b) Thrust-Time Product.

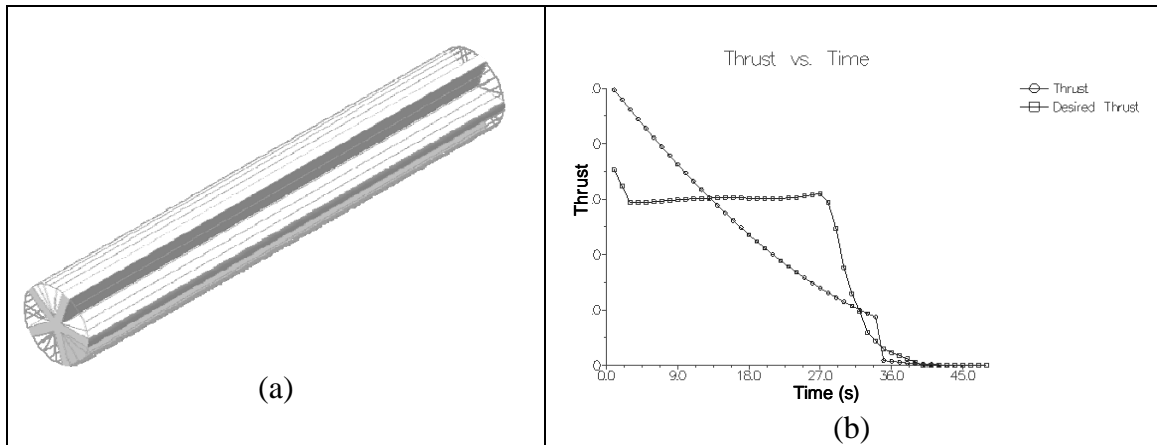


Figure 6-10 – (a) Approximated 5-Fin Star Grain Model and (b) Thrust-Time Product.

### 6-2-3 Internal Ballistic Optimization Strategy Stage 2: Design Optimization

The second stage of the internal ballistic optimization strategy focused on the optimization of the star solid rocket motor grain design. The methodology of this stage was outlined in section 5-1-3, and the goal of this stage was to optimize the two best approximated star grain designs (shown in Figure 6-9 and Figure 6-10) per the thrust-time requirement of the Thiokol XM33E5 Castor solid fueled rocket. This strategy

employed a global optimization routine using the genetic optimization algorithm from the AMOPT optimization interface developed by TechnoSoft. Genetic Algorithms are discussed in section 2-5-3.

First, the AMOPT interface was used to select and prepare each of the two approximated star grains for global optimization. The primary difference between the star grains corresponded to the value of one discrete design variable which manifested itself in the number of slots in the grain geometries. Since the genetic optimization algorithm was not design to optimize while using simultaneously discrete and continuous design variables, each of the two star grains were optimized separately while hold the discrete design variable fixed.

Table 6-10 – Parameter Setting Definitions for the Genetic Algorithm used in Trial #2.

<i>Population Size</i>	25
<i>Number of Generations</i>	25
<i>Noise Power</i>	0.001
<i>Extreme Value</i>	4

Next, four parameter settings of the genetic algorithm were defined. These parameters settings are listed in Table 6-10 and what these parameters represent are discussed in section 5-1-3. The first parameter, *Population Size*, was calculated using Equation 5-1 and the design variable information in Table 6-1. Since the star grain had half the number of design variables as did the multi-cylinder grain from optimization trial #1, it was realistic to see the *Population Size* parameter shrink to have the value used in

trial #1. To ensure enough *generations* to thoroughly mutate the chromosomes used by the genetic algorithm the *Number of Generations* parameter was left unchanged. Next, the third setting, *Noise Power*, represented the design variable increment, and last, the *Extreme Value* setting represented the largest expected objective function response value. If such response values increased beyond the *Extreme Value* setting, the optimization process would terminate.

The optimization process ran successfully and without premature termination; however, referencing the optimization responses from the two star grains plotted in Figure B-2a-b, respectively, under Appendix B-2, the convergence rate drastically differed between the two grains being optimized. The 4-slotted star grain optimization response worsen in the beginning, stagnated throughout almost the entire optimization process, and converged rapidly in the final few design responses. On the other hand, the 5-slotted star grain optimization response rapidly improved in the beginning of the process, continued to gradually improve until approximately two-thirds of the way into the process, and then, stagnated for the last third of the process. It was expected this difference in convergence rates between the two grains was had due to an implied constraint on *total impulse*. Because the thrust-time requirement was defined as a continuous collection of data-points over the thrust-time curve (rather than as segments of data-points) the area under the curve, *total impulse*, had an implicit effect on the optimization response. Additionally, Table B-2 and Table B-3 list every tenth optimization response from a total of 625 responses for each grain, respectively.

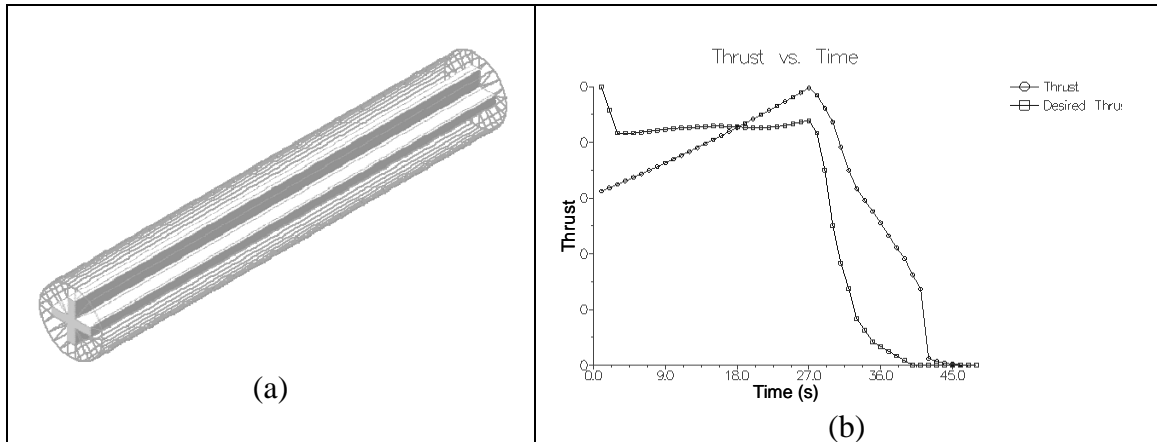


Figure 6-11 – (a) Optimized 4-slotted Star Grain Model and (b) Thrust-Time Product.

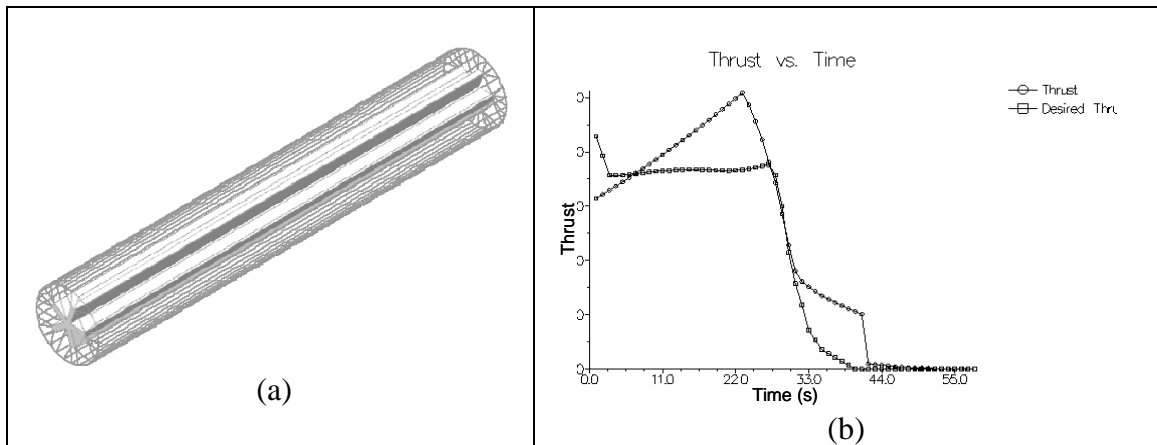


Figure 6-12 – (a) Optimized 5-slotted Star Grain Model and (b) Thrust-Time Product.

In summary, accomplishments from this stage of the internal ballistic optimization strategy included two solid rocket motor star grain designs, a 4-slotted grain and a 5-slotted grain. The merit of these grain designs had improved by 37 percent and 96 percent, respectively. The differences in merit improvement were attributed to the implicit constraint on *total impulse*. Given these differences, the 4-slotted star grain design was dropped, and the 5-slotted star grain was developed further in the next stage of the internal ballistic optimization strategy, high-fidelity optimization.

#### 6-2-4 Internal Ballistic Optimization Strategy Stage 3: High-Fidelity Optimization

The third, and final internal ballistic optimization strategy stage of optimization trial #2 centered on the high-fidelity optimization of the star solid rocket motor grain design. The methodology used in this stage is outlined in section 5-1-4.

To summarize the design optimization progress on the star solid rocket motor grain up to this point, the design had been approximated in internal ballistic optimization strategy stage #1 and globally optimized in stage #2. Stage #1 of the strategy produced two potential star grain designs (one with 4 slots and the other with 5), and stage #2 brought the number of designs back down to one by discovering the 4-slotted star grain design could not satisfy the total impulse constraint imposed as an implicit constraint of the thrust-time requirement. The 5-slotted star grain, conversely, saw a significant merit improvement by global optimization; however, the thrust-time product of the 5-slotted star grain remained significantly progressive to the requirement. Therefore, the goal of this final stage of the internal ballistic optimization strategy was to optimize the 5-slotted star grain design per the Thiokol XM33E5 Castor solid-fueled rocket thrust-time requirement to have an overall merit 90 percent better than the base grain using the high-fidelity BFGS optimization algorithm.

First, the optimized 5-slotted star grain design (see Figure 6-12 in the previous section) was prepared for high-fidelity optimization. With the optimum design from the previous section set as the concurrent design, the design variables were reset within AMOPT to reflect the current design. Next, the objective function was renormalized to a unit value of one, and the BFGS algorithm developed by Vanderplaats Research and

Development was selected. At this point, the model and high-fidelity optimization problem definition was setup; however, parameter settings of the BFGS algorithm remained undefined.

Table 6-11 – Parameter Setting Definitions for the BFGS Algorithm used in Trial #1.

<i>Initial Relative Step Size (DX1)</i>	0.01
<i>Initial Step Size (DX2)</i>	1
<i>Relative Gradient Step (FDCH)</i>	0.001
<i>Min. Gradient Step (FDCHM)</i>	0.0001
<i>Extreme Value</i>	50

Next, five DOT parameter settings were defined to control the BFGS algorithm. These parameter definitions are listed in Table 6-11, and what these parameters represent are discussed in section 5-1-4. All of these parameter definitions were left at their default values except for the *Extreme Value* parameter which was increased to the value shown to avoid premature termination of the optimization process when finite differencing was used to calculate the gradient of the objective function. When this occurred at several instances during the optimization process the response was higher than normal.

After the optimization algorithm parameter settings to the were defined, the objective function was weighted in areas corresponding to the thrust response of the star grain having greater than ten percent departure from the requirement (see Figure 6-12 in

the previous section). This increased response sensitivity in these areas, and thus, the design merit increased more for improvement in weighted areas than non-weighted areas of the thrust-time curve. Additionally, this decreased the chance of premature termination of the optimization process due to poor response sensitivity.

The high-fidelity optimization process executed on the 5-slotted star grain converged quickly to a solution taking just three percent of the CPU time it took to converge in the previous section. The 5-slotted star grain design generated in the process had a merit improvement of 98 percent over the grain design from the second stage of the strategy. The optimized star grain model and a plot of the corresponding thrust-time product are shown in Figure 6-13. This plot indicates the goals of optimization trial #2 were met successfully with the high correlation between the thrust-time product of the grain design and the thrust-time requirement of the Castor solid-fueled rocket. The thrust-time product of the optimized star grain was still slightly progressive as compared to the requirement; however, it was assumed this departure could be attributed to how the chemical propellant and nozzle geometry data taken from the CPIA/M1 Rocket Motor Manual was interpreted. Experimental data proved this hypothesis by perturbing the chemical propellant density and nozzle throat area to retard the progressive thrust-time behavior of the optimum star solid rocket motor grain to make it neutral burning as per the requirement.

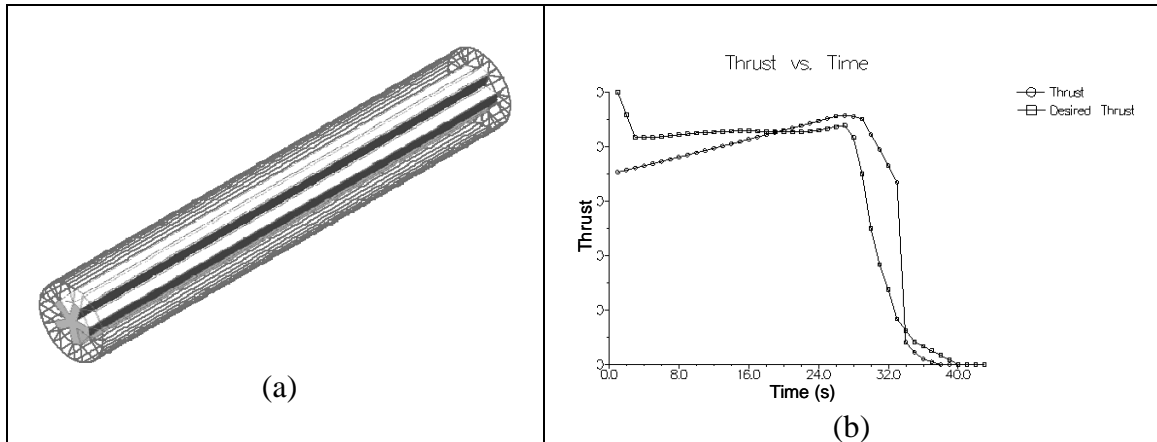


Figure 6-13 – (a) High-Fidelity Optimized 5-slotted Star Grain Model and (b) Thrust-Time Product.

Lastly, this optimum 5-slotted star grain geometry was compared with that of the Castor solid rocket motor grain geometry information published in the CPIA/M1 Rocket Motor Manual. Table 6-12 lists the design variable values for the optimum star grain design (labeled Optimum Design in the table) and for the Thiokol XM33E5 Castor solid-fueled rocket motor grain as would be if the real grain dimensions were divided by the case diameter to encode them the same as the design variables. The optimum grain design variable values were within 9 percent of those of from the Castor grain design.

Table 6-12 – Star grain design variable values for optimum versus Castor grain design.

Variable Name	Variable Description	Optimum Design	Castor Design
<i>dv-fin-thickness</i>	<i>Diameter of Cylinder 1</i>	0.137	0.127
<i>dv-fin-depth</i>	<i>Diameter of Cylinder 2</i>	0.044	0.036
<i>Number-of-Fins</i>	<i>Number of Slots in Array</i>	5	5

In summary, accomplishments from this stage of the optimization strategy included a 5-slotted star rocket motor grain design that satisfied the Thiokol XM33E5 Castor solid-fueled rocket thrust-time requirement, and the grain geometries compared closely to one another. High-fidelity optimization increased the design merit of the grain by 97%, and combined with the design improvement from the previous two stages of the internal ballistic optimization strategy yielded a design merit improvement of 99.92% in relation to the base 5-slotted star grain.

### 6-3 Internal Ballistic Optimization Strategy Trial #3

The third optimization trial of the internal ballistic optimization strategy involved solid rocket motor grain optimization on the merit of burn area versus distance (rather than thrust versus time). Optimizing on this merit decoupled the merit dependence on grain geometry from the nozzle geometry and propellant parameters other than burn-rate, and provided a basis for conceptualizing the design of a grain geometry. The subject grain of this trial was the grain labeled *complex grain* shown below in Figure 6-14a-b along with this grain's burn-area-versus-distance response and burn-area-versus-distance requirement to which it was optimized. The goal of this trial was to quantify the efficiency of the optimization strategy when implemented on complicated grain geometries with a large number of design variables.

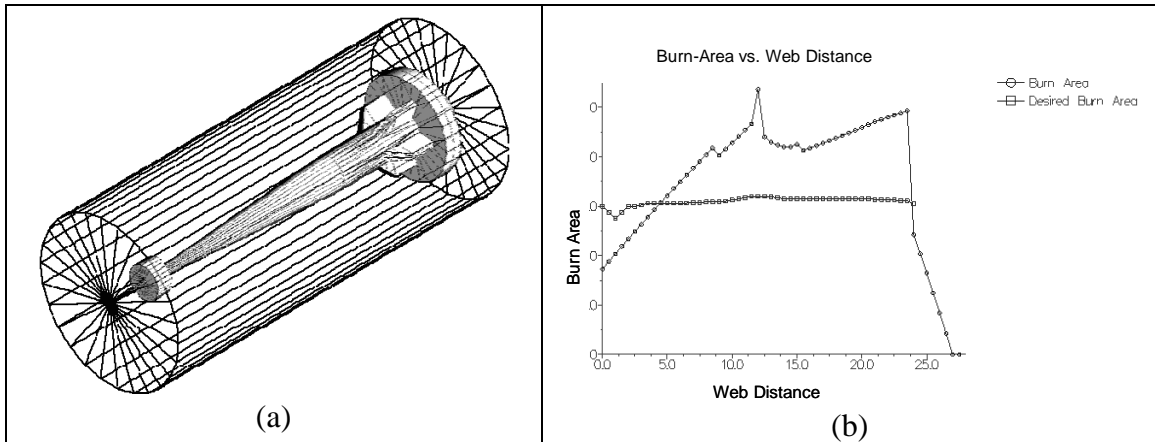


Figure 6-14 – Complex Grain and Burn-Area versus Web-Distance Requirement.

The grain geometry and burn-area versus web-distance requirement used in this optimization trial were extrapolated from figures and plots contained in [8]. This reference used a similar grain to demonstrate computer aided modeling techniques for solid propellant grains. No exact design parameters of the complex grain geometry or burn-area-versus-distance requirement were given by the referenced paper; therefore, in this thesis, the exact geometry and geometric scale of the complex grain, and the amplitude of the burn-area-versus-distance requirement were assumed.

The next four subsections discuss the optimization process of the complex grain starting with the definition of the optimization model.

### 6-3-1 Optimization Model Definition

This section discusses the optimization model definition for the complex solid rocket motor design. The optimization model definition discussed in this section follows a three step process discussed in section 2-1. The process of defining the optimization

model for the complex grain initiated with the selection of the design variables followed by the application of side constraints. Due to the conceptual nature of this problem, design constraints were not employed. Finally, data points from the burn-area- versus- distance requirement were entered and the objective function was formulated.

First, design variables were selected to represent the complex grain geometry. The complex grain geometry was comprised of ten geometric primitives: five cylinders, two spheres, two extrusions, and one cone. Each geometric primitive was defined by at least three dimensional properties and a global position property. This created the potential for 40 design variables and an indeterminate amount of constraints. However through variable decomposition, discussed in section 2-1-2, this large set of possible design variables were reduced to 11, see Figure 6-15.

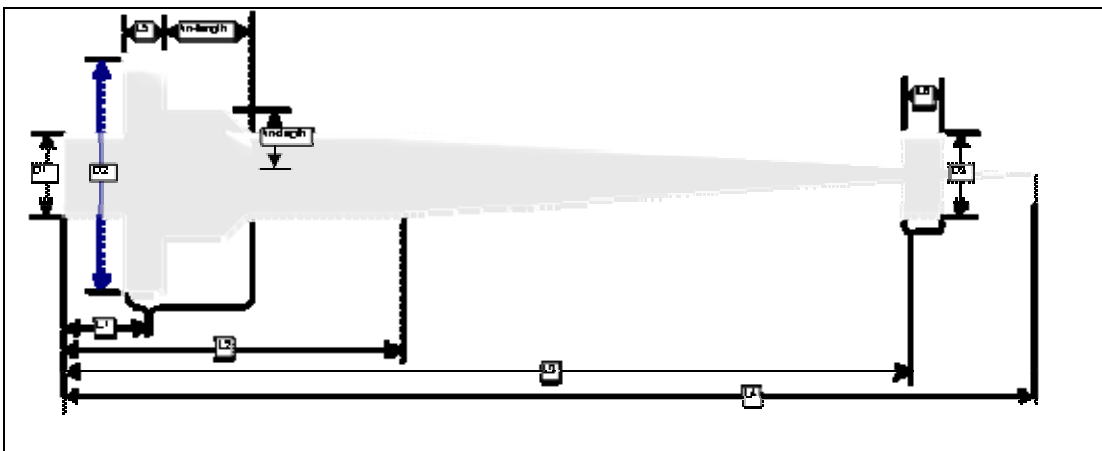


Figure 6-15 – Complex grain with annotated dimensions.

The design variables chosen to represent the complex grain are listed in Table 6-13 below and correspond to the above figure. This table lists variable names along with brief variable descriptions, initial values, and upper (UB) and lower (LB) bounds.

changing the grain geometry and then (2) evaluating the objective function could be seamlessly controlled by optimization algorithms.

The next three sub-sections discuss the results of the optimization process: design approximation with design of experiments, design optimization, and high-fidelity optimization.

### 6-3-2 Internal Ballistic Optimization Strategy Stage 1: Design Approximation

The first stage of the internal ballistic optimization strategy, outlined in section 5-1-2, centered on approximating the complex solid rocket motor design using DOE. The goal of this stage was to approximate the complex grain design driving by a burn-area-versus-distance requirement and identify a grain design approximation(s) that best satisfied that requirement with the intent of optimizing that design(s) in the second stage of the strategy.

The past two optimization trials had used the full-factorial level-three DOE to approximate solid rocket motor grain designs; however, a full-factorial level-three DOE would have required a prohibitive number of experiments to approximate the complex solid rocket motor grain as the complex grain had 11 design variables ( $3^{11} = 177147$  experiments). Therefore, the response sensitivity of each design variable was evaluated and from that experimental data, the number of design variables used in the design approximation was reduced to 6 which reduced the number of experiments required of the DOE approximation to 729.

The complex grain design approximation results are plotted in Figure A-3 under Appendix A-2 and are listed in Table A-3 under Appendix A-5. The

was a conceptual design effort, a non-restrictive solution space was desired; therefore, the side constraints were relatively loose. However, following the first DOE design approximation (discussed in the next section) it was discovered, bounds on the variable titled *DV-fin-depth* were too loose and the fins were allowed to be enveloped by the primary cylinder of the grain. Furthermore, the LB on the corresponding variable was tightened and the fin remained a part of the grain geometry. Lastly, the final set of side constraint bounds are shown per variable in Table 6-13.

Third, the objective function was formulated. The objective function in this and the two previous trials was formulated with the demand-driven dependency-tracking features of AML. This function accepted two inputs, namely lists of burn-surface-area-versus-distance data points from the requirement (entered by the user) and the subject grain (generated by surface recession simulation). The objective function used the damped least squares method to rate the grains' merit of the solid rocket motor grain, see section 4-4 for details.

At this point, the optimization model for solid rocket motor grain was setup, and the demand-driven dependency-tracking features of the objective function were setup such that the process could run seamlessly. The dependency tracking features of the objective function were setup such that calculated values would expire with changes to the grain geometry. For example, any time the grain geometry was altered for improved burn-area-versus-distance response, the objective function property would drop its current value and have to be re-evaluated. Furthermore, the demand-driven features were setup such that when the objective function was demanded, a surface recession simulation would be demanded of the grain. Thus, the optimization process of (1)

changing the grain geometry and then (2) evaluating the objective function could be seamlessly controlled by optimization algorithms.

The next three sub-sections discuss the results of the optimization process: design approximation with design of experiments, design optimization, and high-fidelity optimization.

### 6-3-2 Internal Ballistic Optimization Strategy Stage 1: Design Approximation

The first stage of the internal ballistic optimization strategy, outlined in section 5-1-2, centered on approximating the complex solid rocket motor design using DOE. The goal of this stage was to approximate the complex grain design driving by a burn-area-versus-distance requirement and identify a grain design approximation(s) that best satisfied that requirement with the intent of optimizing that design(s) in the second stage of the strategy.

The past two optimization trials had used the full-factorial level-three DOE to approximate solid rocket motor grain designs; however, a full-factorial level-three DOE would have required a prohibitive number of experiments to approximate the complex solid rocket motor grain as the complex grain had 11 design variables ( $3^{11} = 177147$  experiments). Therefore, the response sensitivity of each design variable was evaluated and from that experimental data, the number of design variables used in the design approximation was reduced to 6 which reduced the number of experiments required of the DOE approximation to 729.

The complex grain design approximation results are plotted in Figure A-3 under Appendix A-2 and are listed in Table A-3 under Appendix A-5. The

aforementioned plot represents the results in two series; The *Raw DOE Response* series represented the responses from all 729 experiments, and the *Sorted Feasible DOE Response* series represented the responses sorted in order of increasing design merit. Results plotted in the former series showed a recurring trend which indicated a response sensitivity to the design variable controlling the length of the fins. However, regardless of this recurring trend, the overarching trend indicated only one appreciable local minimum. This was confirmed by the results plotted in the later series as among the designs of highest merit no significant differences were observed between the designs.

Table 6-14 – Design variable values for best approximated Complex grain design.

Variable Name	Variable Description	Value
<i>DV-D1</i>	<i>Diameter of Cylinder 1</i>	0.3
<i>DV-D2</i>	<i>Diameter of Cylinder 2</i>	0.7
<i>DV-D3</i>	<i>Diameter of Cylinder 3</i>	0.2
<i>DV-L1</i>	<i>Position of Cylinder 2</i>	0.08 (n/a)
<i>DV-L2</i>	<i>Length of Cylinder 1</i>	0.33 (n/a)
<i>DV-L3</i>	<i>Position of Cylinder 3</i>	0.88 (n/a)
<i>DV-L5</i>	<i>Length of Cylinder 2</i>	0.04 (n/a)
<i>DV-L6</i>	<i>Length of Cylinder 3</i>	0.04 (n/a)
<i>DV-fin-length</i>	<i>Length of Fins</i>	0.1
<i>DV-fin-thickness</i>	<i>Thickness of Fins</i>	0.06
<i>DV-fin-depth</i>	<i>Height of Fins</i>	0.25

Finally, the best approximated complex grain design was loaded into AML and validated to be free of defect. The merit value of this design was 0.69 which marked a 31% design improvement relative to the base design. Table 6-14 lists the design variable values for the best approximated grain, and Figure 6-16 shows a model of the best approximated complex solid rocket motor grain design along with a plot of its burn-area-versus-distance product plotted against the requirement and the product of the base grain. This plot shows how discontinuities in the base grain response had somewhat smoothed and a significant design improvement had been made with respect to the requirement.

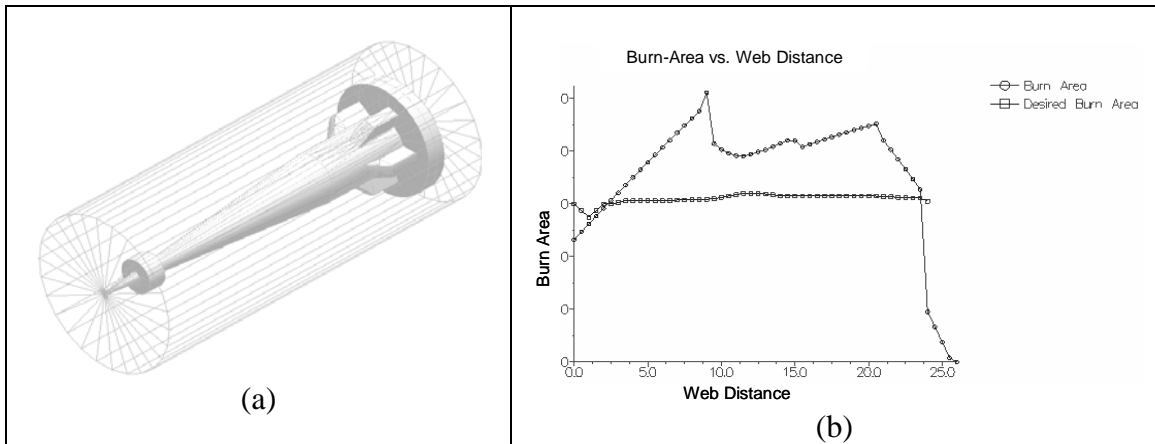


Figure 6-16 – (a) Approximated Complex grain and (b) corresponding burn-area-versus-distance product plotted against the requirement.

### 6-3-3 Internal Ballistic Optimization Strategy Stage 2: Design Optimization

The second stage of the internal ballistic optimization strategy, discussed in section 5-1-3, focused on the optimization of the complex solid rocket motor grain design. The goal of this stage was to optimize the best approximated complex grain

design (shown in Figure 6-16) per that stated burn-area-versus-distance requirement. This strategy employed a global optimization routine using the genetic optimization algorithm from the AMOPT optimization interface developed by TechnoSoft; genetic algorithms are discussed in section 0.

First, the approximated complex grain design (from the first stage of the strategy) was prepared for optimization. The AML optimization interface AMOPT provided an elegant widget for performing this operation. While still in the approximation mode of AMOPT, the DOE experiment producing the best response was selected and set as the concurrent working design. Next, the objective function was renormalized to a unit value of one. At this point, the grain model and optimization model definitions were setup for optimization, however, the parameter settings of the optimization algorithm remained undefined.

Table 6-15 – Parameter Setting Definitions for the Genetic Algorithm used in Trial #3.

<i>Population Size</i>	40
<i>Number of Generations</i>	25
<i>Noise Power</i>	0.001
<i>Extreme Value</i>	4

Next, four parameter settings of the genetic algorithm were defined. These parameters settings are listed in Figure 6-15 and what these parameters represent are discussed in section 5-1-3. The first parameter, *Population Size*, was calculated using

Equation 5-1 and the design variable information in Table 6-1. Based on the convergence rate in optimization processes from the second stage of the previous two optimization trials, it was hypothesized the *Population Size* had been chosen to allow conservative margin. Therefore, even through the number design variables had doubled, it was reasonable to expect design improvement with the *Population Size* defined to have a value between the values of the previous two optimization trials. To ensure enough *generations* to thoroughly mutate the chromosomes used by the genetic algorithm the *Number of Generations* parameter was left unchanged. Next, the third setting, *Noise Power*, represented the design variable increment, and last, the *Extreme Value* setting represented the largest expected objective function response value. If such response values increased beyond the *Extreme Value* setting, the optimization process would terminate.

The optimization process ran successfully and without premature termination. Referencing Figure B-3 in Appendix B-2, the convergence rate was high in the very beginning of the process and then slowed to a more gradual rate. The convergence rate never stagnated, but by the end of the process had slowed a rate of diminishing returns. This was desired! Unlike design responses from the previous two trials, the optimization response for this design had no wasted iterations, and considering the cost per iteration for this design was considerably higher than the past two designs, it was important to not wasted iterations. Additionally, Table B-4 lists every tenth optimization response from a total of 1000 optimization design responses.

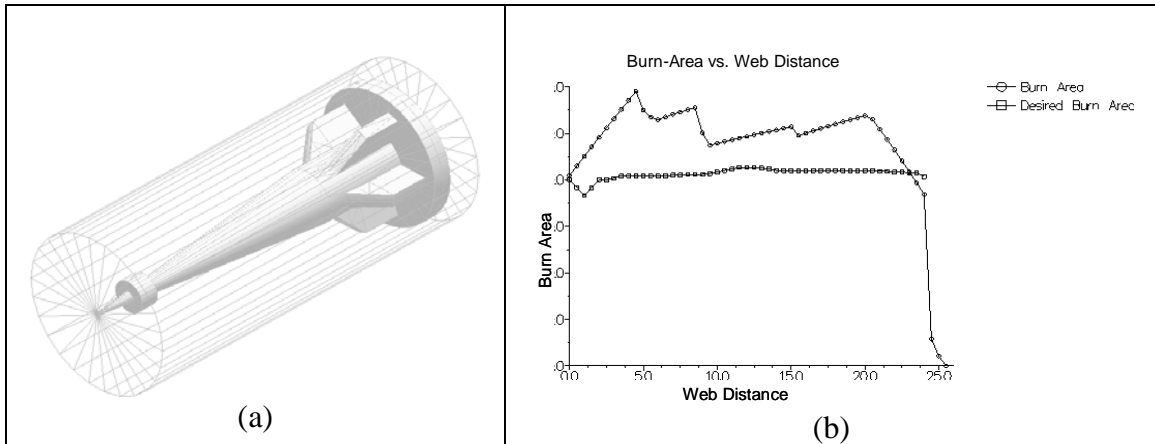


Figure 6-17 – Optimized Complex Grain and corresponding Burn Area versus Distance plotted versus the Requirement.

In summary, accomplishments from this stage of the internal ballistic optimization strategy include complex grain design producing a burn-area-versus-distance response much more neutral, as the requirement, than the base complex grain design from the first section of this trial. The merit of this complex grain at the end of the optimization process had improved by 47 percent. More design improvement could have been had given more iterations by increasing the *Population Size* parameter of the genetic algorithm, however, considering the cost per iteration of this design, it was thought this improvement could be had more efficiently using the high fidelity optimization strategy discussed in the next section.

#### 6-3-4 Internal Ballistic Optimization Strategy Stage 3: High-Fidelity Optimization

The third, and final stage of the internal ballistic optimization strategy for optimization trial #3 centered on the high-fidelity optimization of the complex grain design. The mechanics behind this stage are discussed in section 5-1-4. The baseline

of this stage was the complex grain design product from stage 2 of the internal ballistic optimization strategy; a grain design that had already been approximated and optimized using a global optimization technique. The goal of this final stage was to optimize the complex solid rocket motor grain design per the stated burn-area-versus-distance requirement to have an overall merit 90 percent better than the base grain used at the start the optimization process.

First, the optimized complex grain design (from the second stage of the ballistic optimization strategy) was prepared for high-fidelity optimization. Within the AML optimization interface AMOPT, the optimization iteration producing the optimum design was selected and set as the concurrent design. Next, the objective function was renormalized to a unit value of one. At this point, the model and high-fidelity optimization problem definition was setup, however parameter settings of the optimization algorithm remained unset.

The high-fidelity optimization process utilized the BFGS optimization algorithm developed by Vanderplaats Research and Development. This algorithm is discussed in section 2-5-1. This algorithm had five controlling parameters. These parameters settings are listed in Table 6-16 and what these parameters represent are discussed in section 5-1-4. All of these parameter definitions were left at their default values except for the *Extreme Value* parameter. This parameter was increased to the value shown above to avoid premature termination of the optimization process when finite differences was used to recalculate the gradient of the objective function. When these occurred at several times during the optimization process the response was higher than normal. These settings were made inside the AMOPT interface.

Table 6-16 – Parameter Setting Definitions for the BFGS Algorithm used in Trial #1.

<i>Initial Relative Step Size (DX1)</i>	0.01
<i>Initial Step Size (DX2)</i>	1
<i>Relative Gradient Step (FDCH)</i>	0.001
<i>Min. Gradient Step (FDCHM)</i>	0.0001
<i>Extreme Value</i>	50

After settings to the optimization algorithm were defined, the objective function was weighted. Since the design requirement was to have a neutral burn-area-versus-distance response the objective function was weighted at the beginning and end of the complex grain response corresponding to areas where the response was the least neutral (see Figure 6-17b above) A 5x weighting was applied in these areas. By using weights to increase the objective function sensitivity in areas of needed improvement the probability of premature termination of the optimization process was mitigated.

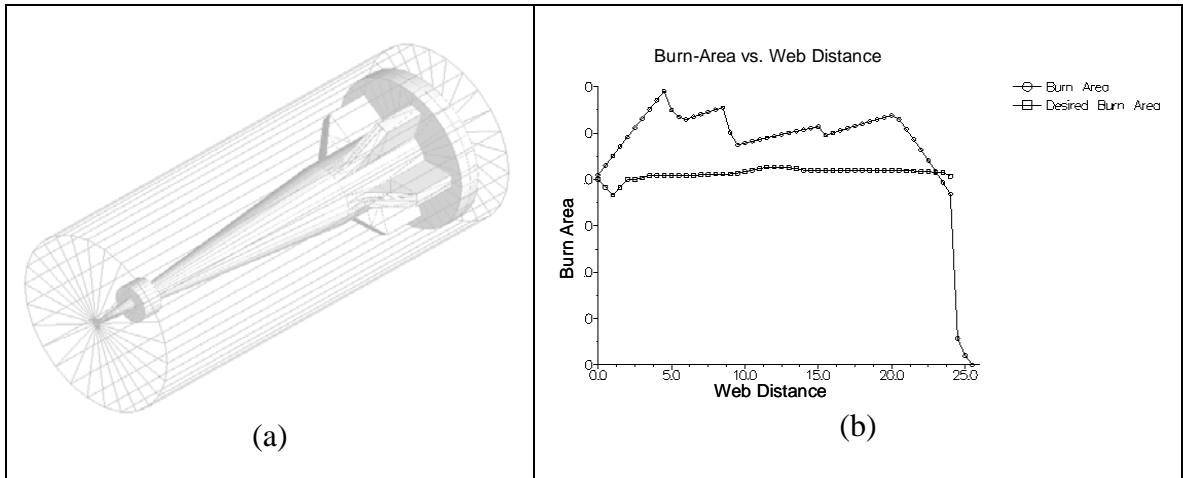


Figure 6-18 – High-Fidelity Optimized Complex Grain and corresponding Burn Area versus Distance plotted versus the Requirement.

The high-fidelity optimization was carried out in AML through the AMOPT interface. The high-fidelity optimization process converged to a solution generating a complex solid rocket grain design with a merit improvement of 31 percent over the grain design produced from the second stage of the ballistic optimization strategy. The optimized grain had a burn-area-versus-distance response much more neutral than the base design. This is shown in Figure 6-18 which shows the optimized complex grain model and a plot of the corresponding burn-area-versus-distance product.

Table 6-17 – Initial design variable configuration for cylinder grain.

Variable Name	Variable Description	Value
<i>DV-D1</i>	<i>Diameter of Cylinder 1</i>	0.32
<i>DV-D2</i>	<i>Diameter of Cylinder 2</i>	0.8
<i>DV-D3</i>	<i>Diameter of Cylinder 3</i>	0.05
<i>DV-L1</i>	<i>Position of Cylinder 2</i>	0.15
<i>DV-L2</i>	<i>Length of Cylinder 1</i>	0.41
<i>DV-L3</i>	<i>Position of Cylinder 3</i>	0.72
<i>DV-L5</i>	<i>Length of Cylinder 2</i>	0.08
<i>DV-L6</i>	<i>Length of Cylinder 3</i>	0.04
<i>DV-fin-length</i>	<i>Length of Fins</i>	0.14
<i>DV-fin-thickness</i>	<i>Thickness of Fins</i>	0.03
<i>DV-fin-depth</i>	<i>Height of Fins</i>	0.22

In summary, accomplishments from this stage of the optimization strategy include a complex solid rocket motor grain design with a burn-area-versus-distance response much more neutral than the base design. The high-fidelity optimization increased the design merit of the grain by 31 percent, and combining this improvement in design merit with that from previous two stages of the ballistic optimization process yielded a design merit improvement of 75 percent. This was 15 percent short of the goal of this optimization trial, however, considering the burn-area-versus-distance response of the

optimum complex grain had a neutral trend similar to the requirement and the response deviated always on the high side of the requirement indicates the requirement may be beyond the capability of the grain. Other steps that could have been performed to improve the merit of the grain further include (1) performing the approximation stage of the ballistic optimization strategy again incorporating the unused design variables, and (2) increase the *Population Size* setting to the genetic algorithm to allow more iterations to improve the design.

#### 6-4 Investigated Optimization Strategies

The section discusses alternative optimization techniques and strategies that were considered. Techniques discussed in this section failed to produce optimum results for an assortment of reasons.

##### 6-4-1 Full-Factorial Design of Experiments Level of Analysis

The full-factorial Design of Experiments technique used to approximate solid rocket motor grain designs had two modes of operation, level-two and level-three. The level-two mode is used to approximate systems with a linear response, and the level-three mode is used to approximation systems with a non-linear response. The level-three DOEs can have a significantly higher cost of operation as for every design variable there are three levels of experiment, rather than two, and if a system has a large number of design variables, this cost can become prohibitive.

Given, there exist designs with large numbers of design variables (large being defined as seven or more), an attempt was made to mitigate the prohibitive cost of

executing a level-three DOE by running a level-two DOE. This approach was tested on several solid rocket motor grains. First, a relatively large design was approximated using a level-three full-factorial DOE. Next, the design was reset to its base configuration and the process was repeated using a level-two DOE. Finally, results were compared on merits of design improvement.

Results compared between the two methods showed poor results. Design merits of approximated designs produced by the level-three DOE were about twice that of what was produced by level-two DOEs. When these respective designs were optimized, the optimizer had a easier time with the design produced by the three-level DOE approximation. Designs produced by two-level DOEs often required heavy weighting of the objective function to increase design sensitivities and eliminate premature termination of the optimization process. Given such, it was concluded the cost savings versus design improvement achieved by using a two-level DOE rather than a three-level DOE was not achieved.

#### 6-4-2 High Fidelity Optimization starting at DOE Optimum

The *internal ballistic optimization strategy* involved a three step design optimization process. First, the design was approximated using DOE. Second, the design was optimized using genetic algorithms, and finally, high-fidelity gradient-based optimization techniques were used to finish the optimization process. The long pole in the tent, so to speak, is the second step of the strategy involving genetic algorithms. Therefore, an attempt was made to eliminate the second stage of the strategy and

optimize the approximated design using high-fidelity gradient-based optimization techniques. This was actually the original attempt at defining an optimization strategy.

Problems were experienced almost immediately with this optimization strategy. Often the optimization process would prematurely terminate due to no change in design merit. Gradient-based optimization algorithms utilize gradient information obtained from the objective function and constraints to calculate a search direction used to manipulate the design variable vector. Apparently, the response sensitivity of design approximations were still fairly low. Thus, finite changes to the design variables had little to no effect to objective function response, and with no improvement, the optimization process would terminate.

When the design sensitivity was high enough, gradient-based optimization algorithms worked successfully. However, when there was not enough sensitivity a great deal of weighting had to be applied. This resulted in an inconsistent optimization strategy and therefore this strategy was not used.

## CHAPTER 7: RESULTS AND DISCUSSION

This chapter focuses on the results of applying the *internal ballistic optimization strategy*, developed in this paper, to the design of solid rocket motor grains. These results include a summary of the optimization design trials per stage of the ballistic optimization strategy and a summary of how the strategy worked as a whole to reduce the cost of obtaining an optimum solution. This chapter ends with a conclusion of the work performed following by recommendations of future work.

### 7-1 Ballistic Optimization Strategy Results

This section discusses the results of applying the internal ballistic optimization strategy to the design of solid rocket motor grains per stage of the strategy. The internal ballistic optimization strategy was comprised of three stages: (1) design approximation, (2) design optimization, and (3) high-fidelity design optimization.

#### 7-1-1 Internal Ballistic Optimization Strategy Stage 1 Results

It was discovered through experimental data and validated through optimization trials 1, 2, and 3 presented in this paper, the full-factorial level-three design of experiments DOE was an effective technique for approximating solid rocket motor grain designs. The design merit of the grain approximations from the three optimization trials showed at least 30 percent improvement from the respective base designs. Also, these

approximated designs provided successful starting designs for global optimization performed in the second stage of the strategy.

Table 7-1 – Summary of approximation results from three optimization trials.

	No. of Design Variables	Cost	Merit Improvement
Optimization Trial #1	5	243	69%
Optimization Trial #2	3	27	61%
Optimization Trial #3	6	729	31%

A summary of the approximation results from the three optimization trials are shown in the Table 7-1. This table lists the number of design variables, cost (number of experiments), and design merit improvement for each respective optimization trial. These results show the first stage of the internal ballistic optimization strategy using a level-three full-factorial DOE was successful at consistently and effectively approximating a variety of solid rocket motor grain designs.

#### 7-1-2 Internal Ballistic Optimization Strategy Stage 2 Results

It was discovered through experimental data and validated through optimization trials 1, 2, and 3 presented in this paper, global optimization performed in the second stage of the ballistic optimization strategy was the most effective stage of optimization solid rocket motor grain designs to ballistic requirements. Global optimization performed a stochastic search that relied on evolution and inheritance to optimize the design.

Table 7-2 – Summary of optimization results from three optimization trials.

	No. of Design Variables	Cost	Merit Improvement
Optimization Trial #1	5	1250	99%
Optimization Trial #2	3	625	96%
Optimization Trial #3	5	1000	47%

A summary of the second stage optimization results from the three optimization trials are shown in the Table 7-2 below. This table lists the number of design variables, cost (number of iterations), and design merit improvement for each respective optimization trial. Note, the merit improvement posted in the table represents the improvement in merit from the second stage of the optimization process alone and does not represent any combined improvement from the first stage of the strategy. These results overwhelmingly show the second stage of the internal ballistic optimization strategy using global optimization techniques of the genetic algorithm was successful at consistently and effectively optimizing a variety of solid rocket motor grain designs.

### 7-1-3 Internal Ballistic Optimization Strategy Stage 3 Results

The final stage of the internal ballistic optimization strategy used high-fidelity gradient-based optimization techniques to fine tune solid rocket motor grain designs to meet internal ballistic requirements of thrust and/or burn-area versus web distance. Through experimental data from optimization trials 1, 2, and 3 presented in this thesis,

the Broyden, Fletcher, Goldfarb, and Shanno (BFGS) algorithm was effective at optimizing solid rocket motor grain designs to meet the requirement. Unique to this stage, weighting was applied to the objective function. This allowed response sensitivity to be increased and areas on a respective grains internal ballistic curve that departed from the requirement were able to be targeted. This proved to be a powerful tool that enabled this stage of the optimization strategy to optimize solid rocket motor grains to the point of satisfying their respective requirements.

Table 7-3 – Summary of high-fidelity optimization results from three optimization trials.

	No. of Design Variables	Cost	Merit Improvement
Optimization Trial #1	5	115	92%
Optimization Trial #2	3	17	97%
Optimization Trial #3	1000	69	31%

A summary of the third stage optimization results from the three optimization trials are shown in the Table 7-3 below. This table lists the number of design variables, cost (number of iterations), and design merit improvement for each respective optimization trial. Note, the merit improvement posted in the table represents the improvement in merit from the third stage of the optimization process alone and does not represent any combined improvement from the first and/or second stages of the strategy.

These results show the third stage of the internal ballistic optimization strategy using a high-fidelity gradient-based optimization algorithm was successful at consistently and effectively optimizing a variety of solid rocket motor grain designs.

#### 7-1-4 Summary Results of Internal Ballistic Optimization Strategy

In summary, the internal ballistic optimization strategy proved to be successful at optimizing solid rocket motor grain designs consistently and effectively. Each stage of the strategy was successful at contributing to the over all success of the strategy, and the methods used in each stage of the strategy compensated for weaknesses of the previous stages. For example, the method in the second stage of the strategy did not suffer the stagnation problems inherit to the method used in the third stage of the strategy.

Table 7-4 – Summary of results from the internal ballistic optimization strategy.

	No. of Design Variables	Merit Improvement
Optimization Trial #1	5	99.9%
Optimization Trial #2	3	99.9%
Optimization Trial #3	5	74.7%

Table 7-4 represents a summary of the design improvements in respective solid rocket motor grain designs produced by the internal ballistic optimization strategy.

Results shown in this table combine the optimization results from all three stages of the

strategy. Designs in optimization trials 1 and 2 met the goal of improving the design by more than 90% with respect to the base design and the design in optimization trial 3 came within 15 percent of the goal.

## 7-2 Conclusion of Work

Ballistic design optimization has been performed on three different solid rocket motor grain designs of varying complexity and practicality. These solid rocket motor grain designs were optimized on the basis of ballistic properties including thrust-time and burn-area-versus-distance requirements. Key contributions of this research are summarized in the following:

1. A three stage optimization strategy was developed (*the internal ballistic optimization strategy*) with the purpose of optimizing solid rocket motor grains for internal ballistic performance.
2. The internal ballistic optimization strategy can successfully fit the internal ballistic product of a solid rocket motor grain (thrust) to a required thrust-time curve.
3. Three solid rocket motor grains of varying complexity were optimized using the internal ballistic optimization strategy.
4. *The ballistic optimization strategy* was developed to work in any AML environment and incorporated the demand-driven dependency-tracking object-oriented features of AML.
5. In addition to the development of the optimization strategy, AML code was written that would create and burn solid rocket motor grains.

Though the use of the AML environment, the optimization process for each individual stage of the optimization strategy was made to run seamlessly during the optimization process. As a result, the computational time was reduced and design efficiency was increased. Also, integrated into this environment was the optimization interface AMOPT developed and supported by TechnoSoft. AMOPT provided an environment for hosting the optimization model (design variable, constraint, and objective function definitions), optimization algorithms, and an interface to third party optimization algorithms developed by Vanderplaats Research and Development (developers of Design Optimization Tools).

The three stage internal ballistic optimization strategy presented herein was developed as a “general purpose” optimization strategy for designing solid rocket propellant grains of any geometry/requirement. This strategy has been applied to solid rocket motor design tools extracted from Interactive Missile Design (IMD) developed by Lockheed Martin, Missiles and Fire Control.

### 7-3 Recommendations

Based on the research presented in this paper, the following text details recommendations from the author for further enhancement and expansion of the ballistic optimization strategy.

First, improvements to the optimization formulation are recommended to allow for the optional inclusion of standard constraints into the objective function formulation. Constraints involving the following solid rocket motor characteristics are considered

standard: *Total Impulse* (the product of thrust and duration), *Space Factor* (the ration of propellant volume to the chamber volume), and *Propellant Weight* (weight of the propellant contained within the combustion chamber). By formulating these constraints into the objective function, the use of extraneous constraints (i.e. inequality constraints) to achieve the same effect would no longer be required. This would allow the genetic algorithm and first-order gradient-based algorithms that normally do not consider constraint responses to allow constraints to effect the design.

Second, it is recommend to understand the benefit of weighting the objective function. This operation will increase response sensitivity at points on the response curve where weights are applied. As the optimization process approaches an optimum, there is a likelihood of significantly decreased response sensitivity. Weighting can be used to mitigate this problem which causes premature termination of the optimization process.

Finally, additionally work should include a better means of handling discrete design variables in the optimization process.

## APPENDIX A: STAGE #1 – DESIGN APPROXIMATION

## A-1 Appendix Overview

Contained in this appendix are the approximation results from three separate solid rocket motor design approximations performed in the first stage of the ballistic optimization strategy described in this paper. Solid rocket motor grain designs were approximated using a level-three full-factorial DOE such that the thrust product of the designs performed better with respect to given thrust-time requirements. The design approximation results are presented in plotted and tabular form. The following lists the contents of each section in this appendix.

Section A-2 contains the approximation responses represented in plotted form.

Section A-3 contains the tabular approximation results for the Multi-cylinder grain.

Section A-4 contains the tabular approximation results for the CASTOR1 grain.

Section A-5 contains the tabular approximation results for the Complex grain.

## A-2 Approximation Response Plots: Trials 1, 2, and 3

The following three figures show the approximation responses graphed versus iteration for three different solid rocket motor grains: the Multi-cylinder grain, the CASTOR grain, and the Complex grain. Figure A-1 plots the approximation response to the multi-cylinder grain design approximation. Figure A-2 plots the approximation response to the CASTOR1 grain design approximation, and Figure A-3 plots the approximation response to the Complex grain design approximation.

Each plot represents the design approximation results in two series. The series labeled “Raw DOE Response” represents the raw approximation response, and next, the series labeled “Sorted Feasible DOE Response” represents only a subset of feasible approximation responses sorted in order of increase design merit (a merit of zero represents the perfect design).

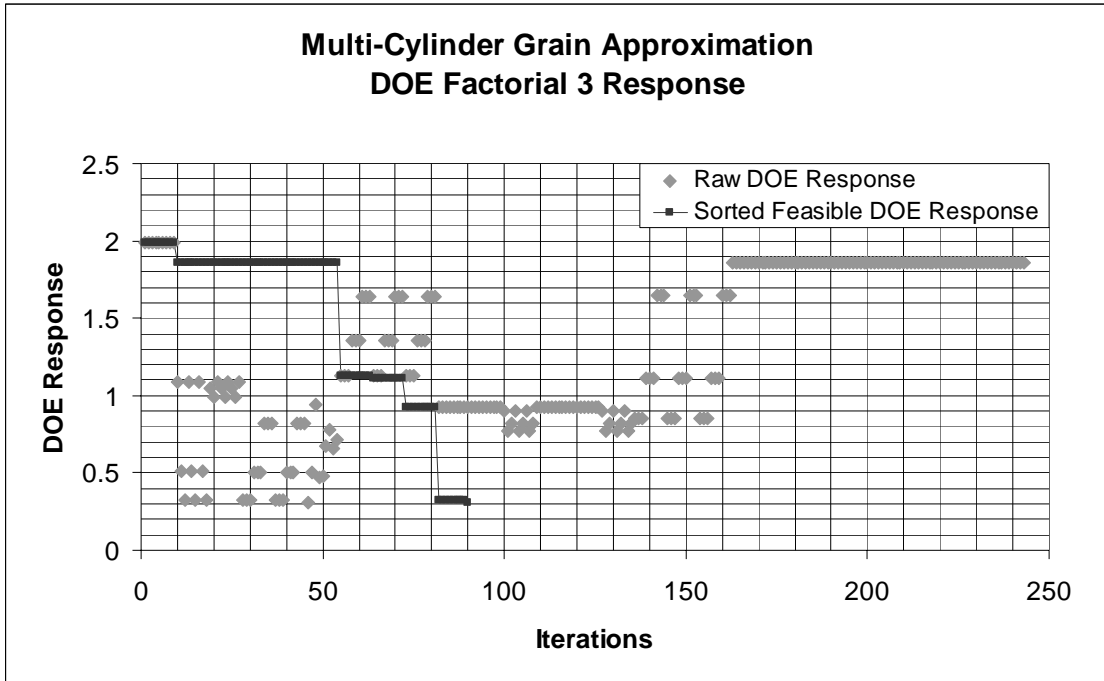


Figure A-1 – DOE approximation responses from the Multi-cylinder grain design.

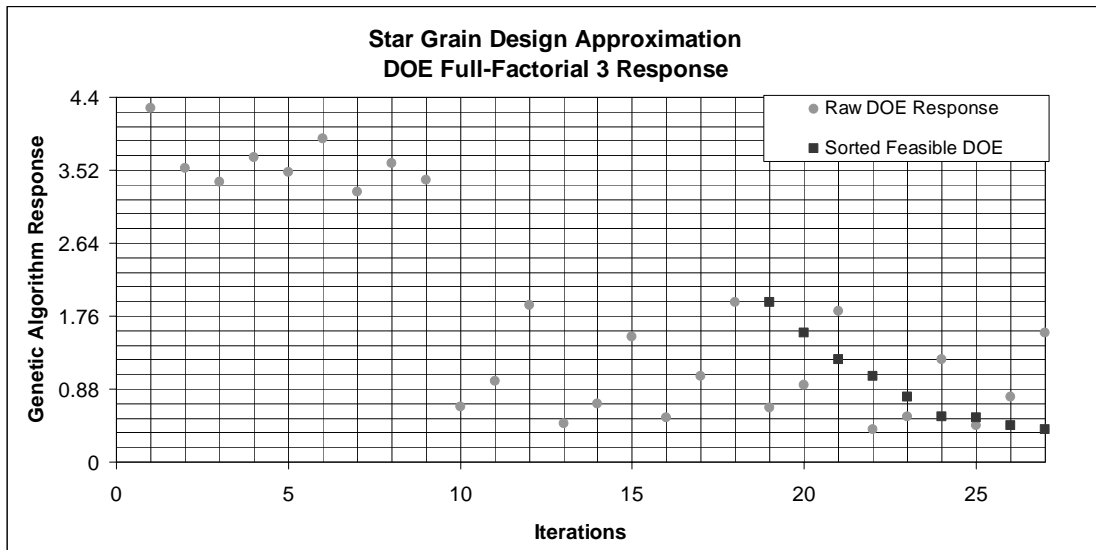


Figure A-2 – DOE approximation responses from the Star grain design.

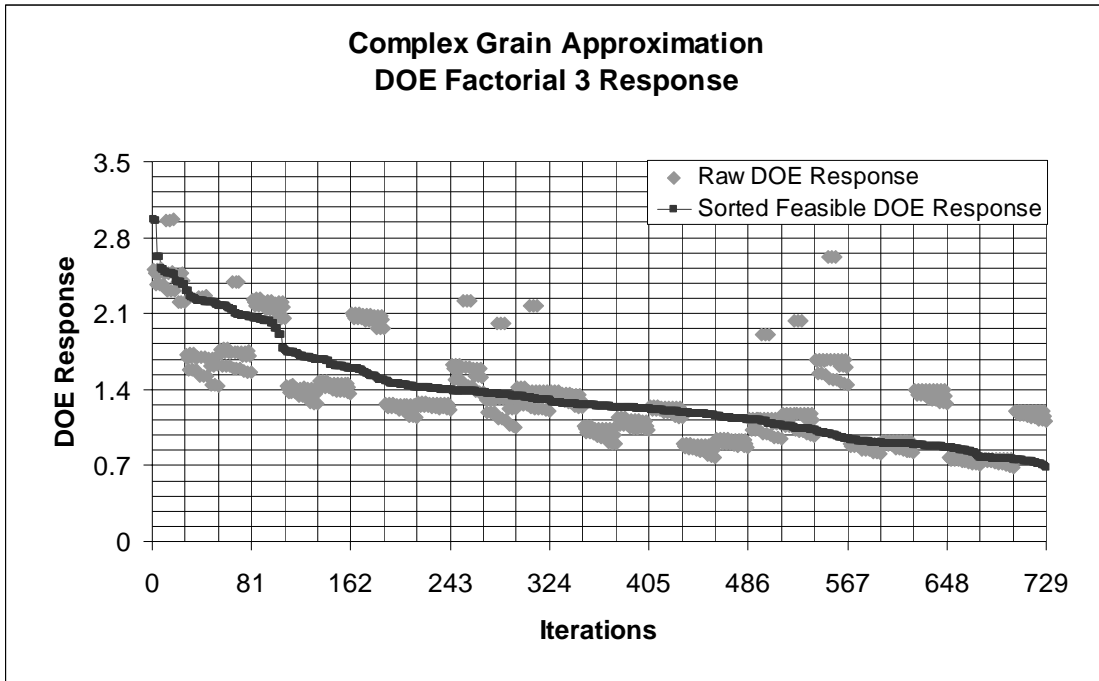


Figure A-3 – DOE approximation responses from the Complex grain design.

### A-3 Approximation Responses: Optimization Trial 1

Table A-1 lists results of a three-level full factorial DOE design approximation performed on the multi-cylinder solid rocket motor grain design. Columns labeled with the prefix *dv-* contain design variable values per iteration for the respective design variable name following the hyphen. Columns labeled *con1* and *con2* contain design constraint responses, and the column labeled *DLSM* (short for *Damped Least Squares Method*) contains the objective-function response per iteration. Note, Iteration 46 produced the approximated design with the highest merit (minimum objective function response).

Table A-1 – Multi-cylinder grain full-factorial 3-level DOE approximation responses.

<i>Iteration</i>	<i>dv-d1</i>	<i>dv-d2</i>	<i>dv-d3</i>	<i>dv-l5</i>	<i>dv-l6</i>	<i>con1</i>	<i>con2</i>	<i>DLSM</i>
1	0.15	0.15	0.15	0.5	0.1	0	0	1.98794
2	0.15	0.15	0.15	0.5	0.275	0	0	1.98794
3	0.15	0.15	0.15	0.5	0.45	0	0	1.98794
4	0.15	0.15	0.15	0.7	0.1	0	0	1.98794
5	0.15	0.15	0.15	0.7	0.275	0	0	1.98794
6	0.15	0.15	0.15	0.7	0.45	0	0	1.98794
7	0.15	0.15	0.15	0.9	0.1	0	0	1.98794
8	0.15	0.15	0.15	0.9	0.275	0	0	1.98794
9	0.15	0.15	0.15	0.9	0.45	0	0	1.98794
10	0.15	0.15	0.525	0.5	0.1	0	-0.71	1.08666
11	0.15	0.15	0.525	0.5	0.275	0	-0.71	0.51449
12	0.15	0.15	0.525	0.5	0.45	0	-0.71	0.32811
13	0.15	0.15	0.525	0.7	0.1	0	-0.71	1.08666
14	0.15	0.15	0.525	0.7	0.275	0	-0.71	0.51449
15	0.15	0.15	0.525	0.7	0.45	0	-0.71	0.32811
16	0.15	0.15	0.525	0.9	0.1	0	-0.71	1.08666
17	0.15	0.15	0.525	0.9	0.275	0	-0.71	0.51449
18	0.15	0.15	0.525	0.9	0.45	0	-0.71	0.32811
19	0.15	0.15	0.9	0.5	0.1	0	-0.83	1.04758
20	0.15	0.15	0.9	0.5	0.275	0	-0.83	0.99198

<i>Iteration</i>	<i>dv-d1</i>	<i>dv-d2</i>	<i>dv-d3</i>	<i>dv-l5</i>	<i>dv-l6</i>	<i>con1</i>	<i>con2</i>	<i>DLMS</i>
21	0.15	0.15	0.9	0.5	0.45	0	-0.83	1.08942
22	0.15	0.15	0.9	0.7	0.1	0	-0.83	1.04758
23	0.15	0.15	0.9	0.7	0.275	0	-0.83	0.99198
24	0.15	0.15	0.9	0.7	0.45	0	-0.83	1.08942
25	0.15	0.15	0.9	0.9	0.1	0	-0.83	1.04758
26	0.15	0.15	0.9	0.9	0.275	0	-0.83	0.99198
27	0.15	0.15	0.9	0.9	0.45	0	-0.83	1.08942
28	0.15	0.525	0.15	0.5	0.1	-0.71	2.5	0.32289
29	0.15	0.525	0.15	0.5	0.275	-0.71	2.5	0.32289
30	0.15	0.525	0.15	0.5	0.45	-0.71	2.5	0.32289
31	0.15	0.525	0.15	0.7	0.1	-0.71	2.5	0.49964
32	0.15	0.525	0.15	0.7	0.275	-0.71	2.5	0.49964
33	0.15	0.525	0.15	0.7	0.45	-0.71	2.5	0.49964
34	0.15	0.525	0.15	0.9	0.1	-0.71	2.5	0.81871
35	0.15	0.525	0.15	0.9	0.275	-0.71	2.5	0.81871
36	0.15	0.525	0.15	0.9	0.45	-0.71	2.5	0.81871
37	0.15	0.525	0.525	0.5	0.1	-0.71	0	0.32289
38	0.15	0.525	0.525	0.5	0.275	-0.71	0	0.32289
39	0.15	0.525	0.525	0.5	0.45	-0.71	0	0.32289
40	0.15	0.525	0.525	0.7	0.1	-0.71	0	0.49964
41	0.15	0.525	0.525	0.7	0.275	-0.71	0	0.49964
42	0.15	0.525	0.525	0.7	0.45	-0.71	0	0.49964
43	0.15	0.525	0.525	0.9	0.1	-0.71	0	0.81871
44	0.15	0.525	0.525	0.9	0.275	-0.71	0	0.81871
45	0.15	0.525	0.525	0.9	0.45	-0.71	0	0.81871
46	0.15	0.525	0.9	0.5	0.1	-0.71	-0.42	0.30934
47	0.15	0.525	0.9	0.5	0.275	-0.71	-0.42	0.50118
48	0.15	0.525	0.9	0.5	0.45	-0.71	-0.42	0.94383
49	0.15	0.525	0.9	0.7	0.1	-0.71	-0.42	0.47144
50	0.15	0.525	0.9	0.7	0.275	-0.71	-0.42	0.47979
51	0.15	0.525	0.9	0.7	0.45	-0.71	-0.42	0.67295
52	0.15	0.525	0.9	0.9	0.1	-0.71	-0.42	0.78148
53	0.15	0.525	0.9	0.9	0.275	-0.71	-0.42	0.65895
54	0.15	0.525	0.9	0.9	0.45	-0.71	-0.42	0.71526
55	0.15	0.9	0.15	0.5	0.1	-0.83	5	1.13199
56	0.15	0.9	0.15	0.5	0.275	-0.83	5	1.13199
57	0.15	0.9	0.15	0.5	0.45	-0.83	5	1.13199
58	0.15	0.9	0.15	0.7	0.1	-0.83	5	1.35649
59	0.15	0.9	0.15	0.7	0.275	-0.83	5	1.35649
60	0.15	0.9	0.15	0.7	0.45	-0.83	5	1.35649
61	0.15	0.9	0.15	0.9	0.1	-0.83	5	1.63909
62	0.15	0.9	0.15	0.9	0.275	-0.83	5	1.63909
63	0.15	0.9	0.15	0.9	0.45	-0.83	5	1.63909
64	0.15	0.9	0.525	0.5	0.1	-0.83	0.714	1.13199
65	0.15	0.9	0.525	0.5	0.275	-0.83	0.714	1.13199
66	0.15	0.9	0.525	0.5	0.45	-0.83	0.714	1.13199

<i>Iteration</i>	<i>dv-d1</i>	<i>dv-d2</i>	<i>dv-d3</i>	<i>dv-l5</i>	<i>dv-l6</i>	<i>con1</i>	<i>con2</i>	<i>DLSM</i>
67	0.15	0.9	0.525	0.7	0.1	-0.83	0.714	1.35649
68	0.15	0.9	0.525	0.7	0.275	-0.83	0.714	1.35649
69	0.15	0.9	0.525	0.7	0.45	-0.83	0.714	1.35649
70	0.15	0.9	0.525	0.9	0.1	-0.83	0.714	1.63909
71	0.15	0.9	0.525	0.9	0.275	-0.83	0.714	1.63909
72	0.15	0.9	0.525	0.9	0.45	-0.83	0.714	1.63909
73	0.15	0.9	0.9	0.5	0.1	-0.83	0	1.13199
74	0.15	0.9	0.9	0.5	0.275	-0.83	0	1.13199
75	0.15	0.9	0.9	0.5	0.45	-0.83	0	1.13199
76	0.15	0.9	0.9	0.7	0.1	-0.83	0	1.35649
77	0.15	0.9	0.9	0.7	0.275	-0.83	0	1.35649
78	0.15	0.9	0.9	0.7	0.45	-0.83	0	1.35649
79	0.15	0.9	0.9	0.9	0.1	-0.83	0	1.63909
80	0.15	0.9	0.9	0.9	0.275	-0.83	0	1.63909
81	0.15	0.9	0.9	0.9	0.45	-0.83	0	1.63909
82	0.525	0.15	0.15	0.5	0.1	2.5	0	0.92808
83	0.525	0.15	0.15	0.5	0.275	2.5	0	0.92808
84	0.525	0.15	0.15	0.5	0.45	2.5	0	0.92808
85	0.525	0.15	0.15	0.7	0.1	2.5	0	0.92808
86	0.525	0.15	0.15	0.7	0.275	2.5	0	0.92808
87	0.525	0.15	0.15	0.7	0.45	2.5	0	0.92808
88	0.525	0.15	0.15	0.9	0.1	2.5	0	0.92808
89	0.525	0.15	0.15	0.9	0.275	2.5	0	0.92808
90	0.525	0.15	0.15	0.9	0.45	2.5	0	0.92808
91	0.525	0.15	0.525	0.5	0.1	2.5	-0.71	0.92808
92	0.525	0.15	0.525	0.5	0.275	2.5	-0.71	0.92808
93	0.525	0.15	0.525	0.5	0.45	2.5	-0.71	0.92808
94	0.525	0.15	0.525	0.7	0.1	2.5	-0.71	0.92808
95	0.525	0.15	0.525	0.7	0.275	2.5	-0.71	0.92808
96	0.525	0.15	0.525	0.7	0.45	2.5	-0.71	0.92808
97	0.525	0.15	0.525	0.9	0.1	2.5	-0.71	0.92808
98	0.525	0.15	0.525	0.9	0.275	2.5	-0.71	0.92808
99	0.525	0.15	0.525	0.9	0.45	2.5	-0.71	0.92808
100	0.525	0.15	0.9	0.5	0.1	2.5	-0.83	0.89922
101	0.525	0.15	0.9	0.5	0.275	2.5	-0.83	0.77337
102	0.525	0.15	0.9	0.5	0.45	2.5	-0.83	0.82068
103	0.525	0.15	0.9	0.7	0.1	2.5	-0.83	0.89922
104	0.525	0.15	0.9	0.7	0.275	2.5	-0.83	0.77337
105	0.525	0.15	0.9	0.7	0.45	2.5	-0.83	0.82068
106	0.525	0.15	0.9	0.9	0.1	2.5	-0.83	0.89922
107	0.525	0.15	0.9	0.9	0.275	2.5	-0.83	0.77337
108	0.525	0.15	0.9	0.9	0.45	2.5	-0.83	0.82068
109	0.525	0.525	0.15	0.5	0.1	0	2.5	0.92808
110	0.525	0.525	0.15	0.5	0.275	0	2.5	0.92808
111	0.525	0.525	0.15	0.5	0.45	0	2.5	0.92808
112	0.525	0.525	0.15	0.7	0.1	0	2.5	0.92808

<i>Iteration</i>	<i>dv-d1</i>	<i>dv-d2</i>	<i>dv-d3</i>	<i>dv-l5</i>	<i>dv-l6</i>	<i>con1</i>	<i>con2</i>	<i>DLMS</i>
113	0.525	0.525	0.15	0.7	0.275	0	2.5	0.92808
114	0.525	0.525	0.15	0.7	0.45	0	2.5	0.92808
115	0.525	0.525	0.15	0.9	0.1	0	2.5	0.92808
116	0.525	0.525	0.15	0.9	0.275	0	2.5	0.92808
117	0.525	0.525	0.15	0.9	0.45	0	2.5	0.92808
118	0.525	0.525	0.525	0.5	0.1	0	0	0.92808
119	0.525	0.525	0.525	0.5	0.275	0	0	0.92808
120	0.525	0.525	0.525	0.5	0.45	0	0	0.92808
121	0.525	0.525	0.525	0.7	0.1	0	0	0.92808
122	0.525	0.525	0.525	0.7	0.275	0	0	0.92808
123	0.525	0.525	0.525	0.7	0.45	0	0	0.92808
124	0.525	0.525	0.525	0.9	0.1	0	0	0.92808
125	0.525	0.525	0.525	0.9	0.275	0	0	0.92808
126	0.525	0.525	0.525	0.9	0.45	0	0	0.92808
127	0.525	0.525	0.9	0.5	0.1	0	-0.42	0.89922
128	0.525	0.525	0.9	0.5	0.275	0	-0.42	0.77337
129	0.525	0.525	0.9	0.5	0.45	0	-0.42	0.82068
130	0.525	0.525	0.9	0.7	0.1	0	-0.42	0.89922
131	0.525	0.525	0.9	0.7	0.275	0	-0.42	0.77337
132	0.525	0.525	0.9	0.7	0.45	0	-0.42	0.82068
133	0.525	0.525	0.9	0.9	0.1	0	-0.42	0.89922
134	0.525	0.525	0.9	0.9	0.275	0	-0.42	0.77337
135	0.525	0.525	0.9	0.9	0.45	0	-0.42	0.82068
136	0.525	0.9	0.15	0.5	0.1	-0.42	5	0.85605
137	0.525	0.9	0.15	0.5	0.275	-0.42	5	0.85605
138	0.525	0.9	0.15	0.5	0.45	-0.42	5	0.85605
139	0.525	0.9	0.15	0.7	0.1	-0.42	5	1.11337
140	0.525	0.9	0.15	0.7	0.275	-0.42	5	1.11337
141	0.525	0.9	0.15	0.7	0.45	-0.42	5	1.11337
142	0.525	0.9	0.15	0.9	0.1	-0.42	5	1.6445
143	0.525	0.9	0.15	0.9	0.275	-0.42	5	1.6445
144	0.525	0.9	0.15	0.9	0.45	-0.42	5	1.6445
145	0.525	0.9	0.525	0.5	0.1	-0.42	0.714	0.85605
146	0.525	0.9	0.525	0.5	0.275	-0.42	0.714	0.85605
147	0.525	0.9	0.525	0.5	0.45	-0.42	0.714	0.85605
148	0.525	0.9	0.525	0.7	0.1	-0.42	0.714	1.11337
149	0.525	0.9	0.525	0.7	0.275	-0.42	0.714	1.11337
150	0.525	0.9	0.525	0.7	0.45	-0.42	0.714	1.11337
151	0.525	0.9	0.525	0.9	0.1	-0.42	0.714	1.6445
152	0.525	0.9	0.525	0.9	0.275	-0.42	0.714	1.6445
153	0.525	0.9	0.525	0.9	0.45	-0.42	0.714	1.6445
154	0.525	0.9	0.9	0.5	0.1	-0.42	0	0.85605
155	0.525	0.9	0.9	0.5	0.275	-0.42	0	0.85605
156	0.525	0.9	0.9	0.5	0.45	-0.42	0	0.85605
157	0.525	0.9	0.9	0.7	0.1	-0.42	0	1.11337
158	0.525	0.9	0.9	0.7	0.275	-0.42	0	1.11337

<i>Iteration</i>	<i>dv-d1</i>	<i>dv-d2</i>	<i>dv-d3</i>	<i>dv-l5</i>	<i>dv-l6</i>	<i>con1</i>	<i>con2</i>	<i>DLMS</i>
159	0.525	0.9	0.9	0.7	0.45	-0.42	0	1.11337
160	0.525	0.9	0.9	0.9	0.1	-0.42	0	1.6445
161	0.525	0.9	0.9	0.9	0.275	-0.42	0	1.6445
162	0.525	0.9	0.9	0.9	0.45	-0.42	0	1.6445
163	0.9	0.15	0.15	0.5	0.1	5	0	1.85633
164	0.9	0.15	0.15	0.5	0.275	5	0	1.85633
165	0.9	0.15	0.15	0.5	0.45	5	0	1.85633
166	0.9	0.15	0.15	0.7	0.1	5	0	1.85633
167	0.9	0.15	0.15	0.7	0.275	5	0	1.85633
168	0.9	0.15	0.15	0.7	0.45	5	0	1.85633
169	0.9	0.15	0.15	0.9	0.1	5	0	1.85633
170	0.9	0.15	0.15	0.9	0.275	5	0	1.85633
171	0.9	0.15	0.15	0.9	0.45	5	0	1.85633
172	0.9	0.15	0.525	0.5	0.1	5	-0.71	1.85633
173	0.9	0.15	0.525	0.5	0.275	5	-0.71	1.85633
174	0.9	0.15	0.525	0.5	0.45	5	-0.71	1.85633
175	0.9	0.15	0.525	0.7	0.1	5	-0.71	1.85633
176	0.9	0.15	0.525	0.7	0.275	5	-0.71	1.85633
177	0.9	0.15	0.525	0.7	0.45	5	-0.71	1.85633
178	0.9	0.15	0.525	0.9	0.1	5	-0.71	1.85633
179	0.9	0.15	0.525	0.9	0.275	5	-0.71	1.85633
180	0.9	0.15	0.525	0.9	0.45	5	-0.71	1.85633
181	0.9	0.15	0.9	0.5	0.1	5	-0.83	1.85633
182	0.9	0.15	0.9	0.5	0.275	5	-0.83	1.85633
183	0.9	0.15	0.9	0.5	0.45	5	-0.83	1.85633
184	0.9	0.15	0.9	0.7	0.1	5	-0.83	1.85633
185	0.9	0.15	0.9	0.7	0.275	5	-0.83	1.85633
186	0.9	0.15	0.9	0.7	0.45	5	-0.83	1.85633
187	0.9	0.15	0.9	0.9	0.1	5	-0.83	1.85633
188	0.9	0.15	0.9	0.9	0.275	5	-0.83	1.85633
189	0.9	0.15	0.9	0.9	0.45	5	-0.83	1.85633
190	0.9	0.525	0.15	0.5	0.1	0.714	2.5	1.85633
191	0.9	0.525	0.15	0.5	0.275	0.714	2.5	1.85633
192	0.9	0.525	0.15	0.5	0.45	0.714	2.5	1.85633
193	0.9	0.525	0.15	0.7	0.1	0.714	2.5	1.85633
194	0.9	0.525	0.15	0.7	0.275	0.714	2.5	1.85633
195	0.9	0.525	0.15	0.7	0.45	0.714	2.5	1.85633
196	0.9	0.525	0.15	0.9	0.1	0.714	2.5	1.85633
197	0.9	0.525	0.15	0.9	0.275	0.714	2.5	1.85633
198	0.9	0.525	0.15	0.9	0.45	0.714	2.5	1.85633
199	0.9	0.525	0.525	0.5	0.1	0.714	0	1.85633
200	0.9	0.525	0.525	0.5	0.275	0.714	0	1.85633
201	0.9	0.525	0.525	0.5	0.45	0.714	0	1.85633
202	0.9	0.525	0.525	0.7	0.1	0.714	0	1.85633
203	0.9	0.525	0.525	0.7	0.275	0.714	0	1.85633
204	0.9	0.525	0.525	0.7	0.45	0.714	0	1.85633

<i>Iteration</i>	<i>dv-d1</i>	<i>dv-d2</i>	<i>dv-d3</i>	<i>dv-l5</i>	<i>dv-l6</i>	<i>con1</i>	<i>con2</i>	<i>DLMS</i>
205	0.9	0.525	0.525	0.9	0.1	0.714	0	1.85633
206	0.9	0.525	0.525	0.9	0.275	0.714	0	1.85633
207	0.9	0.525	0.525	0.9	0.45	0.714	0	1.85633
208	0.9	0.525	0.9	0.5	0.1	0.714	-0.42	1.85633
209	0.9	0.525	0.9	0.5	0.275	0.714	-0.42	1.85633
210	0.9	0.525	0.9	0.5	0.45	0.714	-0.42	1.85633
211	0.9	0.525	0.9	0.7	0.1	0.714	-0.42	1.85633
212	0.9	0.525	0.9	0.7	0.275	0.714	-0.42	1.85633
213	0.9	0.525	0.9	0.7	0.45	0.714	-0.42	1.85633
214	0.9	0.525	0.9	0.9	0.1	0.714	-0.42	1.85633
215	0.9	0.525	0.9	0.9	0.275	0.714	-0.42	1.85633
216	0.9	0.525	0.9	0.9	0.45	0.714	-0.42	1.85633
217	0.9	0.9	0.15	0.5	0.1	0	5	1.85633
218	0.9	0.9	0.15	0.5	0.275	0	5	1.85633
219	0.9	0.9	0.15	0.5	0.45	0	5	1.85633
220	0.9	0.9	0.15	0.7	0.1	0	5	1.85633
221	0.9	0.9	0.15	0.7	0.275	0	5	1.85633
222	0.9	0.9	0.15	0.7	0.45	0	5	1.85633
223	0.9	0.9	0.15	0.9	0.1	0	5	1.85633
224	0.9	0.9	0.15	0.9	0.275	0	5	1.85633
225	0.9	0.9	0.15	0.9	0.45	0	5	1.85633
226	0.9	0.9	0.525	0.5	0.1	0	0.714	1.85633
227	0.9	0.9	0.525	0.5	0.275	0	0.714	1.85633
228	0.9	0.9	0.525	0.5	0.45	0	0.714	1.85633
229	0.9	0.9	0.525	0.7	0.1	0	0.714	1.85633
230	0.9	0.9	0.525	0.7	0.275	0	0.714	1.85633
231	0.9	0.9	0.525	0.7	0.45	0	0.714	1.85633
232	0.9	0.9	0.525	0.9	0.1	0	0.714	1.85633
233	0.9	0.9	0.525	0.9	0.275	0	0.714	1.85633
234	0.9	0.9	0.525	0.9	0.45	0	0.714	1.85633
235	0.9	0.9	0.9	0.5	0.1	0	0	1.85633
236	0.9	0.9	0.9	0.5	0.275	0	0	1.85633
237	0.9	0.9	0.9	0.5	0.45	0	0	1.85633
238	0.9	0.9	0.9	0.7	0.1	0	0	1.85633
239	0.9	0.9	0.9	0.7	0.275	0	0	1.85633
240	0.9	0.9	0.9	0.7	0.45	0	0	1.85633
241	0.9	0.9	0.9	0.9	0.1	0	0	1.85633
242	0.9	0.9	0.9	0.9	0.275	0	0	1.85633
243	0.9	0.9	0.9	0.9	0.45	0	0	1.85633

A-4 Approximation Responses: Optimization Trial 2

Table A-2 lists results of a three-level full factorial DOE design approximation performed on the star solid rocket motor grain design. Columns labeled with the prefix *dv-* contain design variable values per iteration for the respective design variable name following the hyphen. Columns labeled *con1* and *con2* contain design constraint responses, and the column labeled *DLSM* (short for *Damped Least Squares Method*) contains the objective-function response per iteration. Note, Iterations 19 and 20 produced the approximated design with the highest merit (minimum objective function response).

Table A-2 – Star grain full-factorial 3-level DOE approximation responses.

<i>Iterations</i>	<i>dv-fin-depth</i>	<i>dv-fin-thickness</i>	<i>dv-number-of-fins</i>	<i>DLSM</i>
1	0.1	0.01	4	4.16283
2	0.1	0.01	5	1.65183
3	0.1	0.01	6	0.95379
4	0.1	0.055	4	2.16851
5	0.1	0.055	5	1.7457
6	0.1	0.055	6	2.25963
7	0.1	0.1	4	1.76965
8	0.1	0.1	5	2.24865
9	0.1	0.1	6	1.96823
10	0.175	0.01	4	0.40069
11	0.175	0.01	5	0.70575
12	0.175	0.01	6	1.09412
13	0.175	0.055	4	0.80212
14	0.175	0.055	5	1.00955
15	0.175	0.055	6	1.21462
16	0.175	0.1	4	1.10333
17	0.175	0.1	5	1.29002
18	0.175	0.1	6	1.43517
19	0.25	0.01	4	0.40243
20	0.25	0.01	5	0.73408

<i>Iterations</i>	<i>dv-fin-depth</i>	<i>dv-fin-thickness</i>	<i>dv-number-of-fins</i>	<i>DLSM</i>
21	0.25	0.01	6	1.18118
22	0.25	0.055	4	1.13458
23	0.25	0.055	5	1.45254
24	0.25	0.055	6	1.82074
25	0.25	0.1	4	1.93789
26	0.25	0.1	5	2.27808
27	0.25	0.1	6	2.61185

A-5 Approximation Responses: Optimization Trial 3

Table A-3 lists the abridged results from the three-level full factorial DOE design approximation performed on the complex solid rocket motor grain design. Columns labeled with the prefix *dv-* contain design variable values per iteration for the respective design variable name following the hyphen. Columns labeled *con1* and *con2* contain design constraint responses, and the column labeled *DLSM* (short for *Damped Least Squares Method*) contains the objective-function response per iteration. Note, Iteration 702 produced the approximated design with the highest merit (minimum objective function response).

Table A-3 – Complex grain full-factorial 3-level DOE approximation responses.

<i>Iterations</i>	<i>dv-d1</i>	<i>dv-d2</i>	<i>dv-d3</i>	<i>dv-fin-length</i>	<i>dv-fin-thickness</i>	<i>dv-fin-depth</i>	<i>DLSM</i>
1	0.1	0.5	0.1	0.05	0.02	0.15	2.50
2	0.1	0.5	0.1	0.05	0.02	0.2	2.47
3	0.1	0.5	0.1	0.05	0.02	0.25	2.36
4	0.1	0.5	0.1	0.05	0.04	0.15	2.51
5	0.1	0.5	0.1	0.05	0.04	0.2	2.47
6	0.1	0.5	0.1	0.05	0.04	0.25	2.37
7	0.1	0.5	0.1	0.05	0.06	0.15	2.51
8	0.1	0.5	0.1	0.05	0.06	0.2	2.48
9	0.1	0.5	0.1	0.05	0.06	0.25	2.37
10	0.1	0.5	0.1	0.075	0.02	0.15	2.47
20	0.1	0.5	0.1	0.1	0.02	0.2	2.39
30	0.1	0.5	0.2	0.05	0.02	0.25	1.58
40	0.1	0.5	0.2	0.075	0.04	0.15	1.70
50	0.1	0.5	0.2	0.1	0.04	0.2	1.62
60	0.1	0.5	0.3	0.05	0.04	0.25	1.62
70	0.1	0.5	0.3	0.075	0.06	0.15	1.75
80	0.1	0.5	0.3	0.1	0.06	0.2	1.71
90	0.1	0.6	0.1	0.05	0.06	0.25	2.18
100	0.1	0.6	0.1	0.1	0.02	0.15	2.20
110	0.1	0.6	0.2	0.05	0.02	0.2	1.41

<i>Iterations</i>	<i>dv-d1</i>	<i>dv-d2</i>	<i>dv-d3</i>	<i>dv-fin-length</i>	<i>dv-fin-thickness</i>	<i>dv-fin-depth</i>	<i>DLSM</i>
120	0.1	0.6	0.2	0.075	0.02	0.25	1.34
130	0.1	0.6	0.2	0.1	0.04	0.15	1.41
140	0.1	0.6	0.3	0.05	0.04	0.2	1.45
150	0.1	0.6	0.3	0.075	0.04	0.25	1.39
160	0.1	0.6	0.3	0.1	0.06	0.15	1.46
170	0.1	0.7	0.1	0.05	0.06	0.2	2.08
180	0.1	0.7	0.1	0.075	0.06	0.25	2.04
190	0.1	0.7	0.2	0.05	0.02	0.15	1.27
200	0.1	0.7	0.2	0.075	0.02	0.2	1.24
210	0.1	0.7	0.2	0.1	0.02	0.25	1.16
220	0.1	0.7	0.3	0.05	0.04	0.15	1.28
230	0.1	0.7	0.3	0.075	0.04	0.2	1.25
240	0.1	0.7	0.3	0.1	0.04	0.25	1.22
250	0.2	0.5	0.1	0.05	0.06	0.15	1.63
260	0.2	0.5	0.1	0.075	0.06	0.2	2.22
270	0.2	0.5	0.1	0.1	0.06	0.25	1.37
280	0.2	0.5	0.2	0.075	0.02	0.15	1.31
290	0.2	0.5	0.2	0.1	0.02	0.2	1.23
300	0.2	0.5	0.3	0.05	0.02	0.25	1.26
310	0.2	0.5	0.3	0.075	0.04	0.15	1.39
320	0.2	0.5	0.3	0.1	0.04	0.2	1.34
330	0.2	0.6	0.1	0.05	0.04	0.25	1.32
340	0.2	0.6	0.1	0.075	0.06	0.15	1.36
350	0.2	0.6	0.1	0.1	0.06	0.2	1.30
360	0.2	0.6	0.2	0.05	0.06	0.25	1.00
370	0.2	0.6	0.2	0.1	0.02	0.15	1.04
380	0.2	0.6	0.3	0.05	0.02	0.2	1.11
390	0.2	0.6	0.3	0.075	0.02	0.25	1.05
400	0.2	0.6	0.3	0.1	0.04	0.15	1.11
410	0.2	0.7	0.1	0.05	0.04	0.2	1.23
420	0.2	0.7	0.1	0.075	0.04	0.25	1.19
430	0.2	0.7	0.1	0.1	0.06	0.15	1.23
440	0.2	0.7	0.2	0.05	0.06	0.2	0.88
450	0.2	0.7	0.2	0.075	0.06	0.25	0.83
460	0.2	0.7	0.3	0.05	0.02	0.15	0.95
470	0.2	0.7	0.3	0.075	0.02	0.2	0.92
480	0.2	0.7	0.3	0.1	0.02	0.25	0.90
490	0.3	0.5	0.1	0.05	0.04	0.15	1.13
500	0.3	0.5	0.1	0.075	0.04	0.2	1.91
510	0.3	0.5	0.1	0.1	0.04	0.25	0.96
520	0.3	0.5	0.2	0.05	0.06	0.15	1.18
530	0.3	0.5	0.2	0.075	0.06	0.2	2.03
540	0.3	0.5	0.2	0.1	0.06	0.25	0.98
550	0.3	0.5	0.3	0.075	0.02	0.15	1.68
560	0.3	0.5	0.3	0.1	0.02	0.2	1.62
570	0.3	0.6	0.1	0.05	0.02	0.25	0.87

<i>Iterations</i>	<i>dv-d1</i>	<i>dv-d2</i>	<i>dv-d3</i>	<i>dv-fin-length</i>	<i>dv-fin-thickness</i>	<i>dv-fin-depth</i>	<i>DLSM</i>
580	0.3	0.6	0.1	0.075	0.04	0.15	0.91
590	0.3	0.6	0.1	0.1	0.04	0.2	0.86
600	0.3	0.6	0.2	0.05	0.04	0.25	0.89
610	0.3	0.6	0.2	0.075	0.06	0.15	0.93
620	0.3	0.6	0.2	0.1	0.06	0.2	0.88
630	0.3	0.6	0.3	0.05	0.06	0.25	1.35
640	0.3	0.6	0.3	0.1	0.02	0.15	1.39
650	0.3	0.7	0.1	0.05	0.02	0.2	0.77
660	0.3	0.7	0.1	0.075	0.02	0.25	0.74
670	0.3	0.7	0.1	0.1	0.04	0.15	0.78
680	0.3	0.7	0.2	0.05	0.04	0.2	0.76
690	0.3	0.7	0.2	0.075	0.04	0.25	0.72
700	0.3	0.7	0.2	0.1	0.06	0.15	0.77
702	0.3	0.7	0.2	0.1	0.06	0.25	0.69
710	0.3	0.7	0.3	0.05	0.06	0.2	1.19
720	0.3	0.7	0.3	0.075	0.06	0.25	1.14

## APPENDIX B: STAGE #2 – DESIGN OPTIMIZATION

## B-1 Appendix Overview

Contained in this appendix are the optimization results from three separate solid rocket motor design optimizations performed in the second stage of the ballistic optimization strategy described in this paper. Solid rocket motor grain designs were optimized using genetic algorithms such that the thrust product of the designs performed better with respect to given thrust-time requirements. The design optimization results are presented in plotted and tabular form. The following lists the contents of each section in this appendix.

Section B-2 contains the optimization responses represented in plotted form.

Section B-3 contains the tabular optimization results for the Multi-cylinder grain.

Section B-4 contains the tabular optimization results for two Star grains.

Section B-5 contains the tabular optimization results for the Complex grain.

## B-2 Optimization Response Plots: Trials 1, 2, and 3

The following three figures show the optimization responses graphed versus iteration for three different solid rocket motor grains: the Multi-cylinder grain, the Star grain, and the Complex grain. Figure B-1 plots the optimization response for the multi-cylinder grain design optimization. Figure B-2 plots the optimization response for the star grain design optimization, and Figure B-3 plots the optimization response to the complex grain design optimization.

Each plot represents the design optimization results in two series. The series labeled “Raw Optimization Response” represents the raw approximation response, and next, the series labeled “Sorted Optimization Response” represents the optimization responses sorted in order of increasing design merit (a merit of zero represents the perfect design).

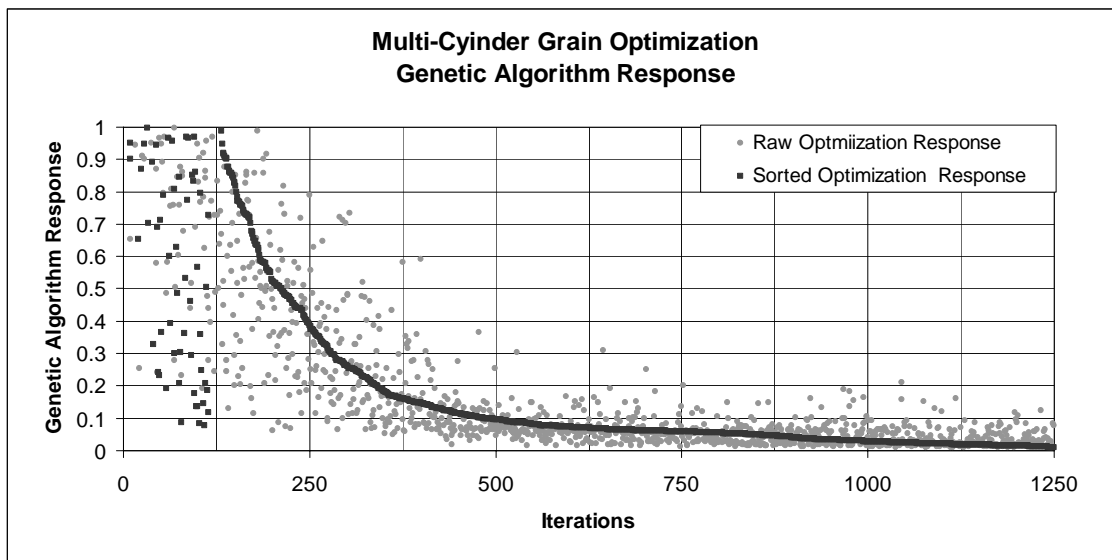
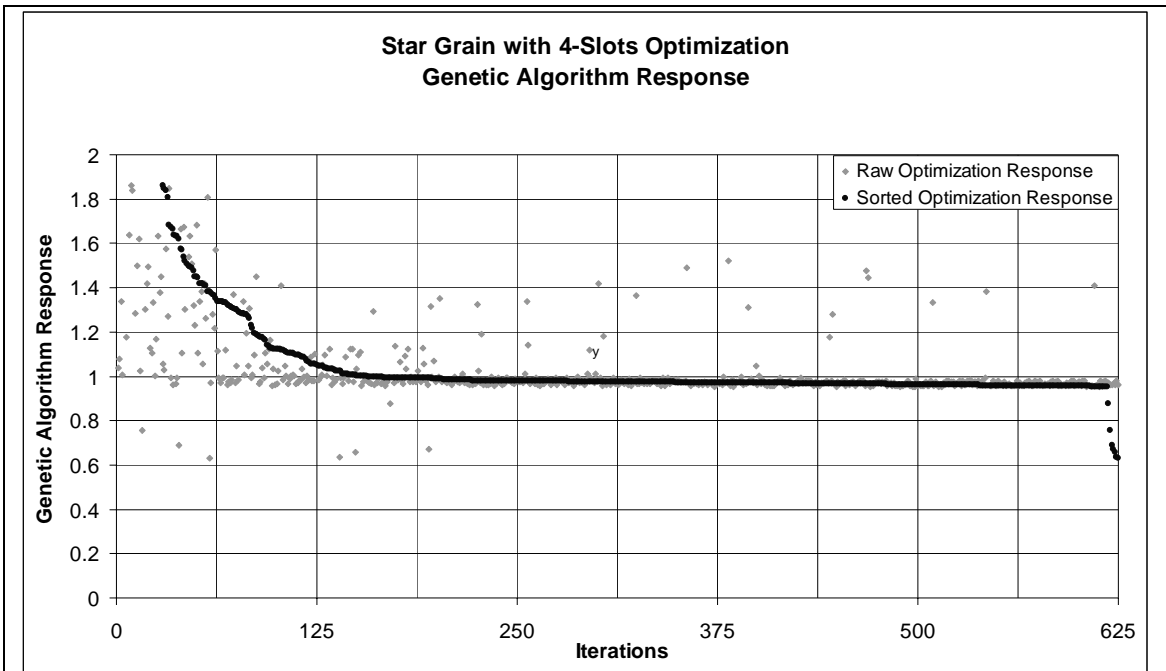
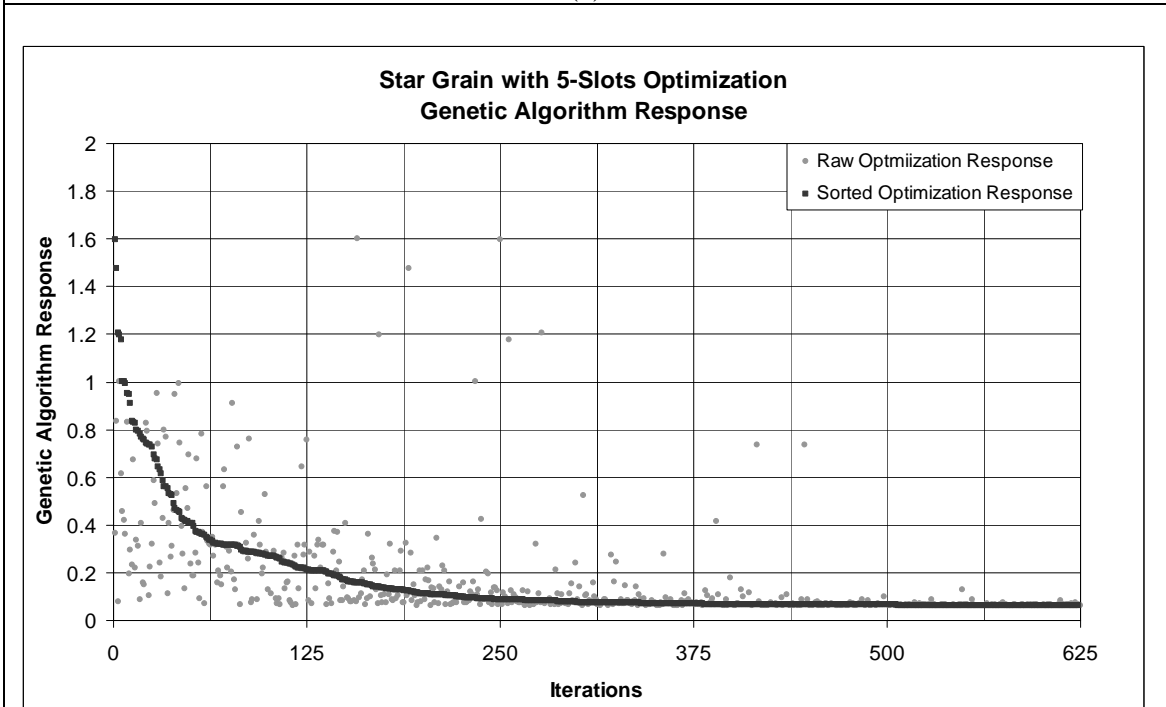


Figure B-1 – Optimization responses from the Multi-Cylinder grain design.



(a)



(b)

Figure B-2 – Optimization responses from (a) the Star grain design with 5-slots and (b) the Star grain design with 4-slots.

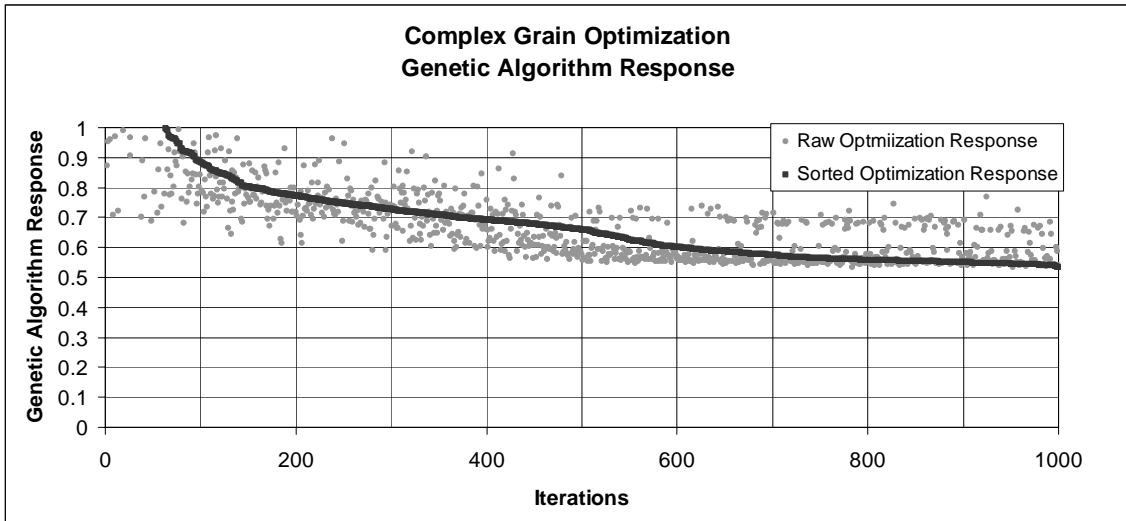


Figure B-3 – Optimization responses from the Complex grain design.

### B-3 Optimization Responses: Optimization Trial 1

Table B-1 lists design optimization results from the experiment of using genetic optimization algorithm to optimize the multi-cylinder solid rocket motor grain design for thrust-time performance. Columns labeled with the prefix *dv-* contain design variable values per iteration for the respective design variable name following the hyphen. The column labeled *DLSM* (short for *Damped Least Squares Method*) contains the objective-function responses, and the column labeled *Penalty* contains constraint response information. A penalty value of zero (0.000) indicates the grain design satisfied all constraints, and a penalty value greater than zero indicates a design violated at least one constraint. Note, Iteration 1220 produced the approximated design with the highest merit (minimum objective function response).

Table B-1 – Multi-cylinder grain abridged genetic optimization response.

<i>Iteration</i>	<i>dv-d1</i>	<i>dv-d2</i>	<i>dv-d3</i>	<i>dv-l5</i>	<i>dv-l6</i>	<i>DLSM</i>	<i>Penalty</i>
10	0.269	0.568	0.247	0.651	0.354	0.654	1.223
20	0.833	0.391	0.393	0.570	0.192	2.642	1.085
30	0.457	0.773	0.327	0.726	0.238	1.769	1.297
40	0.521	0.685	0.775	0.608	0.300	1.928	0.000
50	0.498	0.403	0.795	0.554	0.448	1.235	0.225
60	0.496	0.353	0.515	0.666	0.311	1.157	0.385
70	0.373	0.359	0.540	0.556	0.370	0.504	0.037
80	0.388	0.484	0.788	0.589	0.264	0.847	0.000
90	0.229	0.378	0.743	0.677	0.294	0.439	0.000
100	0.634	0.696	0.610	0.845	0.326	2.270	0.138
110	0.150	0.314	0.900	0.594	0.450	0.863	0.000
120	0.472	0.415	0.817	0.630	0.221	0.970	0.130
130	0.162	0.292	0.851	0.883	0.446	0.739	0.000
140	0.360	0.375	0.288	0.833	0.215	0.601	0.287
150	0.333	0.297	0.484	0.832	0.356	0.293	0.115
160	0.233	0.328	0.732	0.672	0.331	0.255	0.000

<i>Iteration</i>	<i>dv-d1</i>	<i>dv-d2</i>	<i>dv-d3</i>	<i>dv-l5</i>	<i>dv-l6</i>	<i>DLSM</i>	<i>Penalty</i>
170	0.387	0.363	0.571	0.557	0.361	0.567	0.062
180	0.408	0.900	0.900	0.500	0.100	0.988	0.000
190	0.153	0.273	0.704	0.684	0.218	0.206	0.000
200	0.250	0.305	0.591	0.724	0.232	0.063	0.000
210	0.206	0.361	0.729	0.654	0.332	0.354	0.000
220	0.202	0.369	0.821	0.706	0.418	0.523	0.000
230	0.151	0.344	0.890	0.671	0.413	0.581	0.000
240	0.151	0.210	0.712	0.752	0.344	0.477	0.000
250	0.433	0.309	0.558	0.758	0.376	0.789	0.381
260	0.196	0.329	0.841	0.779	0.288	0.259	0.000
270	0.210	0.339	0.582	0.765	0.235	0.297	0.000
280	0.150	0.272	0.661	0.655	0.229	0.150	0.000
290	0.272	0.443	0.694	0.642	0.323	0.722	0.000
300	0.169	0.353	0.636	0.627	0.310	0.238	0.000
310	0.150	0.263	0.640	0.735	0.247	0.157	0.000
320	0.150	0.228	0.543	0.767	0.178	0.476	0.000
330	0.194	0.252	0.689	0.656	0.207	0.254	0.000
340	0.166	0.265	0.790	0.871	0.189	0.307	0.000
350	0.194	0.311	0.792	0.668	0.178	0.169	0.000
360	0.156	0.240	0.530	0.794	0.166	0.435	0.000
370	0.196	0.338	0.900	0.685	0.305	0.298	0.000
380	0.180	0.382	0.683	0.618	0.260	0.353	0.000
390	0.150	0.242	0.587	0.794	0.195	0.280	0.000
400	0.153	0.350	0.665	0.598	0.264	0.158	0.000
410	0.220	0.297	0.637	0.700	0.237	0.082	0.000
420	0.297	0.295	0.564	0.755	0.227	0.119	0.007
430	0.178	0.299	0.648	0.634	0.225	0.076	0.000
440	0.253	0.310	0.596	0.711	0.241	0.067	0.000
450	0.150	0.347	0.730	0.695	0.212	0.275	0.000
460	0.256	0.303	0.632	0.648	0.259	0.062	0.000
470	0.239	0.301	0.598	0.540	0.212	0.047	0.000
480	0.220	0.312	0.633	0.694	0.273	0.071	0.000
490	0.196	0.297	0.658	0.668	0.226	0.097	0.000
500	0.220	0.305	0.616	0.701	0.238	0.048	0.000
510	0.195	0.318	0.626	0.695	0.234	0.108	0.000
520	0.157	0.284	0.635	0.715	0.255	0.086	0.000
530	0.193	0.304	0.630	0.662	0.239	0.043	0.000
540	0.179	0.313	0.662	0.538	0.204	0.055	0.000
550	0.201	0.300	0.592	0.679	0.228	0.048	0.000
560	0.241	0.312	0.615	0.668	0.261	0.047	0.000
570	0.191	0.331	0.596	0.500	0.201	0.034	0.000
580	0.217	0.299	0.619	0.706	0.229	0.066	0.000
590	0.243	0.289	0.578	0.678	0.252	0.080	0.000
600	0.223	0.316	0.610	0.579	0.220	0.026	0.000
610	0.202	0.304	0.609	0.559	0.215	0.017	0.000
620	0.243	0.314	0.597	0.661	0.235	0.055	0.000

<i>Iteration</i>	<i>dv-d1</i>	<i>dv-d2</i>	<i>dv-d3</i>	<i>dv-l5</i>	<i>dv-l6</i>	<i>DLSM</i>	<i>Penalty</i>
630	0.217	0.302	0.606	0.621	0.233	0.021	0.000
640	0.258	0.323	0.628	0.666	0.263	0.112	0.000
650	0.226	0.296	0.602	0.667	0.223	0.061	0.000
660	0.184	0.290	0.619	0.500	0.198	0.076	0.000
670	0.216	0.293	0.606	0.573	0.216	0.055	0.000
680	0.200	0.337	0.592	0.519	0.204	0.074	0.000
690	0.174	0.276	0.631	0.603	0.214	0.118	0.000
700	0.195	0.285	0.584	0.500	0.207	0.098	0.000
710	0.217	0.294	0.633	0.584	0.228	0.059	0.000
720	0.210	0.295	0.607	0.650	0.216	0.059	0.000
730	0.230	0.321	0.619	0.541	0.210	0.030	0.000
740	0.169	0.330	0.635	0.512	0.209	0.036	0.000
750	0.290	0.271	0.544	0.733	0.257	0.135	0.064
760	0.246	0.308	0.617	0.549	0.202	0.041	0.000
770	0.224	0.312	0.636	0.500	0.200	0.067	0.000
780	0.267	0.294	0.620	0.607	0.248	0.082	0.000
790	0.190	0.323	0.603	0.545	0.205	0.025	0.000
800	0.213	0.296	0.600	0.603	0.227	0.051	0.000
810	0.150	0.303	0.590	0.500	0.235	0.072	0.000
820	0.223	0.321	0.632	0.500	0.205	0.024	0.000
830	0.248	0.336	0.619	0.500	0.204	0.076	0.000
840	0.210	0.310	0.621	0.561	0.210	0.020	0.000
850	0.231	0.318	0.611	0.525	0.217	0.021	0.000
860	0.212	0.333	0.588	0.560	0.227	0.042	0.000
870	0.205	0.284	0.596	0.584	0.227	0.064	0.000
880	0.212	0.306	0.634	0.539	0.217	0.033	0.000
890	0.222	0.300	0.606	0.500	0.212	0.029	0.000
900	0.206	0.308	0.590	0.583	0.232	0.026	0.000
910	0.203	0.303	0.618	0.559	0.218	0.020	0.000
920	0.196	0.310	0.611	0.529	0.209	0.019	0.000
930	0.209	0.298	0.585	0.570	0.223	0.066	0.000
940	0.219	0.332	0.636	0.576	0.207	0.068	0.000
950	0.212	0.302	0.622	0.500	0.220	0.021	0.000
960	0.225	0.316	0.612	0.518	0.205	0.027	0.000
970	0.217	0.284	0.604	0.558	0.223	0.061	0.000
980	0.206	0.311	0.596	0.598	0.228	0.030	0.000
990	0.204	0.304	0.613	0.563	0.211	0.018	0.000
1,000	0.222	0.311	0.600	0.668	0.262	0.041	0.000
1,010	0.185	0.314	0.653	0.500	0.223	0.059	0.000
1,020	0.217	0.289	0.607	0.548	0.213	0.065	0.000
1,030	0.199	0.320	0.626	0.500	0.203	0.015	0.000
1,040	0.197	0.297	0.619	0.552	0.189	0.066	0.000
1,050	0.179	0.316	0.614	0.565	0.192	0.076	0.000
1,060	0.202	0.330	0.629	0.522	0.220	0.022	0.000
1,070	0.216	0.306	0.633	0.542	0.217	0.033	0.000
1,080	0.202	0.326	0.623	0.518	0.213	0.016	0.000

<i>Iteration</i>	<i>dv-d1</i>	<i>dv-d2</i>	<i>dv-d3</i>	<i>dv-l5</i>	<i>dv-l6</i>	<i>DLSM</i>	<i>Penalty</i>
1,090	0.199	0.339	0.640	0.500	0.187	0.131	0.000
1,100	0.228	0.314	0.622	0.521	0.210	0.026	0.000
1,110	0.204	0.341	0.629	0.521	0.219	0.064	0.000
1,120	0.200	0.315	0.628	0.545	0.214	0.018	0.000
1,130	0.210	0.286	0.654	0.510	0.211	0.093	0.000
1,140	0.244	0.330	0.644	0.500	0.221	0.058	0.000
1,150	0.217	0.304	0.627	0.500	0.221	0.025	0.000
1,160	0.213	0.313	0.616	0.508	0.215	0.013	0.000
1,170	0.199	0.320	0.623	0.515	0.222	0.014	0.000
1,180	0.202	0.334	0.630	0.500	0.226	0.045	0.000
1,190	0.188	0.327	0.614	0.521	0.227	0.013	0.000
1,200	0.199	0.328	0.630	0.501	0.196	0.087	0.000
1,210	0.213	0.308	0.643	0.500	0.214	0.033	0.000
1,220	0.200	0.319	0.610	0.529	0.249	0.011	0.000
1,230	0.180	0.325	0.599	0.500	0.224	0.031	0.000
1,240	0.209	0.325	0.596	0.500	0.239	0.015	0.000
1,247	0.206	0.312	0.607	0.529	0.245	0.009	0.000
1,250	0.196	0.302	0.567	0.537	0.193	0.077	0.000

## B-4 Optimization Responses: Optimization Trial 2

Table B-2 and Table B-3 lists design optimization results generated in Optimization Trial #2 where stage 2 of the ballistic optimization strategy was used to optimize two star solid rocket motor grain designs: one grain design employing 4 slots and one grain design employing 5 slots. The second stage of the ballistic optimization algorithm use the the genetic algorithm to optimize the star solid rocket motor grain designs for thrust-time performance.

Columns labeled with the prefix *dv-* contain design variable values per iteration for the respective design variable name following the hyphen. The column labeled *DLSM* (short for *Damped Least Squares Method*) contains the objective-function response per iteration. This optimization problem was unconstrained. Note, Iteration 620 produced the approximated design with the highest merit (minimum objective function response).

Table B-2 – Every tenth optimization response for the Star grain design with 4-slots.

<i>Iterations</i>	<i>dv-fin-depth</i>	<i>dv-fin-thickness</i>	<i>dv-number-of-fins</i>	<i>DLSM Response</i>
1	0.379	0.054	4	1.036
10	0.191	0.015	4	1.841
20	0.227	0.091	4	1.494
30	0.175	0.080	4	1.029
40	0.216	0.098	4	1.664
50	0.230	0.018	4	1.682
60	0.238	0.042	4	1.281
70	0.329	0.080	4	0.975
80	0.286	0.084	4	1.009
90	0.386	0.070	4	0.977
100	0.386	0.074	4	0.965
110	0.389	0.087	4	1.008

<i>Iterations</i>	<i>dv-fin-depth</i>	<i>dv-fin-thickness</i>	<i>dv-number-of-fins</i>	<i>DLSM Response</i>
120	0.282	0.081	4	0.985
130	0.388	0.048	4	1.097
140	0.400	0.061	4	0.994
150	0.398	0.055	4	1.032
160	0.184	0.060	4	1.291
170	0.291	0.061	4	0.994
180	0.344	0.096	4	1.091
190	0.382	0.076	4	0.975
200	0.080	0.069	4	8.925
210	0.317	0.067	4	0.970
220	0.364	0.072	4	0.960
230	0.358	0.071	4	0.979
240	0.393	0.065	4	0.968
250	0.347	0.077	4	0.980
260	0.362	0.070	4	0.977
270	0.080	0.059	4	9.235
280	0.400	0.073	4	0.962
290	0.400	0.080	4	0.975
300	0.362	0.077	4	0.984
310	0.328	0.064	4	0.993
320	0.358	0.082	4	0.989
330	0.303	0.066	4	0.970
340	0.286	0.072	4	0.959
350	0.340	0.077	4	0.983
360	0.359	0.074	4	0.965
370	0.292	0.067	4	0.971
380	0.365	0.074	4	0.969
390	0.400	0.083	4	0.998
400	0.400	0.073	4	0.963
410	0.384	0.072	4	0.959
420	0.327	0.070	4	0.978
430	0.400	0.070	4	0.978
440	0.334	0.075	4	0.971
450	0.299	0.070	4	0.977
460	0.354	0.070	4	0.976
470	0.387	0.071	4	0.955
480	0.333	0.070	4	0.978
490	0.370	0.072	4	0.960
500	0.384	0.072	4	0.959
510	0.340	0.071	4	0.956
520	0.390	0.065	4	0.968
530	0.350	0.072	4	0.960
540	0.388	0.071	4	0.979
550	0.331	0.071	4	0.979
560	0.394	0.072	4	0.958
570	0.080	0.058	4	9.252

<i>Iterations</i>	<i>dv-fin-depth</i>	<i>dv-fin-thickness</i>	<i>dv-number-of-fins</i>	<i>DLSM Response</i>
580	0.362	0.073	4	0.962
590	0.360	0.072	4	0.957
600	0.379	0.069	4	0.974
610	0.194	0.063	4	1.409
620	0.341	0.073	4	0.961
621	0.342	0.072	4	0.960
622	0.381	0.074	4	0.965
623	0.368	0.073	4	0.963
624	0.350	0.071	4	0.980
625	0.369	0.073	4	0.961

Table B-3 – Every tenth optimization response for the Star grain design with 5-slots.

<i>Iterations</i>	<i>dv-fin-depth</i>	<i>dv-fin-thickness</i>	<i>dv-number-of-fins</i>	<i>DLSM Response</i>
1	0.080	0.081	5	0.367
10	0.319	0.017	5	0.197
20	0.133	0.074	5	0.148
30	0.274	0.024	5	0.242
40	0.177	0.083	5	0.948
50	0.147	0.058	5	0.238
60	0.215	0.056	5	0.562
70	0.095	0.073	5	0.150
80	0.180	0.068	5	0.730
90	0.103	0.062	5	0.086
100	0.096	0.064	5	0.129
110	0.128	0.029	5	0.284
120	0.149	0.100	5	0.133
130	0.088	0.096	5	0.272
140	0.104	0.015	5	0.091
150	0.227	0.042	5	0.409
160	0.142	0.086	5	0.113
170	0.099	0.082	5	0.129
180	0.106	0.091	5	0.088
190	0.145	0.100	5	0.102
200	0.080	0.015	5	0.209
210	0.116	0.080	5	0.070
220	0.107	0.057	5	0.075
230	0.103	0.065	5	0.085
240	0.118	0.069	5	0.089
250	0.193	0.100	5	1.599
260	0.121	0.072	5	0.095
270	0.132	0.100	5	0.065

<i>Iterations</i>	<i>dv-fin-depth</i>	<i>dv-fin-thickness</i>	<i>dv-number-of-fins</i>	<i>DLSM Response</i>
280	0.140	0.095	5	0.082
290	0.102	0.083	5	0.108
300	0.128	0.090	5	0.087
310	0.086	0.023	5	0.157
320	0.115	0.100	5	0.064
330	0.110	0.077	5	0.070
340	0.146	0.100	5	0.107
350	0.132	0.095	5	0.077
360	0.100	0.038	5	0.086
370	0.103	0.048	5	0.079
380	0.107	0.057	5	0.074
390	0.161	0.100	5	0.416
400	0.120	0.099	5	0.067
410	0.136	0.099	5	0.066
420	0.130	0.100	5	0.063
430	0.130	0.099	5	0.066
440	0.127	0.100	5	0.062
450	0.136	0.100	5	0.063
460	0.135	0.098	5	0.071
470	0.128	0.100	5	0.062
480	0.129	0.099	5	0.064
490	0.124	0.100	5	0.064
500	0.121	0.099	5	0.066
510	0.138	0.100	5	0.064
520	0.138	0.099	5	0.067
530	0.131	0.100	5	0.065
540	0.125	0.100	5	0.063
550	0.127	0.098	5	0.066
560	0.127	0.100	5	0.062
570	0.134	0.100	5	0.065
580	0.125	0.100	5	0.063
590	0.129	0.100	5	0.062
600	0.130	0.100	5	0.064
610	0.130	0.100	5	0.064
620	0.127	0.100	5	0.062
621	0.126	0.100	5	0.063
622	0.141	0.100	5	0.075
623	0.127	0.099	5	0.064
624	0.128	0.098	5	0.065
625	0.129	0.100	5	0.063

## B-5 Optimization Responses: Optimization Trial 3

Table B-4 lists design optimization results from the experiment of using genetic optimization algorithm to optimize the complex solid rocket motor grain design for thrust-time performance. Columns labeled with the prefix *dv-* contain design variable values per iteration for the respective design variable name following the hyphen. The column labeled *DLSM* (short for *Damped Least Squares Method*) contains the objective-function responses. This optimization problem was unconstrained. Note, Iteration 970 produced the approximated design with the highest merit (minimum objective function response).

Table B-4 – Complex grain abridged genetic optimization response.

<i>Iterations</i>	<i>dv-d1</i>	<i>dv-d2</i>	<i>dv-d3</i>	<i>dv-fin-length</i>	<i>dv-fin-depth</i>	<i>DLSM</i>
1	0.150	0.813	0.220	0.123	0.256	1.135
10	0.374	0.613	0.261	0.087	0.299	1.723
20	0.200	0.557	0.201	0.085	0.299	1.298
30	0.332	0.757	0.237	0.107	0.153	1.320
40	0.241	0.582	0.201	0.055	0.208	1.418
50	0.296	0.692	0.252	0.093	0.288	1.313
60	0.150	0.850	0.300	0.059	0.350	1.247
70	0.447	0.842	0.147	0.050	0.186	0.777
80	0.336	0.627	0.112	0.071	0.153	1.143
90	0.369	0.803	0.207	0.070	0.183	0.914
100	0.322	0.850	0.144	0.140	0.199	0.842
110	0.318	0.842	0.147	0.127	0.194	0.838
120	0.341	0.840	0.130	0.096	0.271	0.769
130	0.349	0.808	0.205	0.079	0.191	0.919
140	0.401	0.850	0.128	0.072	0.181	0.786
150	0.421	0.793	0.175	0.079	0.160	0.766
160	0.285	0.794	0.175	0.100	0.261	0.801
170	0.335	0.839	0.138	0.095	0.265	0.740
180	0.342	0.829	0.178	0.106	0.212	0.750
190	0.230	0.819	0.197	0.101	0.321	0.750
200	0.310	0.800	0.170	0.128	0.254	0.719
210	0.405	0.793	0.189	0.061	0.188	0.729

<i>Iterations</i>	<i>dv-d1</i>	<i>dv-d2</i>	<i>dv-d3</i>	<i>dv-fin-length</i>	<i>dv-fin-depth</i>	<i>DLSM</i>
220	0.294	0.846	0.166	0.120	0.206	0.877
230	0.349	0.832	0.180	0.132	0.242	0.701
240	0.374	0.811	0.174	0.127	0.227	0.711
250	0.376	0.808	0.184	0.092	0.208	0.689
260	0.267	0.850	0.194	0.150	0.237	0.684
270	0.353	0.837	0.149	0.130	0.259	0.730
280	0.424	0.808	0.130	0.150	0.201	0.798
290	0.343	0.825	0.144	0.113	0.264	0.752
300	0.401	0.788	0.228	0.079	0.151	1.160
310	0.404	0.797	0.197	0.082	0.187	0.749
320	0.268	0.842	0.188	0.129	0.263	0.620
330	0.252	0.835	0.185	0.106	0.298	0.645
340	0.382	0.812	0.162	0.140	0.273	0.717
350	0.347	0.827	0.133	0.112	0.274	0.771
360	0.178	0.850	0.198	0.079	0.350	1.006
370	0.324	0.836	0.171	0.128	0.281	0.642
380	0.394	0.817	0.186	0.114	0.150	0.704
390	0.283	0.834	0.185	0.122	0.276	0.597
400	0.268	0.835	0.177	0.106	0.297	0.759
410	0.301	0.832	0.180	0.116	0.276	0.718
420	0.296	0.832	0.187	0.122	0.284	0.588
430	0.335	0.818	0.164	0.133	0.311	0.718
440	0.397	0.828	0.167	0.150	0.316	0.638
450	0.294	0.826	0.189	0.120	0.257	0.634
460	0.291	0.828	0.186	0.126	0.237	0.638
470	0.282	0.836	0.184	0.122	0.277	0.588
480	0.296	0.843	0.191	0.122	0.316	0.579
490	0.286	0.841	0.192	0.119	0.326	0.583
500	0.279	0.835	0.187	0.127	0.318	0.577
510	0.295	0.843	0.186	0.112	0.350	0.552
520	0.298	0.850	0.188	0.115	0.343	0.594
530	0.299	0.834	0.189	0.116	0.343	0.574
540	0.295	0.841	0.183	0.118	0.341	0.698
550	0.325	0.831	0.191	0.123	0.295	0.587
560	0.304	0.827	0.186	0.122	0.280	0.587
570	0.296	0.838	0.186	0.108	0.347	0.559
580	0.328	0.833	0.182	0.123	0.280	0.693
590	0.325	0.845	0.180	0.129	0.262	0.681
600	0.304	0.838	0.188	0.115	0.347	0.563
610	0.288	0.845	0.184	0.122	0.322	0.553
620	0.311	0.835	0.187	0.123	0.310	0.560
630	0.296	0.845	0.187	0.122	0.319	0.558
640	0.302	0.831	0.189	0.118	0.343	0.578
650	0.289	0.846	0.186	0.107	0.350	0.558
660	0.299	0.843	0.182	0.115	0.345	0.687
670	0.297	0.844	0.186	0.116	0.348	0.555

<i>Iterations</i>	<i>dv-d1</i>	<i>dv-d2</i>	<i>dv-d3</i>	<i>dv-fin-length</i>	<i>dv-fin-depth</i>	<i>DLSM</i>
680	0.313	0.844	0.184	0.107	0.350	0.540
690	0.282	0.847	0.182	0.119	0.338	0.716
700	0.292	0.844	0.191	0.104	0.350	0.575
710	0.297	0.839	0.186	0.118	0.344	0.557
720	0.301	0.848	0.186	0.120	0.333	0.555
730	0.290	0.850	0.185	0.101	0.350	0.594
740	0.296	0.836	0.185	0.118	0.344	0.555
750	0.301	0.844	0.186	0.115	0.347	0.553
760	0.304	0.849	0.182	0.119	0.333	0.685
770	0.313	0.842	0.188	0.110	0.350	0.552
780	0.321	0.848	0.182	0.101	0.346	0.666
790	0.305	0.848	0.182	0.110	0.347	0.680
800	0.304	0.840	0.187	0.116	0.350	0.552
810	0.311	0.842	0.191	0.107	0.348	0.566
820	0.302	0.847	0.193	0.086	0.350	0.586
830	0.299	0.844	0.186	0.111	0.346	0.555
840	0.305	0.843	0.184	0.114	0.350	0.546
850	0.325	0.850	0.181	0.104	0.350	0.694
860	0.309	0.842	0.181	0.115	0.345	0.672
870	0.314	0.850	0.186	0.109	0.346	0.585
880	0.313	0.834	0.181	0.120	0.340	0.681
890	0.307	0.844	0.183	0.113	0.349	0.683
900	0.313	0.844	0.186	0.113	0.344	0.547
910	0.312	0.833	0.184	0.114	0.350	0.555
920	0.341	0.844	0.186	0.120	0.349	0.547
930	0.344	0.850	0.187	0.116	0.346	0.586
940	0.317	0.850	0.181	0.099	0.346	0.668
950	0.313	0.842	0.181	0.106	0.348	0.670
960	0.322	0.841	0.184	0.115	0.347	0.540
970	0.264	0.822	0.186	0.105	0.341	0.613
980	0.313	0.837	0.184	0.116	0.344	0.545
990	0.310	0.844	0.184	0.105	0.344	0.543
1000	0.322	0.838	0.184	0.119	0.350	0.540

## APPENDIX C: STAGE #3 – HIGH-FIDELITY OPTIMIZATION

## C-1 Appendix Overview

Contained in this appendix are the high-fidelity optimization results from three separate solid rocket motor high-fidelity (HF) design optimization trials performed in the third stage of the ballistic optimization strategy described in this paper. High fidelity solid rocket motor grain designs optimization was carried out using the BFGS gradient based optimization algorithm to improve the thrust-time product the respective solid rocket motor grains. The design optimization results are presented in plotted and tabular form. The following lists the contents of each section in this appendix.

Section C-2 contains the high-fidelity optimization responses represented in plotted form.

Section C-3 contains the tabular HF optimization results for the Multi-cylinder grain.

Section C-4 contains the tabular HF optimization results for the CASTOR1 grain.

Section C-5 contains the tabular HF optimization results for the Complex grain.

## C-2 High-Fidelity Optimization Response Plots: Trials 1, 2, and 3

The following three figures show high-fidelity optimization responses graphed versus iteration for three different solid rocket motor grains: the Multi-cylinder grain, the Star grain, and the Complex grain. Figure C-1 plots the high-fidelity optimization response of the multi-cylinder grain design optimization. Figure C-2 plots the high-fidelity optimization response of the star grain design optimization, and Figure C-3 plots the high-fidelity optimization response of the complex grain design optimization.

Each plot represents the design optimization results in two series. The series labeled “Raw Optimization Response” represents the raw approximation response, and next, the series labeled “Sorted Optimization Response” represents the optimization responses sorted in order of increasing design merit (a merit of zero represents the perfect design).

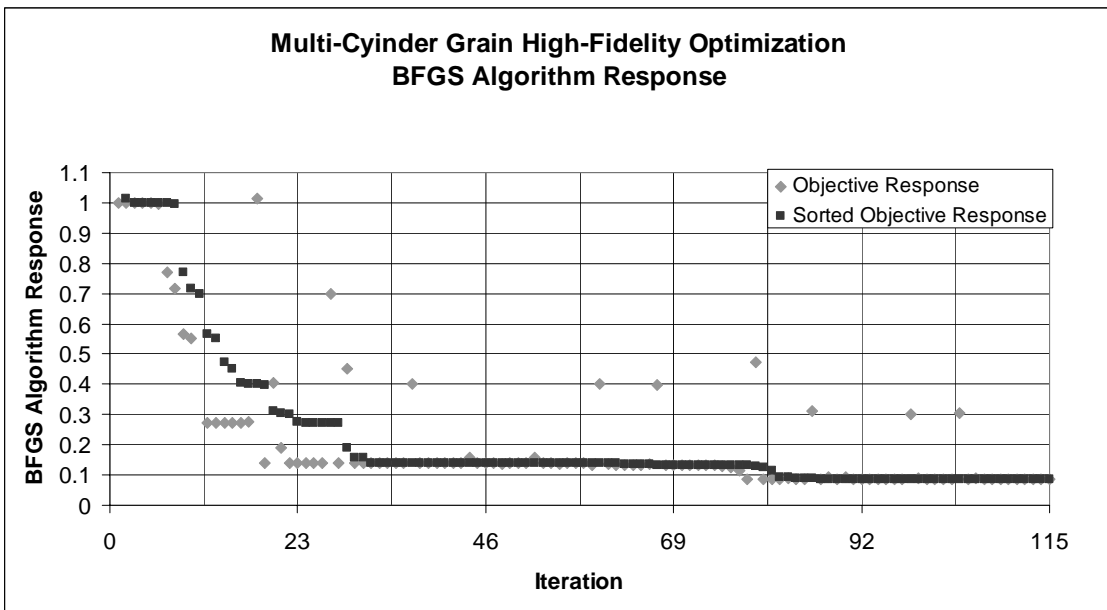


Figure C-1 – Optimization Response Plot of the Multi-Cylinder Grain Design.

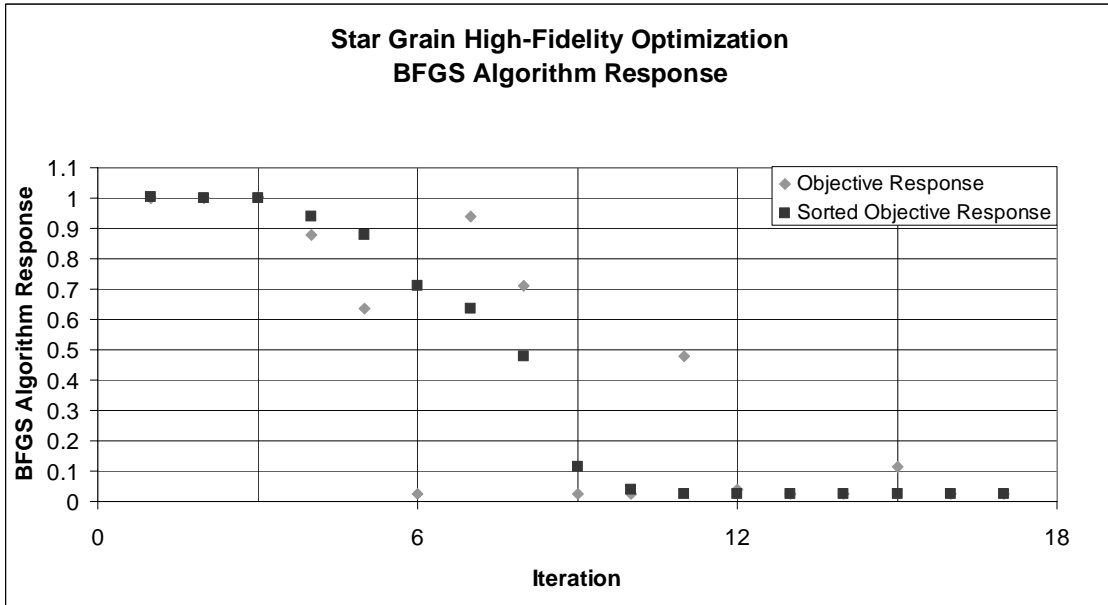


Figure C-2 – Optimization Response Plot of the Star Grain Design.

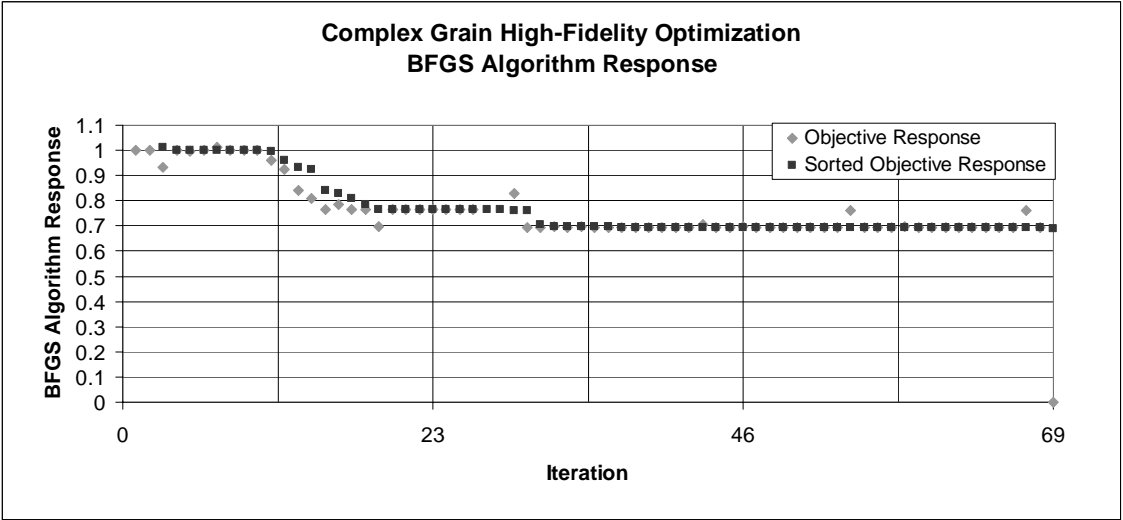


Figure C-3 – Optimization Response Plot of the Complex Grain Design.

### C-3 High-Fidelity Opt. Responses: Optimization Trial 1

Table C-1 lists design high-fidelity optimization results from the experiment of using the BFGS gradient based algorithm to optimize the multi-cylinder solid rocket motor grain design for thrust-time performance. Columns labeled with the prefix *dv*- contain design variable values per iteration for the respective design variable name following the hyphen. The column labeled *DLSM* (short for *Damped Least Squares Method*) contains the objective-function responses. Note, Iteration 115 produced the approximated design with the highest merit (minimum objective function response).

Table C-1 – Multi-cylinder grain high-fidelity optimization response.

<i>Iterations</i>	<i>dv-d1</i>	<i>dv-d2</i>	<i>dv-d3</i>	<i>dv-l5</i>	<i>dv-l6</i>	<i>DLSM</i>
1	0.19647	0.30002	0.56678	0.53671	0.1941	1.00019
2	0.19667	0.30002	0.56678	0.53671	0.1941	0.99939
3	0.19647	0.30032	0.56678	0.53671	0.1941	1.00143
4	0.19647	0.30002	0.56734	0.53671	0.1941	0.99826
5	0.19647	0.30002	0.56678	0.53724	0.1941	1.00031
6	0.19647	0.30002	0.56678	0.53671	0.1943	0.99763
7	0.19832	0.29813	0.56833	0.5366	0.20012	0.77014
8	0.20132	0.29507	0.57084	0.53643	0.20985	0.71607
9	0.20916	0.28706	0.57741	0.53597	0.23533	0.56658
10	0.22969	0.2661	0.59461	0.53479	0.30203	0.55246
11	0.28343	0.21121	0.63965	0.53169	0.45	8.59756
12	0.22067	0.2753	0.58706	0.53531	0.27273	0.27294
13	0.22089	0.2753	0.58706	0.53531	0.27273	0.27275
14	0.22067	0.27558	0.58706	0.53531	0.27273	0.27212
15	0.22067	0.2753	0.58764	0.53531	0.27273	0.27336
16	0.22067	0.2753	0.58706	0.53584	0.27273	0.27274
17	0.22067	0.2753	0.58706	0.53531	0.27301	0.27462
18	0.23198	0.31338	0.5779	0.54019	0.1941	1.01443
19	0.22324	0.28394	0.58498	0.53642	0.2549	0.13987
20	0.22532	0.29096	0.58329	0.53732	0.24039	0.4045
21	0.22243	0.28121	0.58563	0.53607	0.26053	0.19015
22	0.22346	0.28394	0.58498	0.53642	0.2549	0.13976
23	0.22324	0.28422	0.58498	0.53642	0.2549	0.13938

<i>Iterations</i>	<i>dv-d1</i>	<i>dv-d2</i>	<i>dv-d3</i>	<i>dv-l5</i>	<i>dv-l6</i>	<i>DLSM</i>
24	0.22324	0.28394	0.58556	0.53642	0.2549	0.14027
25	0.22324	0.28394	0.58498	0.53695	0.2549	0.13975
26	0.22324	0.28394	0.58498	0.53642	0.25515	0.14089
27	0.2201	0.27213	0.56714	0.53555	0.24659	0.69764
28	0.22317	0.2837	0.58462	0.5364	0.25473	0.13938
29	0.22274	0.28205	0.58213	0.53628	0.25357	0.45057
30	0.2232	0.28381	0.58478	0.53641	0.25481	0.13961
31	0.2234	0.2837	0.58462	0.5364	0.25473	0.13928
32	0.22317	0.28399	0.58462	0.5364	0.25473	0.13891
33	0.22317	0.2837	0.58521	0.5364	0.25473	0.1398
34	0.22317	0.2837	0.58462	0.53694	0.25473	0.13926
35	0.22317	0.2837	0.58462	0.5364	0.25499	0.1404
36	0.22379	0.28366	0.58362	0.53651	0.25474	0.13844
37	0.22478	0.28359	0.582	0.53668	0.25475	0.40309
38	0.2236	0.28368	0.58394	0.53647	0.25474	0.13874
39	0.22401	0.28366	0.58362	0.53651	0.25474	0.13833
40	0.22379	0.28395	0.58362	0.53651	0.25474	0.13797
41	0.22379	0.28366	0.58421	0.53651	0.25474	0.13886
42	0.22379	0.28366	0.58362	0.53704	0.25474	0.13832
43	0.22379	0.28366	0.58362	0.53651	0.25499	0.13946
44	0.22433	0.28329	0.58342	0.53751	0.25448	0.15803
45	0.2238	0.28365	0.58362	0.53653	0.25473	0.13841
46	0.22389	0.28359	0.58358	0.5367	0.25469	0.13823
47	0.22412	0.28359	0.58358	0.5367	0.25469	0.13813
48	0.22389	0.28388	0.58358	0.5367	0.25469	0.13777
49	0.22389	0.28359	0.58417	0.5367	0.25469	0.13866
50	0.22389	0.28359	0.58358	0.53723	0.25469	0.13812
51	0.22389	0.28359	0.58358	0.5367	0.25494	0.13926
52	0.22489	0.28288	0.58386	0.53665	0.25438	0.15853
53	0.2239	0.28359	0.58359	0.5367	0.25469	0.13823
54	0.22412	0.28359	0.58359	0.5367	0.25469	0.13813
55	0.2239	0.28387	0.58359	0.5367	0.25469	0.13777
56	0.2239	0.28359	0.58417	0.5367	0.25469	0.13866
57	0.2239	0.28359	0.58359	0.53723	0.25469	0.13812
58	0.2239	0.28359	0.58359	0.5367	0.25494	0.13926
59	0.22402	0.28399	0.58341	0.53675	0.25369	0.13348
60	0.22421	0.28465	0.58311	0.53684	0.25207	0.40027
61	0.22399	0.28389	0.58345	0.53674	0.25394	0.13465
62	0.22424	0.28399	0.58341	0.53675	0.25369	0.13339
63	0.22402	0.28428	0.58341	0.53675	0.25369	0.13306
64	0.22402	0.28399	0.58399	0.53675	0.25369	0.13392
65	0.22402	0.28399	0.58341	0.53729	0.25369	0.13338
66	0.22402	0.28399	0.58341	0.53675	0.25394	0.13447
67	0.22412	0.28438	0.58321	0.5368	0.25269	0.39946
68	0.22402	0.284	0.5834	0.53675	0.25368	0.13345
69	0.22402	0.28401	0.5834	0.53675	0.25364	0.13327

<i>Iterations</i>	<i>dv-d1</i>	<i>dv-d2</i>	<i>dv-d3</i>	<i>dv-l5</i>	<i>dv-l6</i>	<i>DLSM</i>
70	0.22425	0.28401	0.5834	0.53675	0.25364	0.13317
71	0.22402	0.28429	0.5834	0.53675	0.25364	0.13285
72	0.22402	0.28401	0.58398	0.53675	0.25364	0.1337
73	0.22402	0.28401	0.5834	0.53729	0.25364	0.13316
74	0.22402	0.28401	0.5834	0.53675	0.25389	0.13425
75	0.22447	0.28501	0.58379	0.53681	0.25321	0.13025
76	0.22521	0.28663	0.58443	0.53691	0.25251	0.12552
77	0.22712	0.29086	0.58611	0.53716	0.25069	0.11419
78	0.23213	0.30196	0.59051	0.53783	0.24592	0.08746
79	0.24524	0.33099	0.60203	0.53957	0.23343	0.47314
80	0.23281	0.30347	0.59112	0.53792	0.24527	0.08733
81	0.23305	0.30347	0.59112	0.53792	0.24527	0.08733
82	0.23281	0.30378	0.59112	0.53792	0.24527	0.08744
83	0.23281	0.30347	0.59171	0.53792	0.24527	0.08787
84	0.23281	0.30347	0.59112	0.53846	0.24527	0.08737
85	0.23281	0.30347	0.59112	0.53792	0.24551	0.08765
86	0.25228	0.30338	0.58076	0.53113	0.24701	0.31103
87	0.23314	0.30347	0.59094	0.5378	0.2453	0.0872
88	0.23531	0.30346	0.58979	0.53705	0.24549	0.09244
89	0.23316	0.30347	0.59093	0.5378	0.2453	0.08719
90	0.23339	0.30347	0.59093	0.5378	0.2453	0.09331
91	0.23316	0.30378	0.59093	0.5378	0.2453	0.0873
92	0.23316	0.30347	0.59152	0.5378	0.2453	0.08772
93	0.23316	0.30347	0.59093	0.53834	0.2453	0.08723
94	0.23316	0.30347	0.59093	0.5378	0.24554	0.08752
95	0.23315	0.30413	0.58993	0.53689	0.24563	0.08688
96	0.23315	0.30519	0.58832	0.53542	0.24618	0.08638
97	0.23313	0.30797	0.58408	0.53158	0.2476	0.08506
98	0.2331	0.31525	0.57299	0.52152	0.25133	0.30217
99	0.23337	0.30797	0.58408	0.53158	0.2476	0.09118
100	0.23313	0.30828	0.58408	0.53158	0.2476	0.08515
101	0.23313	0.30797	0.58466	0.53158	0.2476	0.08557
102	0.23313	0.30797	0.58408	0.53211	0.2476	0.08509
103	0.23313	0.30797	0.58408	0.53158	0.24785	0.08538
104	0.23312	0.30852	0.58301	0.52473	0.24754	0.30618
105	0.23313	0.30797	0.58407	0.53155	0.2476	0.08506
106	0.23337	0.30797	0.58407	0.53155	0.2476	0.09117
107	0.23313	0.30828	0.58407	0.53155	0.2476	0.08514
108	0.23313	0.30797	0.58466	0.53155	0.2476	0.08556
109	0.23313	0.30797	0.58407	0.53208	0.2476	0.08509
110	0.23313	0.30797	0.58407	0.53155	0.24785	0.08537
111	0.23213	0.30796	0.58404	0.53155	0.24755	0.08501
112	0.23052	0.30795	0.58399	0.53155	0.24747	0.08497
113	0.22628	0.3079	0.58385	0.53154	0.24727	0.08504
114	0.22969	0.30794	0.58396	0.53154	0.24743	0.08496
115	0.22969	0.30794	0.58396	0.53154	0.24743	0.08496

C-4 High-Fidelity Opt. Responses: Optimization Trial 2

Table C-2 lists design optimization results from the experiment of using the BFGS gradient based algorithm to optimize the star solid rocket motor grain design for thrust-time performance. Columns labeled with the prefix *dv-* contain design variable values per iteration for the respective design variable name following the hyphen. The column labeled *DLSM* (short for *Damped Least Squares Method*) contains the objective-function responses. This optimization problem was unconstrained. Note, Iteration 17 produced the approximated design with the highest merit (minimum objective function response).

Table C-2 – Star grain high-fidelity optimization response.

<i>Iterations</i>	<i>dv-fin-depth</i>	<i>dv-fin-thicknes</i>	<i>number-of-fins</i>	<i>DLSM</i>
1	0.010	0.175	5	1.000
2	0.010	0.175	5	0.999
3	0.010	0.175	5	1.002
4	0.014	0.168	5	0.879
5	0.020	0.157	5	0.636
6	0.036	0.128	5	0.023
7	0.079	0.100	5	0.938
8	0.052	0.100	5	0.710
9	0.036	0.128	5	0.023
10	0.036	0.128	5	0.023
11	0.031	0.155	5	0.478
12	0.035	0.133	5	0.039
13	0.036	0.128	5	0.023
14	0.036	0.128	5	0.023
15	0.034	0.140	5	0.113
16	0.036	0.130	5	0.025
17	0.036	0.128	5	0.023

C-5 High-Fidelity Opt. Responses: Optimization Trial 3

Table C-3 lists design optimization results from the experiment of using BFGS gradient based algorithm to optimize the complex solid rocket motor grain design for thrust-time performance. Columns labeled with the prefix *dv-* contain design variable values per iteration for the respective design variable name following the hyphen. The column labeled *DLSM* (short for *Damped Least Squares Method*) contains the objective-function responses. This optimization problem was unconstrained. Note, Iteration 69 produced the approximated design with the highest merit (minimum objective function response).

Table C-3 – Complex grain high-fidelity optimization response.

<i>It'ns</i>	<i>dv-d1</i>	<i>dv-d2</i>	<i>dv-d3</i>	<i>dv-l1</i>	<i>dv-l2</i>	<i>dv-l3</i>	<i>dv-l5</i>	<i>dv-l6</i>	<i>dv-fin-length</i>	<i>DLSM</i>
1	0.3	0.7	0.1	0.1	0.4	0.8	0.06	0.06	0.100	1.000
2	0.303	0.7	0.1	0.1	0.4	0.8	0.06	0.06	0.100	0.999
3	0.3	0.707	0.1	0.1	0.4	0.8	0.06	0.06	0.100	0.931
4	0.3	0.7	0.101	0.1	0.4	0.8	0.06	0.06	0.100	1.002
5	0.3	0.7	0.1	0.101	0.4	0.8	0.06	0.06	0.100	0.997
6	0.3	0.7	0.1	0.1	0.404	0.8	0.06	0.06	0.100	0.999
7	0.3	0.7	0.1	0.1	0.4	0.808	0.06	0.06	0.100	1.010
8	0.3	0.7	0.1	0.1	0.4	0.8	0.061	0.06	0.100	0.999
9	0.3	0.7	0.1	0.1	0.4	0.8	0.06	0.061	0.100	1.000
10	0.3	0.7	0.1	0.1	0.4	0.8	0.06	0.060	0.101	0.999
11	0.3	0.709	0.098	0.102	0.4	0.799	0.061	0.060	0.101	0.962
12	0.301	0.723	0.095	0.106	0.401	0.797	0.063	0.059	0.101	0.924
13	0.303	0.76	0.087	0.115	0.402	0.792	0.068	0.058	0.104	0.840
14	0.308	0.8	0.065	0.14	0.406	0.779	0.08	0.054	0.110	0.808
15	0.32	0.8	0.05	0.15	0.415	0.745	0.08	0.043	0.126	0.765
16	0.352	0.8	0.05	0.15	0.439	0.7	0.08	0.040	0.150	0.786
17	0.327	0.8	0.05	0.15	0.42	0.727	0.08	0.04	0.135	0.763
18	0.33	0.8	0.05	0.15	0.42	0.727	0.08	0.04	0.135	0.765
19	0.327	0.792	0.05	0.15	0.42	0.727	0.08	0.04	0.135	0.699
20	0.327	0.8	0.051	0.15	0.42	0.727	0.08	0.04	0.135	0.764
21	0.327	0.8	0.05	0.149	0.42	0.727	0.08	0.04	0.135	0.764
22	0.327	0.8	0.05	0.15	0.424	0.727	0.08	0.04	0.135	0.765

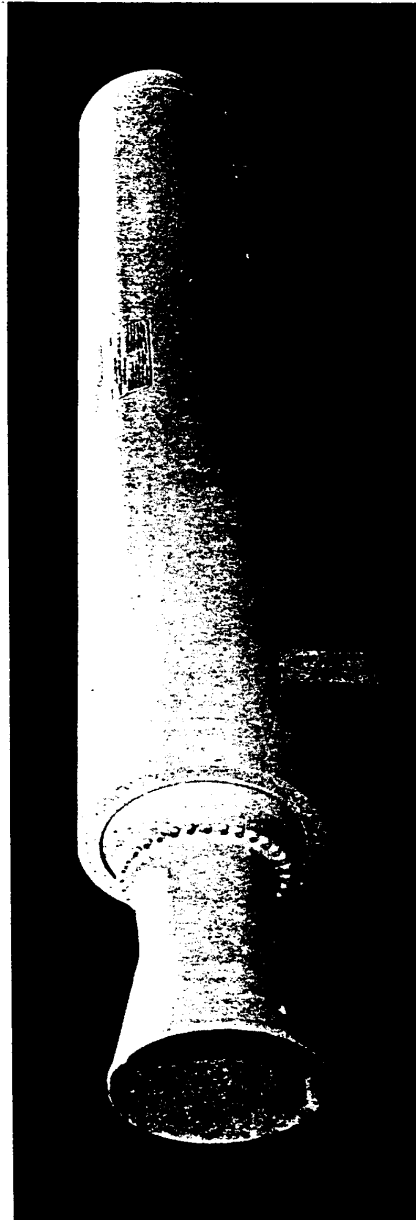
<i>It'ns</i>	<i>dv-d1</i>	<i>dv-d2</i>	<i>dv-d3</i>	<i>dv-l1</i>	<i>dv-l2</i>	<i>dv-l3</i>	<i>dv-l5</i>	<i>dv-l6</i>	<i>dv-fin-length</i>	<i>DLSM</i>
23	0.327	0.8	0.05	0.15	0.42	0.734	0.08	0.04	0.135	0.764
24	0.327	0.8	0.05	0.15	0.42	0.727	0.079	0.04	0.135	0.765
25	0.327	0.8	0.05	0.15	0.42	0.727	0.08	0.041	0.135	0.763
26	0.327	0.8	0.05	0.15	0.42	0.727	0.08	0.04	0.136	0.763
27	0.302	0.6	0.05	0.15	0.394	0.719	0.08	0.04	0.140	1.164
28	0.315	0.6	0.05	0.15	0.408	0.723	0.08	0.04	0.137	1.154
29	0.323	0.715	0.05	0.15	0.416	0.726	0.08	0.04	0.136	0.827
30	0.327	0.8	0.05	0.15	0.42	0.727	0.08	0.04	0.135	0.694
31	0.33	0.8	0.05	0.15	0.42	0.727	0.08	0.04	0.135	0.695
32	0.327	0.792	0.05	0.15	0.42	0.727	0.08	0.04	0.135	0.699
33	0.327	0.8	0.051	0.15	0.42	0.727	0.08	0.04	0.135	0.694
34	0.327	0.8	0.05	0.149	0.42	0.727	0.08	0.04	0.135	0.696
35	0.327	0.8	0.05	0.15	0.424	0.727	0.08	0.04	0.135	0.695
36	0.327	0.8	0.05	0.15	0.42	0.734	0.08	0.04	0.135	0.695
37	0.327	0.8	0.05	0.15	0.42	0.727	0.079	0.04	0.135	0.695
38	0.327	0.8	0.05	0.15	0.42	0.727	0.08	0.041	0.135	0.694
39	0.327	0.8	0.05	0.15	0.42	0.727	0.08	0.04	0.136	0.694
40	0.326	0.799	0.05	0.15	0.419	0.727	0.08	0.04	0.135	0.693
41	0.324	0.799	0.05	0.15	0.417	0.726	0.08	0.04	0.136	0.693
42	0.321	0.798	0.05	0.15	0.413	0.725	0.08	0.04	0.137	0.692
43	0.311	0.796	0.05	0.15	0.402	0.72	0.08	0.04	0.141	0.704
44	0.322	0.798	0.05	0.15	0.414	0.725	0.08	0.04	0.137	0.692
45	0.325	0.798	0.05	0.15	0.414	0.725	0.08	0.04	0.137	0.692
46	0.322	0.79	0.05	0.15	0.414	0.725	0.08	0.04	0.137	0.698
47	0.322	0.798	0.051	0.15	0.414	0.725	0.08	0.04	0.137	0.693
48	0.322	0.798	0.05	0.149	0.414	0.725	0.08	0.04	0.137	0.694
49	0.322	0.798	0.05	0.15	0.418	0.725	0.08	0.04	0.137	0.693
50	0.322	0.798	0.05	0.15	0.414	0.732	0.08	0.04	0.137	0.693
51	0.322	0.798	0.05	0.15	0.414	0.725	0.079	0.04	0.137	0.694
52	0.322	0.798	0.05	0.15	0.414	0.725	0.08	0.041	0.137	0.692
53	0.322	0.798	0.05	0.15	0.414	0.725	0.08	0.04	0.138	0.692
54	0.322	0.8	0.05	0.15	0.413	0.724	0.08	0.04	0.137	0.761
55	0.322	0.799	0.05	0.15	0.414	0.725	0.08	0.04	0.137	0.692
56	0.322	0.799	0.05	0.15	0.414	0.725	0.08	0.04	0.137	0.692
57	0.325	0.799	0.05	0.15	0.414	0.725	0.08	0.04	0.137	0.692
58	0.322	0.791	0.05	0.15	0.414	0.725	0.08	0.04	0.137	0.698
59	0.322	0.799	0.051	0.15	0.414	0.725	0.08	0.04	0.137	0.693
60	0.322	0.799	0.05	0.149	0.414	0.725	0.08	0.04	0.137	0.694
61	0.322	0.799	0.05	0.15	0.418	0.725	0.08	0.04	0.137	0.693
62	0.322	0.799	0.05	0.15	0.414	0.732	0.08	0.04	0.137	0.693
63	0.322	0.799	0.05	0.15	0.414	0.725	0.079	0.04	0.137	0.694
64	0.322	0.799	0.05	0.15	0.414	0.725	0.08	0.041	0.137	0.692
65	0.322	0.799	0.05	0.15	0.414	0.725	0.08	0.04	0.138	0.692
66	0.322	0.8	0.05	0.15	0.414	0.725	0.08	0.04	0.137	0.692
67	0.322	0.8	0.05	0.15	0.414	0.725	0.08	0.04	0.137	0.761
68	0.322	0.799	0.05	0.15	0.414	0.725	0.08	0.04	0.137	0.692

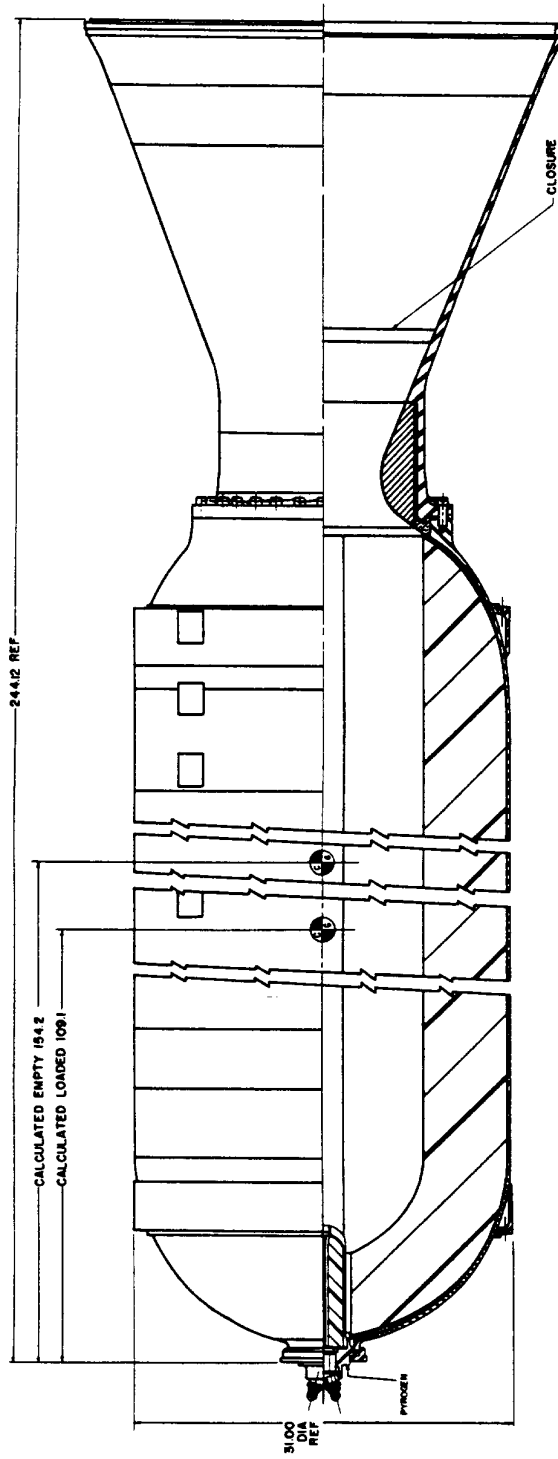
<i>It'ns</i>	<i>dv-d1</i>	<i>dv-d2</i>	<i>dv-d3</i>	<i>dv-l1</i>	<i>dv-l2</i>	<i>dv-l3</i>	<i>dv-l5</i>	<i>dv-l6</i>	<i>dv-fin-length</i>	<i>DLSM</i>
69	0.322	0.8	0.05	0.15	0.414	0.725	0.08	0.04	0.137	0.691

## APPENDIX D: XM33E5 CASTOR SOLID FUELED ROCKET

D-1 XM33E5 Castor Solid Fueled Rocket Datasheet

Contained in this appendix are excerpts from the Chemical Propulsion Information Analysis Center CPIA/M1 Rocket Motor Manual published by John Hopkins University containing information on the Thiokol XM33E5 Castor solid fueled rocket motor. Information contained in the excerpts includes grain geometry, a thrust-time performance requirement, and propellant information.





Purpose: Second stage propulsion for Scout Vehicle  
Status: Development

PRINCIPAL DATA:

Length (overall)(in)	246.7
Diameter (in):	
principal	31.0
maximum (nozzle exit cone)	40.0
Weight (lb):	
loaded	8867
expended	1440
Time of burning ( $t_b @ 77^\circ\text{F}$ )(sec)	27.28
Thrust (average over $t_b$ )(lbf) <sup>(a)</sup>	53850
Total impulse (lbf-sec) <sup>(a)</sup>	1632000
Location of center of gravity (inches from fwd face of pyrogen retaining ring):	
loaded	109.1
expended	154.2
Nozzle expansion cone angle (degrees)	43°20'
Temperature limits (°F):	
firing	20 to 100
storage	10 to 110

(a) at sea level, optimum expansion; approx. 17% higher under design conditions

WEIGHTS AND DIMENSIONS OF INERT PARTS:

	Wt. (lb)	O. D. (in.)	I. D. (in.)	Length (in.)	Material
Chamber	807	31.00	30.78	202.00	4130 steel
Nozzle	525 <sup>(b)</sup>	40.00 <sup>(c)</sup>	9.69 <sup>(d)</sup>	41.50	4130 steel
nozzle insert					graphite
Igniter assembly	13.7	5.49		15.59	fiberglass
Insulation	28				polysulfide-asbestos
Liner	168				polysulfide rubber
Attachment rings and bolts	12.3				
Total weight (lb)	1554				

(b) incl. insert

(c) at end of cone

(d) throat diameter

L

PROPELLANT DATA:

Propellant designation	TP-H8038A
Propellant composition	Am. perchlorate/PBAA/aluminum
Flame temperature (adiabatic)(°F)	5165
Method of manufacture	Cast, cured in case
Physical characteristics of grain:	
number	One
configuration	5 pt. star
length (in)	198.47
diameter (in)	30.54
web (in)	6.85
grain weight (lb)	7313
propellant weight (lb)	7313

<b>Liner:</b>					
material		Polysulfide rubber			
place of attachment		Bonded between case and propellant			
method of application		Applied as liquid, cured in place			
weight (lb)		168			
thickness (in)		0.12			
<b>Design parameters:</b>					
surface-to-throat area ratio, $K_n$ average		219			
port-to-throat area ratio, 1/J		1.35			
surface-to-port area ratio, G		162			
design progressivity		Essentially neutral			
<b>Exhaust gas ingredients</b>		H <sub>2</sub> O	HCl	CO	CO <sub>2</sub>
		N <sub>2</sub>	SO <sub>2</sub>	S	H <sub>2</sub>
		H <sub>2</sub> S	Cl	NO	Al <sub>2</sub> O <sub>3</sub>

IV. PERFORMANCE: (e)

	10°F	77°F	110°F
Burning time, $t_b$ (sec)	29.44	29.28	28.31
Maximum pressure, $P_{max}$ (psi)	630	683	698
Average pressure, $\bar{P}_b$ , over $t_b$ (psi)	471	512	533
Maximum thrust $F_{b, max}$ (lbf)	57360	67960	76200
Average thrust, $\bar{F}_b$ , over $t_b$ (lbf)	49150	53850	56150
Total impulse, I (lbf-sec)	1606400	1632000	1644500
Propellant specific impulse, $I_{sp}$ (lbf-sec/lbm)	220	223	225
Thrust-to-pressure conversion factor	0.0955	0.0953	0.0950

(e) at sea level, optimum expansion; approx. 17% higher under design conditions

	<u>Maximum</u>	<u>End of Burning</u>
<b>Temperature of outside motor wall (°F):</b>		
nozzle	1903	1600
nozzle end of motor	580	135
midpoint of motor	235	110
head end of motor	220	135

V. IGNITION:

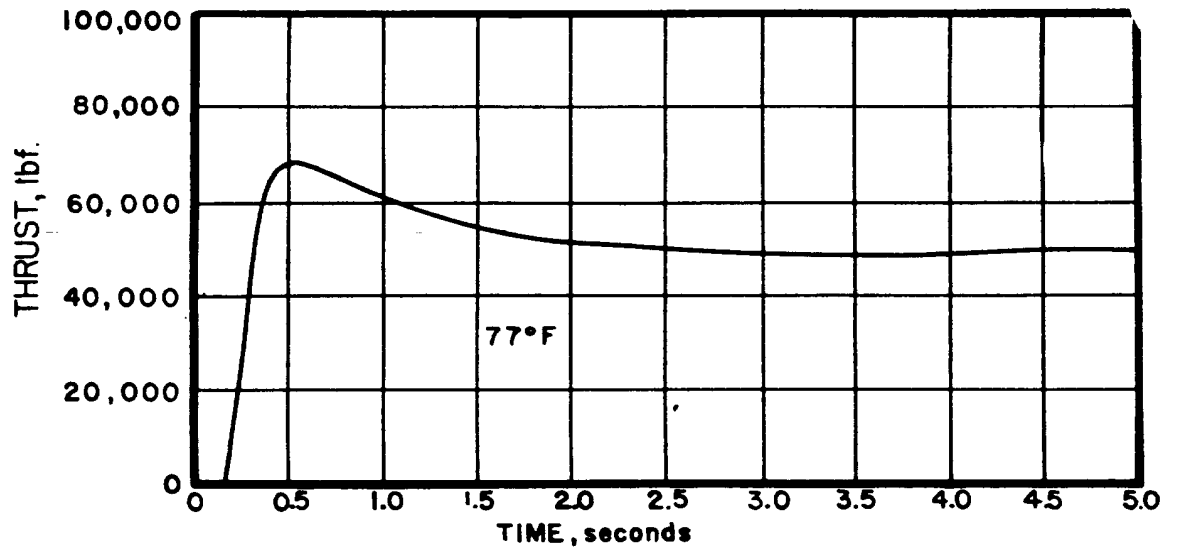
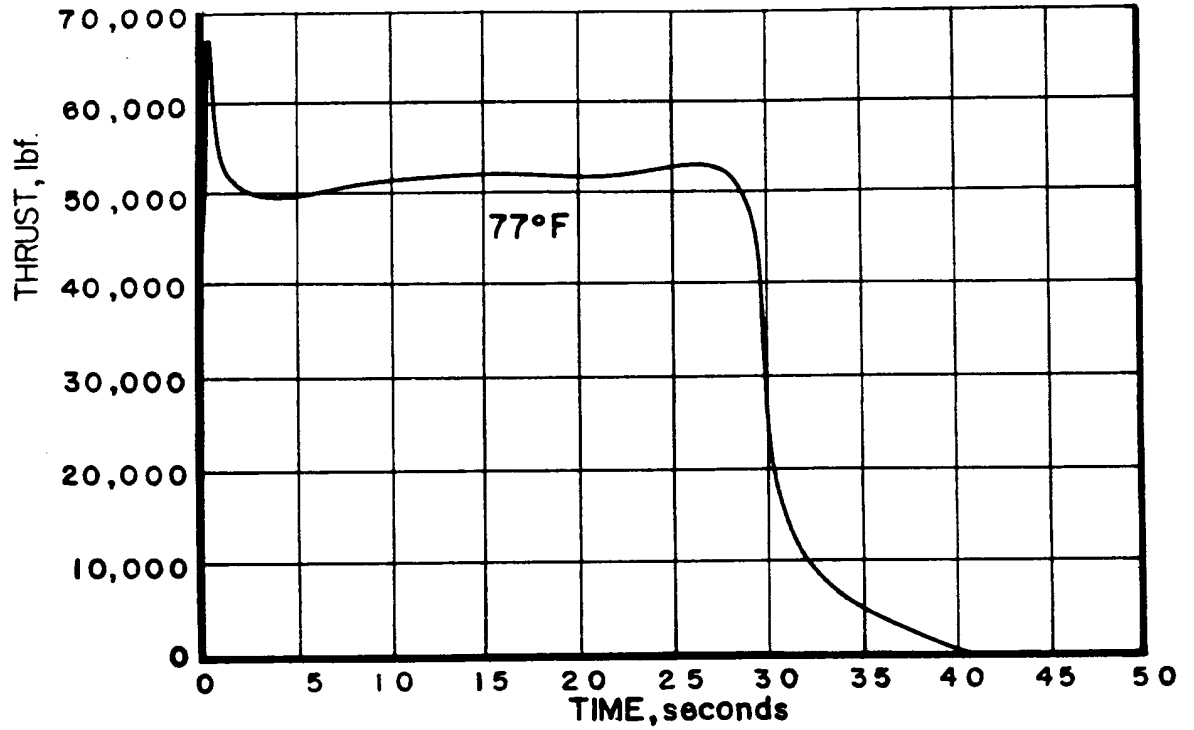
Igniter designation	TX-22-12
Igniter description	Pyrogen 3 x 9 fiberglass (Durez insert)
Igniter charge	Two MS-125 squibs with SP-16877-01 pellets
Ignition delay, $t_i$ (msec)	160
Igniter resistance (ohm)	1
Minimum current for reliable ignition (amp)	5

VI. PROCUREMENT INFORMATION:

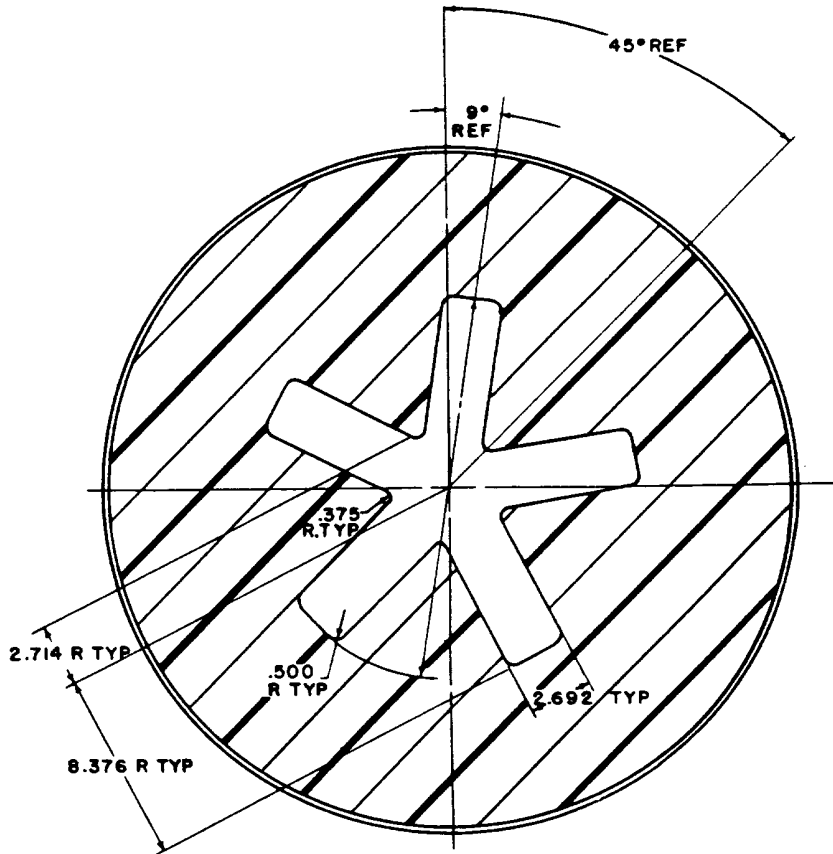
Sponsoring agency	NASA
Design and development agency	Thiokol/Redstone
Number and type of Service tests	11 static and 5 flight tests
Extent of Service use	Experimental use only. Modified versions of this motor for use with the "Little Joe" (XM33E2, E4) and "Mach 20" (XM33E3) Vehicles.

REFERENCES:

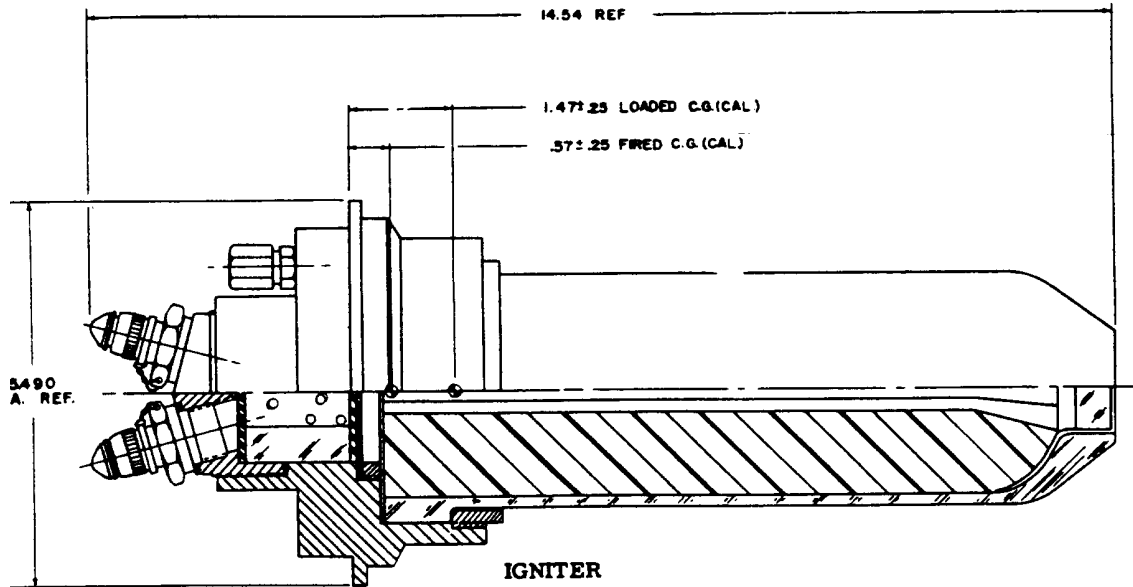
- (1) SPIA/M1 Questionnaire from Thiokol/Redstone (M. Weber, Jr.) August 1960.
- (2) "Rocket Propulsion Data" MCN-11072-60 (CONFIDENTIAL), Thiokol Chemical Corp., Second Edition - July 1960.
- (3) Supplementary Data from Thiokol/Redstone (B. C. Keith) April 1961.



PERFORMANCE CURVES



GRAIN CONFIGURATION



## REFERENCES

- [1] Raphael T. Haftka, and Zafer Gürdal, “Elements of Structural Optimization, third revised and expanded edition,” Kluwer Academic Publishers, 1996.
- [2] John S. Gero, Ed., “Design Optimization,” Orlando, FL, Academic Press, 1985.
- [3] Jabir S. Arora, “Introduction to Optimum Design,” New York: McGraw-Hill, 1989.
- [4] Ralph H. Pennington, “Introductory Computer Methods and Numerical Analysis,” 2<sup>nd</sup> Edition, First Printing, Toronto, ON, Collier-Macmillan Canada, 1970.
- [5] <http://www.sinopt.com/learning1/optsoft/optimization/optimization.htm>
- [6] <http://science.howstuffworks.com/rocket.htm>
- [7] George P. Sutton, “Rocket Propulsion Elements,” 2<sup>nd</sup> Edition, New York: John Wiley & Sons, 1956.
- [8] P. Richard Zarda, and Daniel J. Hartman, “Computer-Aided Propulsion Burn Analysis,” 24<sup>th</sup> AIAA/ASME/SAE/ASEE Joint Propulsion Conference, Boston, MA, July 11-13, 1988. AIAA Paper No. 88-3342.
- [9] Srinivas Kodiyalam, Jian Su Lin and Brett A. Wujek, “Design of Experiments Based Surface Models for Design Optimization,” Proceedings of the 39<sup>th</sup> AIAA/ASME/ASCE/AHS/ASC Structures, Structural Dynamics and Materials Conference, Long Beach, CA, April 20-23, 1998.
- [10] M. Alexandra Ahlqvist, “Dependency-Tracking Object-Oriented Multidisciplinary Design Optimization (MDO) Formulation on a Large-Scale System,” Ph.D. dissertation, University of Central Florida, Orlando, FL, 2001.
- [11] Garret N. Vanderplaats, “Numerical Optimization Techniques for Engineering Design with Applications,” New York, NY: McGraw-Hill. 1984.
- [12] Lawrence Hasdorff, “Gradient Optimization and Nonlinear Control,” New York: John Wiley & Sons, 1976.
- [13] Mitsuo Gen, and Runwei Cheng, “Genetic Algorithms and Engineering Design,” New York: John Wiley & Sons, 1997.

- [14] VR&D, “DOT – Design Optimization Tools”. Vanderplaats Research and Development Inc., Copyright 1999, Colorado Springs, CO.